Application of SWAT modeling for watershed restoration and protection in a tribal watershed setting

by

Anish Holla

B.E., Malnad College of Engineering, 2013
M.Tech, Indian Institute of Technology-Bombay, 2017

A THESIS

submitted in partial fulfillment of the requirements for the degree

MASTER OF SCIENCE

Department of Civil Engineering
Carl R. Ice College of Engineering

KANSAS STATE UNIVERSITY
Manhattan, Kansas

2026

Approved by:

Major Professor
Trisha Moore

Copyright

Abstract

Agricultural nonpoint source pollution is one of the major causes of water quality challenges across rural watersheds. There are more complexities involved in tribal watersheds settings where tribal sovereignty, fragmented land ownership, and climate vulnerability intersect. This study developed and applied a hydrologic and water quality model using the Soil and Water Assessment Tool (SWAT) to evaluate existing conditions in the Soldier Creek Watershed in northeast Kansas, a watershed where part of the drainage area falls within the Prairie Band Potawatomi Nation (PBPN) reservation boundary.

The SWAT model was calibrated and validated for streamflow, sediments, total nitrogen and total phosphorus against the observed data. Model performance for monthly streamflow exceeded NSE of 0.7 for both calibration locations, with satisfactory agreement for sediment and nutrient loads given the sparsity of observed water quality data. Twelve BMP scenarios were evaluated, including filter strips, no-till agriculture, and regenerative agriculture (RA) assumption applied across combinations of PBPN owned and privately owned croplands within the reservation area.

Filter strips applied at the watershed scale produced the largest sediment reductions, reaching approximately 70% at the subwatershed-scale and 15–28% at the PBPN boundary outlet; however, reductions were substantially diminished when BMP application was restricted to PBPN owned parcels, reflecting the constraints imposed by the checkerboard land ownership. No-till as a standalone BMP yielded limited water quality benefits but improved performance when combined with filter strips. The combination of RA and no-till across all croplands within the reservation produced effective reductions in water quality impediments.

Climate change analysis using an 18-model CMIP5 ensemble under RCP 4.5 and RCP 8.5 pathways was then conducted to examine potential impacts on hydrological processes within the tribal area. The ensemble of models projected a consistent warming trend expected to reduce average monthly runoff by 30–40% during the historically wet season by late century (2071-2099), alongside a substantial increase in moderate to extreme drought frequency.

This study found that watershed scale water quality improvement within the PBPN requires cooperative BMP adoption by both tribal and non-tribal landowners. The modeling framework developed here provides a practical tool to support conservation planning, prioritize management interventions, and develop long-term water resource resilience in the Soldier Creek Watershed within the PBPN.

Table of Contents

List of Figures

List of Tables

Acknowledgements

I would like to express my sincere gratitude to everyone who helped me complete my master's thesis work. This would not have been possible without the support of my advisor, Dr. Trisha Moore, who helped me continue my graduate program and provided guidance throughout my thesis. I especially appreciate her patience and continued support when I took a break from the master's program.

I am truly grateful for her willingness to always be available to discuss questions and provide directions whenever needed. I also appreciate the opportunities she provided for me to explore open-source data collection sensors and present my work at a conference. Her flexibility, encouragement, and support throughout the changes in my graduate journey were invaluable.

I would also like to thank my committee members, Dr. Aleksey Sheshukov and Dr. Dilini Herath, for their time, guidance, and support throughout this process. I am especially grateful to Dr. Sheshukov for his guidance and support when I faced challenges with the SWAT model. His help in troubleshooting model-related issues was very valuable to the successful completion of this work.

I would also like to sincerely thank Anu and her parents for their encouragement, understanding, and support throughout this journey.

Finally, I am thankful to my family, friends, and everyone who supported and encouraged me throughout my graduate studies.

Chapter 1 - Introduction

1.1 Problem Statement

Water resources form an integral part of society, providing various critical ecosystem services. Some of the services delivered are drinking water, fish production, recreation, and irrigation (Brauman et al., 2007; Grizzetti *et al*., 2016). Over the years, water resource management transformed from focusing on technical management to a participatory management approach, involving various stakeholders such as government bodies, local communities, universities to address water issues and challenges (Pahl-Wostl *et al*., 2007). Further, the intricate relationship between water resources and humans evolved, presenting new directions, challenges, and behaviors to be addressed when modelling coupled human-water systems (Shivapalan *et al*., 2011).

Sustainable water resource management is required to support drinking water needs, food security, recreation, and other commercial activities. Water resources challenges in terms of water quality and quantity are becoming more complex. They vary spatially and temporally along with local socio-political factors which require a collaborative partnership in water management (Biswas, 2008; Richard D Margerum *et al*., 2015).

Water quality issues will impact society's well-being by way of crop yield reduction, water availability, and land-use management challenges. A recent study shows how Iowa's intensive agricultural production has led to long term nitrate contamination of water resources which has directly impacted public water systems (Mantey *et al*., 2025).

According to the Intergovernmental Panel on Climate Change (IPCC)'s sixth Assessment Report, global warming is predicted to result in temperature increases in the range of 2.1°C to 3.5°C for intermediate greenhouse gas emission scenarios and 3.3°C to 5.7°C under high greenhouse gas (GHG) emission scenarios (IPCC, 2021). Numerous studies have shown that changing climate affects runoff water quality (Alamdari *et al*., 2020; Najjar *et al*., 2010). However, considerable uncertainty exists in climate change impact assessments due to differences among greenhouse gas emission scenarios, climate models, downscaling techniques, and hydrologic model structures, resulting in a range of potential future outcomes for water resources (Kundzewicz *et al*., 2018). Additionally, there is a social dimension of climate change, where socially vulnerable communities are impacted by their ability to recover post-disaster, increased food prices, and resource scarcity (Otto *et al*., 2017). The review by Berberian *et al*. (2022) showed that climate change is having a disparate impact on the health of people of color in the United States, finding that Black, Latinx, Native American, Pacific Islander, and Asian communities face higher risks of climate-related health impacts than White populations. The analysis documents racial disparities across a broad range of health outcomes including mortality, respiratory and cardiovascular disease, mental health, and heat-related illness driven by exposures such as extreme heat, flooding, hurricanes, and wildfires. Indigenous tribes' dependence on natural resources for subsistence, commercial activities, and cultural values associated in the form of fishing, hunting, agriculture, and tourism is threatened by increasing frequency of wildfire, droughts, and flooding. In some cases, federal and state legal regulations may act as an additional hurdle for tribes trying to adapt to climate change as well (Jantarasami *et al*., 2018).

Today's challenge is to understand this water resource management and hydroclimatic changes to develop mitigation strategies at the smaller community level. Watershed modeling is an integrated tool commonly used to support sustainable solutions (Xin Li *et al*., 2018; Reid *et al*., 2010; Devia *et al*., 2015). There is a limited amount of research on the application of these models at the tribal level. Therefore, developing a watershed model for tribal regions accounting for their local challenges is required to support climate change mitigation measures.

1.2 Objectives

The goal of this research is to understand the impacts of land use and climate change on the water quality, hydrologic functions and watershed management practices to support the water uses and ecological values of the Prairie Band Pottawatomie Nation (PBPN), a federally recognized tribe located in a predominantly rural watershed in Jackson County, northeast Kansas, north of Topeka. A physically based hydrologic model was used to model the existing condition and assess various best management practices (BMPs) to reduce pollutants in the watershed. The research herein will address the following questions:

1. What are the most effective BMPs to address the pollutant concerns faced by the tribal watershed? What are the challenges in implementing those BMPs?
2. How will projected climate change affect key hydrological characteristics in the Soldier Creek Watershed over future time horizons?

1.3 Research Significance

Surface water resources in Kansas are affected by various non-point pollution sources. A planning and management framework called Watershed Restoration and Protection Strategy (WRAPS) was developed to address various water quality issues across Kansas' watersheds (KDHE, 2020). These plans were developed in a participatory fashion, i.e., the stakeholders included government and non-government agencies, residents, universities, and watershed groups. The main objective of this program was to focus on streams across Kansas which did not meet water quality standards defined under the U.S. Clean Water Act. Funding for the

WRAPS program is provided by EPA's Clean Water Act Section 319 and the Kansas State Water Plan.

The WRAPS program contains four stages (W. L. Hargrove *et al*., 2005): 1) Development, 2) Assessment, 3) Planning, and 4) Implementation. In the development stage, stakeholders across the spectrum from rural landowners to universities and government agencies are identified. Local project cooperators interested in the watershed and with extensive knowledge of the area are identified to provide leadership. A WRAPS committee is set up to guide the program and can include diverse stakeholders. Once these items are completed, activities are undertaken to generate public awareness and interest in water quality issues. This may include creating awareness about water resource threats and related activities like fishing, local cultural values, and drinking water. Furthermore, stakeholder involvement includes public education, public participation, and public relations, which is critical for the successful implementation of the WRAPS program. The Assessment stage entails assessing the current condition of the watershed. This process may include information on geography of the area, socioeconomic conditions, water quality, land use, flora, fauna, and wildlife. Analysis is carried out to identify the locations/regions that are major contributors to water quality impairments. Watershed models are also used to simulate hydrological processes in the watershed and to evaluate the impact of mitigation measures. Input obtained from this assessment is used to develop management plans. In the Planning stage, focus group discussions are carried out with stakeholders to discuss existing water quality issues, sources of pollution and explore management options to improve the water quality. Streams with critical water quality issues are identified and mitigation/protection goals are determined. An implementation plan is developed which includes the following causes of pollution, protection measures, estimated reduction in loads and technical/financial resources, timeline, and evaluation criteria. The implementation stage is the final stage of the WRAPS program and follows the strategy laid out in the implementation plan. Diverse stakeholders are part of the implementation process and efforts are made to maintain local interest in the program. Periodic evaluations are carried out to mark the progress and revisit the strategy.

Kansas was divided into twelve major river basins forming the planning units for the WRAPS program. One of the river basins is Middle Kansas WRAPS, which includes numerous stream segments that are impaired for various TMDL pollutants as summarized in Table 1-1.

Table 1: Middle Kansas WRAPS Project Area Impediments

Water Segment	TMDL Pollutant	Priority
Kansas River at Topeka	Ammonia	High
Kansas River at Topeka	Fecal Coliform Bacteria	Medium
Kansas River below Topeka	Biology	Medium
Kansas River below Topeka	Fecal Coliform Bacteria	Medium
Kansas River near Wamego	Fecal Coliform Bacteria	Medium
Mill Creek	Fecal Coliform Bacteria	High
Upper Soldier Creek	Biology, Sediments	High
Rock Creek	E. coli Bacteria	High
Vermillion Creek	Fecal Coliform Bacteria	High
Wildcat Creek	Fecal Coliform Bacteria	High
Wildcat Creek	Fecal Coliform Bacteria	High

Among the impaired stream segments identified in the Middle Kansas WRAPS plan is the Upper Soldier Creek. The majority of Upper Soldier Creek flows through the Prairie Band Potawatomi Nation (PBPN), a federally recognized tribe headquartered near the center of the Soldier Creek Watershed. The tribal nation is considering adopting the WRAPS program for the part of creek flowing through the nation. As part of the assessment requirement, PBPN wants to understand the current conditions of Soldier Creek and analyze the impact of best management practices (BMPs) in reducing pollutant loads. One major focus of load reduction was reduction in sediment loading into the Soldier Creek. This research aims to develop a watershed model to support the assessment component of WRAPS. This research used a physically based semi-distributed hydrologic model to develop an existing conditions model. This research aims to determine effectiveness of various BMPs to achieve the TMDL reduction targets. This research will also analyze the impact of future climate scenarios on the hydrological conditions within the watershed. The findings from this research will support the PBPN in adopting BMPs to achieve the water quality requirements under the WRAPS project.

Chapter 2 - Literature Review

2.1 Hydrologic Modelling and SWAT

Hydrological modelling is used to simulate runoff, water quality, and flow routing using numerical models and tools. Watershed models answer fundamental questions such as "What happens to rainwater? Where does it go and how?" They are interdisciplinary linking anthropogenic activities to the natural world. Some modeling applications support flood control, reservoir management, groundwater management, water quality assessment, soil conservation, and land-use evaluation. A hydrological model can be further described as a mathematical representation of one or more components of the hydrological cycle, designed to simulate catchment behavior and to define the relationship between precipitation inputs and streamflow outputs (Singh and Woolhiser, 2002). Understanding water quantity and quality within a watershed is the essential first step before any management decision can be made; some of the core components such as water operation policies, governance, and management feedback follow the initial assessment. Over time, hydrology has been further subdivided into ecohydrology, global hydrology, and social hydrology, each emphasizing the growing importance of stakeholder participation and governance (He and James, 2021).

Watershed models are classified according to how they represent the flow of water in the natural watershed system. In terms of physical representation, models may be physical (scale models), analogue (such as electrical circuit analogues of groundwater flow), or mathematical; mathematical models have become dominant with the growth of computing power (Jajarmizadeh et al., 2012). Models may simulate a discrete storm event referred to as event-based model or operate continuously over months to decades, also known as continuous models. Event-based models are particularly well-suited to support hydrological design applications, such stormwater management systems for which the design is based on specific design storms. Continuous hydrologic models simulate both wet and dry phases of the hydrological cycle and are generally preferred where long-term nonpoint-source pollution loading and land management evaluation are the primary concern (Borah and Bera, 2003). The continuous model is more appropriate for current study which analyzes long term loading in the system. Models also can be classified according to their spatial representation of the watershed as either lumped and non-lumped. Lumped models treat the entire catchment as a single unit and are fast to run but unable to represent spatial variability. By contrast, fully distributed models have parameters which vary spatially and temporally. They are the most physically rigorous and require heavy data and computational demands while semi-distributed models occupy an intermediate position, partitioning the catchment into sub-basins or hydrological response units (HRUs) and assuming homogeneity within each unit while allowing differences between units (Okiria et al., 2022). Finally, hydrologic models may be classified according to their consideration of uncertainty. Deterministic models produce a single output for a given set of inputs, while stochastic models incorporate probabilistic elements suited to forecasting under uncertainty. Most widely used models are fundamentally deterministic but may be embedded within Monte Carlo frameworks for uncertainty and sensitivity analysis.

In a comparison of different integrated hydrology and water quality models, Hydrological Simulation Program (HSPF) and Soil and Water Assessment Tool (SWAT) are consistently identified as the highest-performing options, with MIKE SHE approaching comparable functionality when its ECO water quality module is deployed (Keller et al., 2023). Precipitation Runoff Modelling System (PRMS) and Hydrologic Engineering Center (HEC-HMS) both lack water quality components and are therefore unsuitable as standalone tools for water quality assessment. HSPF, though capable of sub-daily time steps and mixed land-use simulation, conceptualizes overland flow as levelled detention storage. This limits its performance in intense single-event flood scenarios, and its user interface has been described as dated (Borah and Bera, 2003; Keller et al., 2023). Direct model comparisons reinforce these conclusions: Golmohammadi et al. (2014) evaluated SWAT, MIKE SHE, and APEX on the 52.6 km^2 Canagagigue Creek watershed and found that all three met accepted performance criteria during validation (NSE of 0.73, 0.71, and 0.70 respectively), while SWAT offered greater calibration flexibility than the Agricultural Policy/Environmental eXtender Model (APEX). Jaiswal et al. (2020) acknowledged that SWAT's ability to simultaneously simulate land-use change, climate change, and water quality loading which were usually absent from lumped models made it the better choice for agricultural watersheds.

Regardless of the model classification, hydrological models all require meteorological data as inputs (e.g., precipitation, temperature, solar radiation, and evapotranspiration) to represent climatic forcing functions. Land surface information, such as elevation, slope, drainage networks, and soils, are also key model inputs, as are anthropogenic factors such as land use, land cover, and management practices. Many hydrologic models are set up using Geographic Information Systems (GIS) to help manage and process multiple spatial data layers. In addition to modelling flow, point source and non-point source water quality modelling involves loading impediment data distributed across the watershed and through time (Keller et al., 2023). Models then determine surface flows in the form of overland, channel, and stream flows, as well as subsurface and groundwater contributions, to support decision-making on the impacts of climate change, land-use change, best management practices (BMPs), and water quality impediments.

For this study, SWAT was selected as the most appropriate model. It is well suited to represent agricultural watersheds, allows explicit representation of changes in agricultural land management practices. There are specific modules to support BMP implementation and can simulate both hydrologic and water quality processes. SWAT offers flexibility, which can represent individual fields to large basins supporting continuous simulation at daily, monthly and annual time steps. Tools like SWAT-CUP can be paired with the model for calibration and uncertainty analysis to strengthen confidence in the model outputs. Further it supports integrating future climate scenarios into the model. These capabilities make SWAT a suitable tool for examining the research questions of this study. The hydrology component uses the SCS curve number method with lateral subsurface flow and groundwater percolation; the sediment component applies the Modified Universal Soil Loss Equation (MUSLE); and the water quality component tracks nitrogen, phosphorus, and bacteria through the plant-soil-runoff-stream continuum (Borah and Bera, 2003). SWAT's semi-distributed HRU structure captures land use, soil, and management practice, and SWAT has been widely adopted for evaluating agricultural BMPs and informing TMDL standards under the USEPA's BASINS system (Gassman et al., 2007). One of the studies noted that SWAT is one of the few models that can represent land-use change within a single continuous simulation run, making it particularly well-suited to integrated climate change and scenario assessments (Keller et al., 2023). Gassman et al. (2007) catalogued over 250 peer-reviewed SWAT applications across watersheds from less than 1 km^2 to over 490,000 km^2, demonstrating satisfactory performance across diverse climatic zones and land-use types; Tan et al. (2020) subsequently reviewed around 111 articles , of which most of them reported acceptable NSE and R^2 values of 0.5 and 0.6 for streamflow exceeding satisfactory threshold mentioned by Moriasi et al. (2007). By 2021, SWAT publications had grown to more than 4,500 publication (CARD, 2021), demonstrating the model's extensive and continually expanding application. Further SWAT is freely available, supported by USEPA and USDA, and accompanied by the SWAT-CUP platform that provides various algorithms like SUFI-2, GLUE, MCMC, and PSO to support calibration and uncertainty framework.

2.2 Water Quality in Agricultural Watersheds

Nonpoint source pollution (NPS) is impacting various water bodies across United States with nutrient pollution from nitrogen and phosphorus being one of the leading impediments. Some of the well-known examples are the hypoxic zone in Gulf of Mexico (Rabalais and Turner, 2019) which is caused by the nitrogen and phosphorus loads from the Mississippi River Watershed due to contribution by agricultural activities. Moss (2008) argued that agriculture's impact extends well beyond nutrients to drainage, channel modification, and catchment alteration, with management implications far more profound. Regional water-quality studies in Kansas and Missouri have shown that nonpoint-source runoff can be a major contributor to stream impairment. In the Blue River Basin, a USGS report by Wilkison et al. (2009) found that nutrient and bacteria loads were influenced by a combination of nonpoint-source runoff, wastewater-treatment plant discharge, and combined sewer overflows, with nonpoint sources contributing substantially to annual nutrient and bacteria loads. The study also reported declines in suspended-sediment concentrations following erosion and runoff-reduction efforts, showing that sediment management can also reduce sediment associated pollutant transport. Further, numerous studies in agricultural watersheds have recorded Escherichia coli (E. coli) enters streams via runoff from manured fields, livestock access to channels, failing onsite wastewater systems, and wildlife, and that it can persist in stream bed and riparian sediments (Gazio-Hadzick et al.,2010; Afolabi et al.,2023).

Kamrath & Yuan (2022) analyzed long-term monitoring data across Lake Erie Basin and the Mississippi River Basin watersheds and found that top 10% of the flow transported more than half of the annual nutrient load. The annual loads during high flow saw an increase as the agricultural landuse increased but reduced when watershed size increased. This shows the importance of high flows in water quality in a watershed. Similarly, Dodds and Oakes (2008) found that landuse in eastern Kansas watersheds was strongly related to downstream nutrient concentrations, particularly total nitrogen, nitrate, and total phosphorus. Their results showed that headwater stream areas can strongly influence downstream water quality, suggesting that nonpoint-source pollution management should consider upland and headwater riparian zones rather than focusing only on downstream stream corridors. Watershed modeling has been widely used to support TMDL development and nonpoint-source pollution management in agricultural watersheds. In a Kansas based study of the Marmaton River Watershed, Wang et al. (2009) used AnnAGNPS to evaluate sediment, total nitrogen, and total phosphorus loading and found that agricultural nonpoint sources were the dominant contributors to nutrient impairment. Results showed that targeted management of critical source areas required substantially less land treatment than random BMP implementation, highlighting the value of spatially explicit watershed modeling for identifying effective pollutant-reduction strategies. In another example Yasarer et al. (2016) applied the SWAT model in the Perry Lake watershed in northeast Kansas to evaluate how landuse changes due to biofuel related activities could affect sediment, total nitrogen, and total phosphorus loads. Their scenario analysis showed that converting hay land to corn or grain sorghum increased nutrient and sediment export, demonstrating the usefulness of SWAT for comparing land-management alternatives and water-quality impacts in Kansas agricultural watersheds.

2.3 Best Management Practices for Sediments and Nutrient Reduction

Best Management Practices (BMPs) measures implemented to mitigate impediments from a target site. In case of agricultural watersheds these can be structural, vegetative or policy level measures. They are used to reduce the impact of pollutants and achieve Total Maximum Daily Load (TMDL) or regulatory targets. BMPs can be applied at the source i.e. reduce pollutant generation at the origin or can be applied along the flow path to intercept pollutants before they reach stream channels. Effective watershed management typically involves a combination of both types, applied strategically across the landscape to maximize load reductions (Gassman et al., 2007; Chaubey et al., 2010).

Some of the BMPs used in the agricultural watersheds are filter strips, no till and regenerative agriculture. Filter strips (FS) are narrow bands of permanent vegetation, usually dense grasses or mixed herbaceous cover, established between agricultural areas (cropland or pasture) and adjacent streams or drainageways. They function primarily by intercepting shallow overland flow, reducing runoff velocity, enhancing infiltration, and improving deposition of sediment and sediment bound nutrients before they reach the stream (Cibin et al., 2018; Chaubey et al., 1995; White & Arnold, 2009). Within the SWAT, FS are represented as edge of field BMPs applied at the hydrologic response unit (HRU) scale, with performance parameterized by strip width, field-to-strip area ratio, and the fraction of flow that remains as sheet flow. When implemented along stream corridors, FS act as a riparian buffer system that also contribute to channel-bank stabilization.

Studies reported sediment (TSS) reductions of 40–85% at the field scale, total phosphorus (TP) reductions of 30–70%, and total nitrogen (TN) reductions of 20–60%, with effectiveness dependent on strip width, slope steepness, vegetation density, and flow characteristics (White & Arnold, 2009; Vigiak et al., 2016). At the watershed scale, simulated and observed load reductions from VFS are typically lower than field-scale trapping rates because only a portion of the landscape is treated, untreated upstream areas continue to contribute pollutants, and in-stream processes redistribute sediment and nutrients (Chaubey et al., 2010; Leh et al., 2018; Vigiak et al., 2016).

No-till (NT) farming eliminates mechanical soil disturbance, retaining crop residue on the surface and seeding directly into undisturbed soil. NT increases infiltration capacity, reduces surface detachment and builds soil organic carbon relative to conventional tillage. Wang et al. (2013) quantified these dynamics in the Pataha Creek Watershed in Washington State, finding effective hydraulic conductivity under NT to be 44% higher than under conventional tillage on average but these tillage impacts on hydrological processes are site specific and watershed dependent. In SWAT, NT is represented by low soil mixing efficiency (EFFMIX = 0.05, representing the fraction of surface residue, nutrients, and soil properties mixed within the tillage layer), shallow tillage depth (25 mm), an increased Manning's roughness coefficient for overland flow (OV_N), and a modest curve number (CN2) reduction to reflect improved infiltration (Wang et al., 2013; Ricci et al., 2020; Li et al., 2018).

The pollutant reduction efficiency of NT varies considerably across watersheds. In the semi-arid Lake Mogan watershed in Turkey, Özcan et al. (2017) reported NT reductions of 1.46% in nitrate and 4.50% in total phosphorus, with negligible sediment reduction. In more erosive environments NT performed more strongly. Ricci et al. (2020) found NT to be the most effective single BMP for sediment reduction in the Carapelle basin in Italy, and also the most economically favorable practice. Conversely, Wu et al. (2022) found NT to be the least effective of six BMPs in the highly erodible Yanhe River watershed on China's Loess Plateau, achieving only 3.18% annual sediment reduction. This shows the varying efficiency of NT across different watersheds and regions. Despite this variability, NT consistently performs better as part of integrated BMP suites than as a standalone BMP. Li et al. (2018) found NT improved freshwater provisioning by up to 11.4% in agriculturally dominated watersheds across the Upper Mississippi River Basin, with effectiveness maintained under projected future climate scenarios. Their study also found that combined BMP scenarios outperformed NT alone across all watershed types. Parajuli et al. (2016) modelled three tillage scenarios i.e. conventional, reduced tillage (three tillage passes, closer to conservation tillage) and a near no till (two passes: fall sub-soiling and a pre-planting roller pass, closest to no-till) scenarios. Study found that near NT practices produced the lowest sediment yields under future climate projections in the Big Sunflower River Watershed in Mississippi. So, NT's role as a simple and cost-effective conservation practice is most effective when paired with complementary management measures.

Regenerative agriculture (RA) is an emerging, holistic approach to farming that seeks to restore and improve soil health, biodiversity, and ecosystem services through integrated management practices. RA typically combines practices of including no-till or minimal tillage, cover cropping, diversified crop rotations, integration of livestock, and reduced synthetic inputs, all oriented toward building soil organic matter and biological activity (Schreefel et al., 2020; Newton et al., 2020). Regenerative farming systems have been shown to significantly increase soil infiltration rates compared to conventional agriculture. A study by Panta (2025) reported increases in soil infiltration rates of 86–198% in regeneratively managed fields compared to conventional controls, suggesting substantially reduced surface runoff and erosion potential. However, the scientific evidence base for quantifying RA's hydrological impacts at the field and watershed scale remains limited, and significant variability exists across sites, climates, and practice combinations.

2.4 Climate Change Impacts on Water Resources

There has been a higher frequency of severe heat waves, extreme rainfall and droughts across the world due to climate change (AR5, 2015). As water resources are one of the important components impacted by these, several studies (Jha et al.,2013; Mueller-Warrant et al., 2019; Marin et al., 2020) have analyzed the effects of climate on the runoff and nutrients within a watershed. The study carried out by Jha et al. (2013) in the upper Mississippi River basin showed a decrease in annual streamflow reduced by 5% during the mid-century period (2046-2065). This study also highlighted the spatial variability in nutrient results with Illinois sub watersheds showing a positive increase in nitrate-nitrogen loading while Iowa sub watershed having a mix of results.

SWAT is one of the most widely applied models for climate change impact assessment on a watershed scale with publication growing between 2001 to 2013 from three to around eighty annually (Krysanova & White, 2015; Krysanova & Arnold, 2015). Future climate projections are obtained from global climate models (GCM) ensembles like CIMP5 for different Representative Concentration Pathway (RCP) scenarios. Some studies then introduced GCM into the calibrated model either through delta change method (Jha et al., 2013) or bias corrected statistical downscaling method, such as used by Gharibodusti et al. (2019) and Kujawa et al. (2022). In most cases, no single GCM is considered appropriate as each model will have inherent bias and assumptions (Alamdari et al., 2020); thus, multiple climate models are used to simulate the calibrated model, and the ensemble mean and range of outcomes is used to communicate uncertainty (Jha et al., 2013; Kujawa et al., 2020; Gharibodusti et al; 2019). Acknowledging the uncertainty from various sources, Kundzewicz et al. (2018) suggests adopting an ensemble-based approach which will provide a spread of outcomes and help develop adapting strategy considering the range of future possibilities. In this study, the focus was to identify the impact of climate change on the study area stream flow for mid- and long-term future conditions. A suite of GCMs were simulated and the model output was averaged to understand the impact of climate change on the hydrologic performance of the watershed.

2.5 Tribal Water Resources, Environment Governance, and Climate Vulnerability

Native Americans have a unique relationship with the local ecology and water is considered sacred. It is an integral part of their culture and used in practices like purification and blessing rituals (Cozzeto et al., 2013). Tribal communities depend on water resources both surface and groundwater for domestic water supply, fishing, hunting, agricultural irrigation and the maintenance of aquatic ecosystems to support cultural practices (Jantarasami et al., 2018). According to Cozzetto et al. (2013), groundwater supplies around 93% of Native American drinking water systems. The protection and sustainability of water resources are critical for the Tribal nations.

Tribal nations have inherent sovereign authority over their land and natural resources but exercising of this authority is complicated by historic dispossession and overlapping jurisdictional relationships with state and federal agencies. Water resources within the Tirbal nation are legally protected by the 1908 Winters decision which mentions that tribes reserved the water rights necessary to fulfill the purpose of their reservations. However, many of these water rights have not been fully settled, and in cases where tribes have won the rights there is lack of funding required to build infrastructure needed to use that water (Cozzeto et al., 2013).

Prairie Band Potawatomi Nation (PBPN) deals with the challenge of a checkerboard pattern of tribal and non-tribal land ownership within reservation boundaries. The Indian Removal Act of 1850, subsequent relocations and allotment policies under the Dawes Act of 1887 resulted in this checkerboard pattern of land ownership (Mehl et al., 2021). Despite the PBPN's resistance to individual allotment well into late nineteenth century by 1895 the remaining land had been divided into 80–160-acre parcels resulting in fragmented land parcel structures that complicated land management and watershed scale conservation coordination (Mehl et al., 2021). Further, off-reservation water use, and pollution compound this problem as tribes are frequently underrepresented in water resource management discussions and decision-making processes (Cozzetto et al., 2013).

Climate change impacts the Indigenous communities, as they face greater exposure to climate hazards and have fewer resources to adapt compared to the broader population. Berberian et al. (2022) analyzed the data from 2017-2022 to show that people of color including Native American communities faced an elevated risk of climate related health impacts driven by exposure to extreme heat, flooding, hurricanes and wildfires. While the National Climate Assessment report 4 (NCA4) mentions that Indigenous health is grounded in interconnected social and ecological systems, and climate driven impacts to lands, water, foods and culturally significant species pose threats not only to physical health but to cultural heritage, identify and mental wellbeing (Jantarasami et al., 2018). Some of the other threats documented by Cozzetto et al. (2013) include disruption of subsistence activities, deterioration of water quality and availability, and increasing frequency of extreme weather events. Also, federal and state policies may further act as institutional barriers to tribal climate adaptation, including through limited access to traditional territories and funding mechanisms that fail to account for the unique conditions of Indigenous communities (Jantarasami et al., 2018).

Despite these challenges, there is growing recognition of developing watershed management plans tailored to tribal contexts and building adaptive capacity. As the NCA4 notes, successful adaptation in indigenous contexts depends on integrating traditional knowledge systems, resiliency and proactive efforts by the state and federal to reduce institutional barriers (Jantarasami et al., 2018). The study by Mehl et al., (2021) noted that sustainable land priorities like cover crops, riparian buffers and health stream ecosystems are linked to deeply held community values around stream condition, fish and fishing, and cultural continuity.

Hydrological modeling applications specifically designed for or applied in tribal watershed settings remain relatively scarce in the published literature. This gap represents both a research need and an opportunity to develop methodologies and frameworks that address the unique jurisdictional dimensions of water resource management in PBPN reservation. The development of SWAT models for tribal watersheds can provide critical information to support TMDL development, BMP planning, and climate adaptation strategies grounded in the ecological and cultural priorities of the community.

Chapter 3 - Methods and Materials

3.1 Study Area

The study area is the watershed of Soldier Creek (HUC# 1027010208) in northeast Kansas. The creek flows across three counties with the headwaters starting in Nemaha County, while the majority of the creek's flow path is in Jackson County. Soldier Creek ultimately drains into Kansas River near Topeka in Shawnee county (Figure 1). Little Soldier Creek is the major tributary to Soldier Creek and other smaller tributaries are Crow Creek, James Creek, Dutch Creek, Messhoss Creek, Halfday Creek and Walnut Creek.

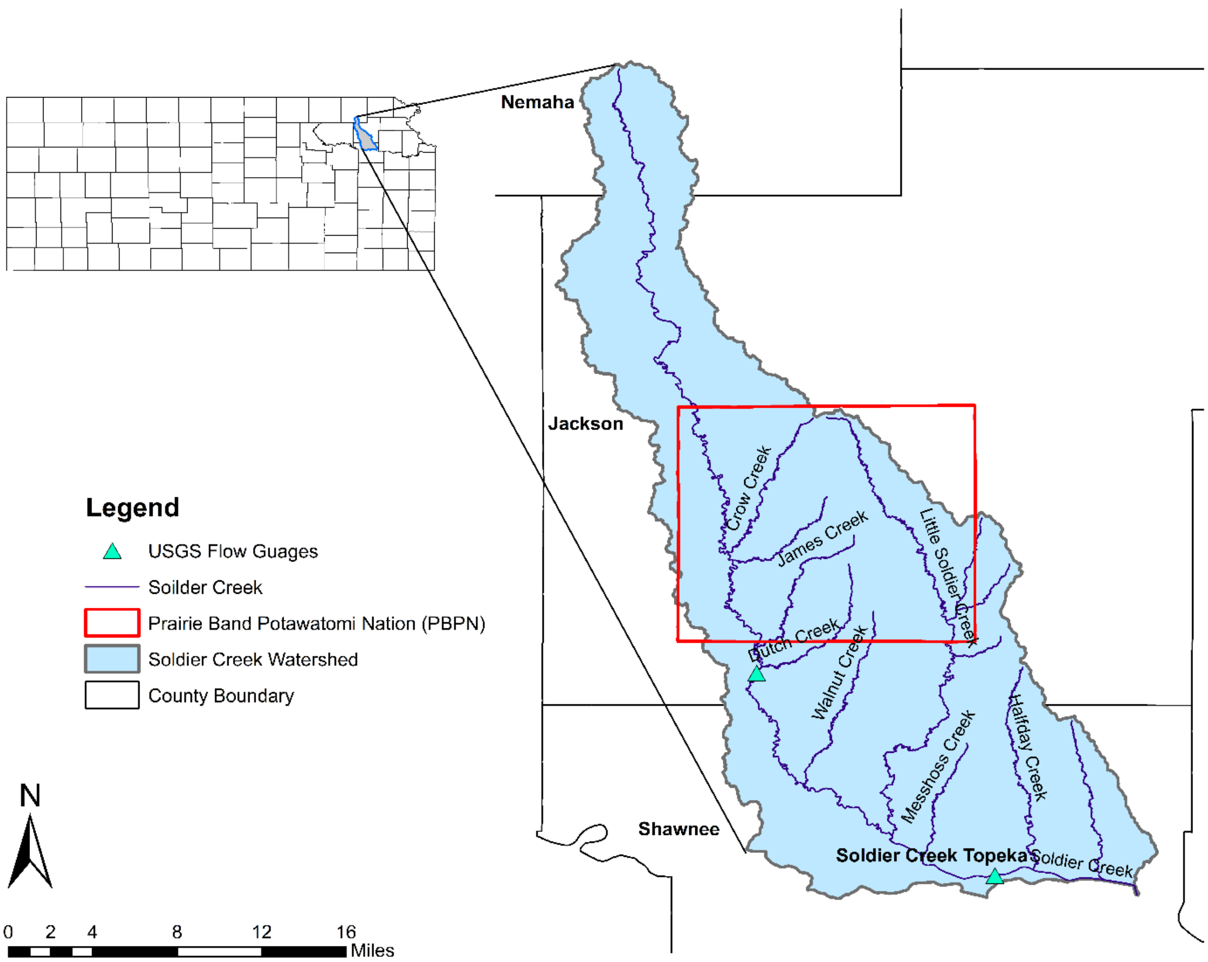

Figure 1: Location of Soldier Creek and tributaries.

The Soldier Creek watershed area is 873 km^2 , with approximately 31.15% of this area within the PBPN administrative boundary. There are eight HUC-12 level sub-watersheds within the Soldier Creek watershed. Flow data is recorded through two USGS gages, including the Delia gage (06889200) situated upstream south the PBPN boundary and Topeka gage (06889500) near the outlet of the watershed (Figure 1). Streamflow characterization analysis done by USGS (Juracek, 2017) found substantial variation between years but no defined long-term trends in the annual mean stream flow. Their analysis also showed that bseflow comprised around 20 percent of the annual streamflow. Streamflow tends to peak in the spring and is lowest during the winter depicting the wet season in the watershed. Based on the historical data during extreme droughts there were periods of no flow in the creek which varied from one to several months (Juracek, 2017) showing that creek can dry up during prolonged drought periods.

3.2 PBPN Land History

Regarding the history associated with PBPN, Prairie Band Potawatomie Nation is originally from the Great Lakes area. The tribe was forced to migrate west following the 1830 Indian Removal Act, and during the migration in the mid-1830s and 1840s the tribe made temporary stops in Missouri and Iowa (*PBPN webpage*). Initially when the tribe moved into Kansas the reservation area was around 230,000 ha. The passage of the Kansas-Nebraska Act of 1854 led to immigration of white settlers in tribal reservations. This was followed by two treaties in 1861 and 1867 which further divided the land to meet railroad and religious group interests. By 1867, the reservation area had decreased 87% to 31,300 ha. Finally, the Dawes Act was passed in 1887 by Congress, which would provide private land to Indians families to become a farmer. This was opposed by the tribe, as it went against the culture of the tribe which believed and practiced land holding as common property of the community and not individual.

As part of the Dawes Act, the land was divided into 80- to160-acre parcels and allocated to each household head (Heidi Mehl *et al*.,2021). Many tribal community members were not accustomed to the economic value of the land, as in many cases sold the land to non-tribal members at a low value. Heidi Mehl *et al*. (2021) noted the result of fractionation and escheat provision resulted in checkerboard pattern of land tenure seen today (Figure 2). The current reservation area is 31,517 ha, and PBPN owns around 45% of the land parcels.

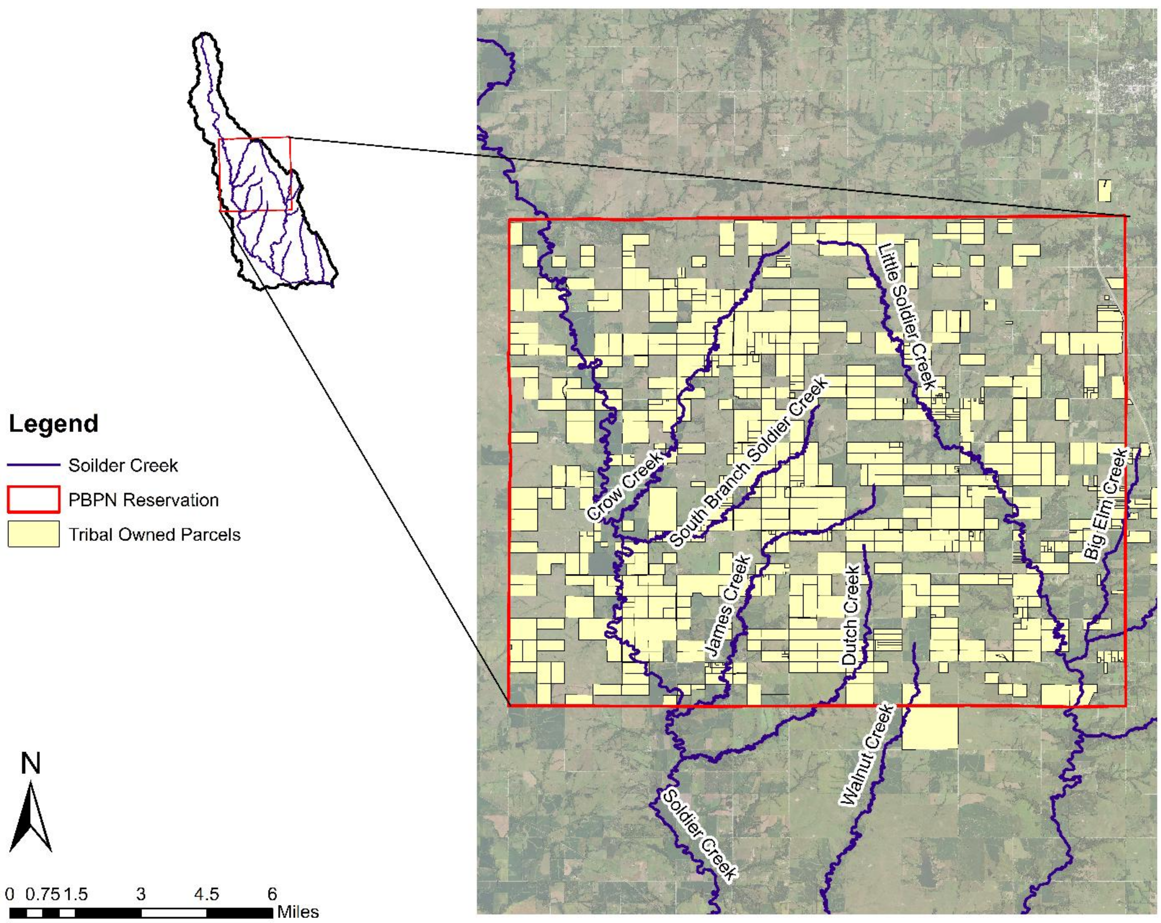

Figure 2: PBPN Land ownership within PBPN Reservation

3.3 Watershed Parameters

3.3.1 Soldier Creek Land Use

The major land use in the watershed is pasture/grassland (48%), crop land (21%), and deciduous forest (15%). Table 2 provides the major land use classification for the watershed based on the USDA Crop Data Layer (CDL) for 2019.

Table 2: Major Land use Classification in Soldier Creek Watershed (CDL 2019)

Land use	Area (ha)	% of Watershed
Grass/Pasture	42425.46	48.33
Deciduous Forest	13272.48	15.12
Soybeans	9856.98	11.23
Corn	8546.49	9.74
Other Hay/Non Alfalfa	5266.71	6
Developed/Open Space	3072.15	3.5
Developed/Low Intensity	1755.45	2
Winter Wheat	541.98	0.62

Figure 3 represents the spatial distribution of land use. Most cropland, which includes primarily corn and soybean, are located along the creek. Additionally, there is a cluster of croplands at the headwaters of Soldier Creek and within the floodplain of the Kansas River in the southern portion of the watershed. There is a practice of crop rotation involving corn-soybean cycle in the watershed.

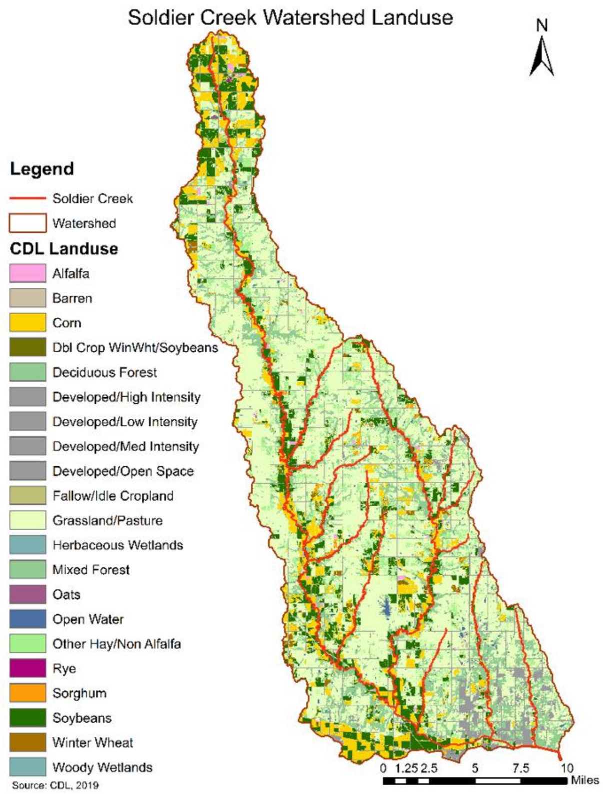

Figure 3: Watershed Level Land Use

Land use analysis was carried out using the USDA CDL between 2006 and 2019. Over this time, soybean cropping area increased by 29% (Figure 4) while grassland/pasture decreased by 20%. While corn cropping area fluctuated from year to year, there was a decreasing trend in winter wheat cropping area. In 2006, approximately 1,207 ha of winter wheat was grown in the watershed, but only 215 ha by 2019. Regardless, winter wheat still represents a small portion of the total watershed landcover (< 1%) and so is not represented in Figure 5. The reduction in winter wheat was compensated for by increasing cropping area for soybeans.

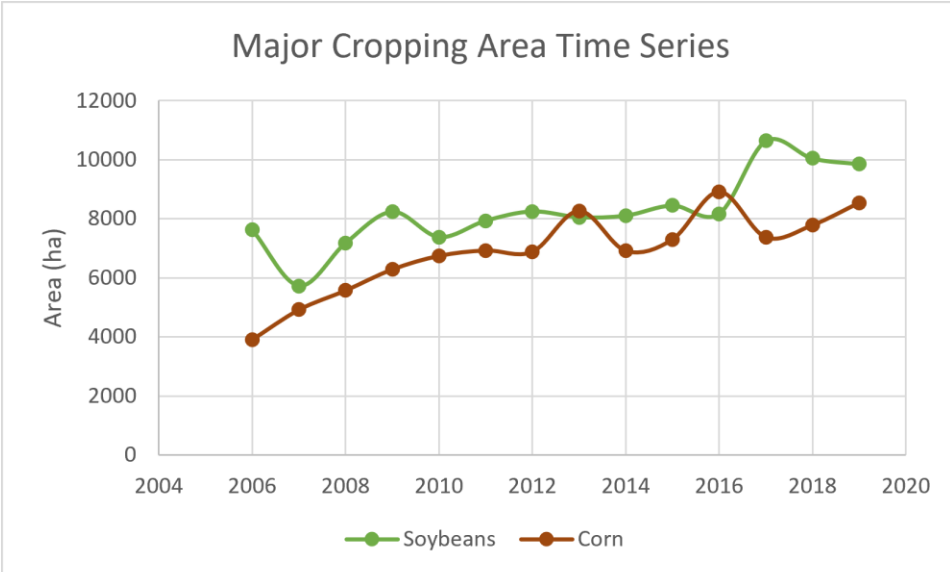

Figure 4: Major Crops Trend Analysis

3.3.2 PBPN Land Use

Land use within the PBPN reservation area follows a similar pattern as seen across the watershed. Table 3 shows pasture as the prominent land use type with 54.76% followed by deciduous forest while row crops like corn and soybean constitute around 14% of the land use. Though most of these agricultural and pasture lands are owned privately as discussed in Section 3.2.

Table 3: Land Use Distribution within PBPN

Land use	Area (ha)	% of Watershed
Grassland/Pasture	14875.83	54.76
Deciduous Forest	4453.83	16.39
Soybeans	2264.22	8.33
Other Hay/Non Alfalfa	2235.87	8.23
Corn	1608.66	5.92
Developed/Open Space	672.48	2.48

3.4 Hydrologic Modeling: Soil Water Assessment Tool (SWAT)

The Soil and Water Assessment Tool, also known as SWAT, is a physically based, spatially distributed deterministic model developed by the USDA. SWAT is widely used for hydrological assessment studies, to predict flows and water quality from point and non-point loading sources (Douglas-Mankin *et al*.,2010). As the tool helps meet this study's objective, SWAT was used for modelling the Soldier Creek watershed. It is an open source-based model which can be added to ArcGIS or QGIS applications. The basic principle of a water balance across the watershed is used to determine the flows and other parameters. The routing of flows can be generally divided into landscape and streamflow routing. The landscape routing phase, which happens at sub-watershed level, determines the loading of water, nutrients, and sediments into the main channel. Following the landscape routing phase, resulting runoff and materials (e.g., sediment, nutrients, etc.) are routed through the watershed stream network to the watershed outlet. The basic water balance calculated by SWAT is presented in Equation 1, where the final water content in the soil (SW_t) is obtained by taking the initial soil water content, SW_0, and adding the net sum of rainfall, R_{day}, surface runoff, Q_{surf}, evapotranspiration, E_a, seepage (the amount of water entering the vadose zone from the soil), w_{seep}, and the amount of return flow, Q_{gw}. All the units are in mm of H_2O and calculated on a daily timestep.

$$SW_t = SW_o + \sum_{i=1}^{t}(R_{day} - Q_{surf} - E_a - w_{seep} - Q_{gw} \qquad (1)$$

Surface runoff (Q_{surf}) is calculated based on the SCS curve number method (Neitsch *et al*., 2009), and the difference between rainfall and runoff is used to approximate infiltration and evapotranspiration. Equation 2 calculate the amount of runoff (Q_{surf})

$$Q_{surf} = \frac{(R_{day} - 0.2S)^2}{(R_{day} + 0.8S)^2} \qquad (2)$$

R_{day} = Depth of rainfall for the day in mm and S = Parameter for retention in mm

Evapotranspiration is determined using either the Penman-Monteith, Hargreaves, or Priestley-Taylor equations based on the available data. Penman-Monteith method was applied in this study given its more accurate representation of the evapotranspiration process and the availability of required input data for the study watershed.

Streamflow routing in SWAT can be performed using either the variable storage or Muskingum routing method. The variable storage method is based on the continuity equation and storage–discharge relationships, whereas the Muskingum method routes flow through channels using a storage-based approach and Muskingum routing coefficients (Neitsch *et al*., 2009). Groundwater contributions to streamflow are simulated through a shallow, unconfined aquifer that discharges baseflow to the main channel, and a deep confined aquifer assumed to leave the watershed as underflow (Arnold et al., 1993). Percolation leaving the soil profile reaches the shallow aquifer after a delay governed by the aquifer delay time, and a user-specified fraction of this recharge is diverted to the deep aquifer via the deep aquifer percolation coefficient. Baseflow is generated once the shallow aquifer volume exceeds a threshold. The regions where there is snow melt contributing to the hydrology, SWAT simulates that using a temperature index approach.

Variable storage methods were adopted for modelling the study area as this method requires fewer input parameters than the Muskingum method and the study emphasized watershed-scale processes rather than detailed channel routing. SWAT assumes the main channel has a trapezoidal cross section with channel side slope of 2:1 and data from DEM is used to calculate the channel cross-sectional area and hydraulic radius. SWAT uses manning's n equation for uniform flow to obtain the flow rate and velocity in each reach for the given time step as represented in equation 3 and 4.

$$q_{ch} = \frac{A_{ch} \cdot R_{ch}^{2/3} .slp_{ch}^{1/2}}{n} \tag{3}$$

$$v_c = \frac{R_{ch}^{2/3} . slp_{ch}^{1/2}}{n} \quad (4)$$

Where q_{ch} is the rate of flow in the channel (m^3/s), A_{ch} is the cross section of flow in the channel (m^2), R_{ch} is the hydraulic radius for a given depth of flow (m), slp_{ch} is the slope along the channel length (m/m), n is Manning's n coefficient and v_c is the flow velocity (m/s). Flow is then routed downstream using the variable storage coefficient method (Williams, 1969), which was adopted for this study. This method is based on the continuity equation applied to a reach segment:

$$V_{in} - V_{out} = \Delta V_{stored} \quad (5)$$

Where V_{in} and V_{out} are the volumes of inflow and outflow during the timestep and V_{stored} is the resulting change in channel storage. Travel time is calculated as the storage volume divided by the discharge rate. The flow rate, time and storage are used to calculate inflow and outflow rate through subbasins to outlet.

Erosion and sediments delivery are calculated using the Modified Universal Soil Loss Equation (MUSLE) shown in equation 6.

$$Sed = 11.8 \cdot * \left(Q_{surf} \cdot q_{peak} \cdot area_{hru}\right)^{0.56} \cdot K_{USLE} \cdot C_{USLE} \cdot P_{USLE} \cdot LS_{USLE} \cdot CFRG \quad (6)$$

Where sed is the sediment yield on a given day (metric tons), Q_{surf} is the surface runoff volume (mm H_2O/ha), q_{peak} is the peak runoff rate (m^3/s), $area_{hru}$ is the area of HRU (ha), K_{USLE} is the soil erodibility factor, C_{USLE} is the USLE cover management factor, P_{USLE} is the USLE support practice factor, LS_{USLE} is the USLE topographic factor and CFRG is coarse fragment factor. Sediment is routed downstream through the channel network using the simplified Bagnold (1977) stream power equation, the default method in SWAT (Williams, 1980). This method calculates the maximum sediment concentration that a reach segment can transport as a function of peak channel velocity.

Nitrogen and phosphorus loading to the stream network is generated through two linked sets of processes in SWAT's land phase: transformations among the soil nutrient pools (mineralization, denitrification, sorption) that control how much nitrogen and phosphorus is available for transport and the transport equations themselves, which move nitrate, organic N, soluble P, and sediment-bound P from the HRU to the main channel (Neitsch et al., 2009). Equation 7 and 8 provide the nitrate and soluble phosphorous loss to surface runoff.

$$NO3_{surf} = \beta_{NO3} \cdot conc_{NO3,mobile} \cdot Q_{surf} \tag{7}$$

Where $NO3_{surf}$ is the nitrate removed in surface runoff (kg N/ha), β_{NO3} is the nitrate percolation factor coefficient, $conc_{NO3,mobile}$ is the concentration of nitrate in the mobile water for the top 10 mm of soil (kg N/mm H_2O), and Q_{surf} is the surface runoff generated on a given day (mm H_2O).

$$P_{surf} = \frac{P_{solution,surf} \cdot Q_{surf}}{\rho_b \cdot depth_{surf} \cdot k_{d,surf}} \tag{8}$$

Where P_{surf} is the amount of soluble phosphorus lost to surface runoff 9kg P/ha), $P_{solution,surf}$ is the amount of phosphorus in solution in the top 10mm (kg P/ha), $Q_{,surf}$ is the amount of surface runoff on a given day (mm H_2O), p_b is the bulk density, $depth_{surf}$ is the depth of "surface" layer (10mm), and $k_{d,surf}$ is the phosphorus soil partitioning coefficient (m^3/Mg). Phosphorus behaves very differently from nitrate because it sorbs strongly to soil particles and is far less mobile in solution and they are bound to sediments.

SWAT divides the watersheds into sub-catchments, which are further divided into hydrological response units (HRUs). Within sub-catchments, each HRU contains homogenous soils, landuse type, and slope. HRUs are not spatially connected and are the smallest unit of the model. Runoff and water quality are calculated at the HRU level and then aggregated to the subbasin level for further processing (Neitsch *et al*., 2009). SWAT uses gridded inputs for topology through digital elevation model (DEM), landuse, and soil type grids. Other inputs like point source loading, management practices, cattle count and weather data can be added using the GIS interface. Figure 5 provides the flow chart depicting the SWAT workflow.

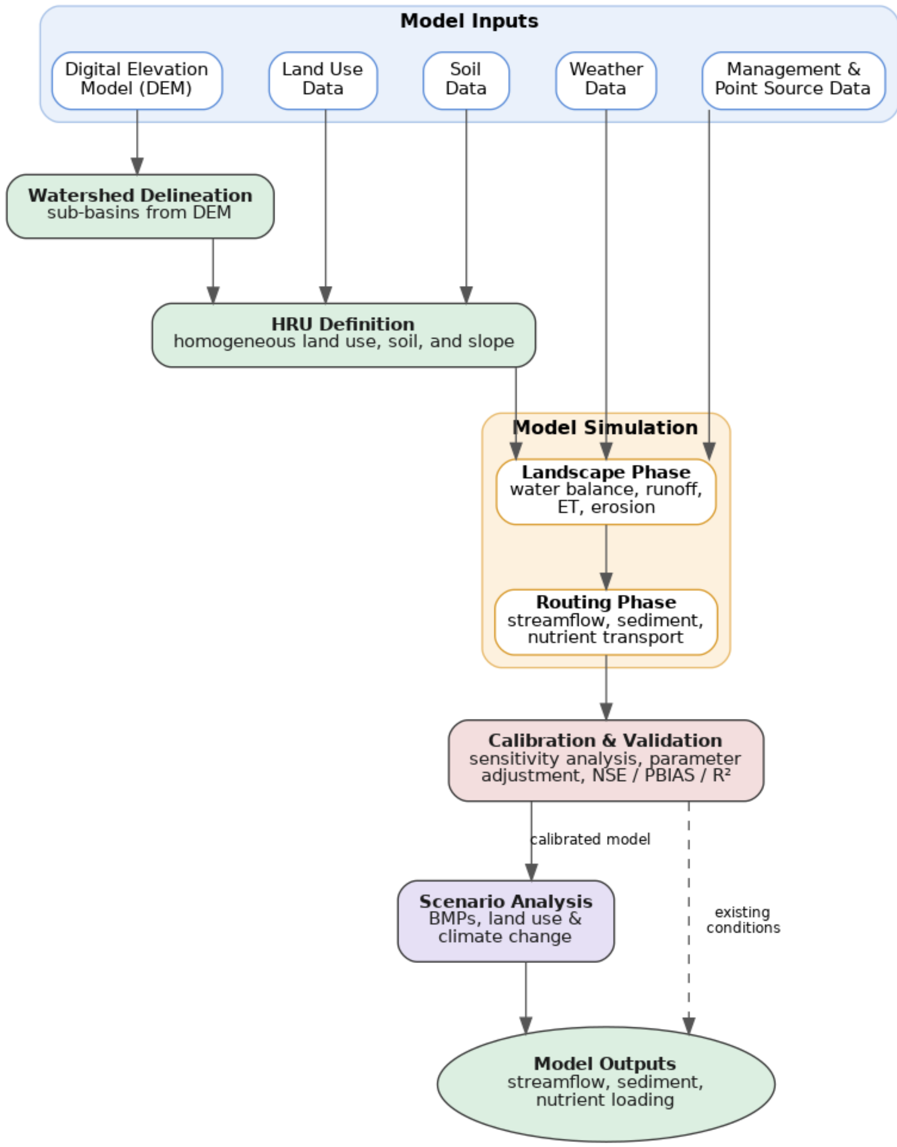

Figure 5: General SWAT Model Workflow

3.5 Model Inputs

As described, various inputs were prepared for the model, and this section discusses inputs used in it.

3.5.1 Digital Elevation Model (DEM)

The DEM is an important input for the SWAT hydrological model. Previous studies have shown that the SWAT model is sensitive to DEM resolution, with DEM resolution being the most influential parameter affecting streamflow simulation accuracy compared to data source and resampling technique (Tan *et al.,* 2015). A 10-m DEM (1/3 arc-second) was downloaded from United States Geological Survey (USGS) 3D elevation program dataset. The SWAT auto watershed delineator was used to delineate the watershed. Autogenerated basins and reaches were further refined by adjusting the outlet points to match HUC12 boundaries within the HUC10 Soldier Creek watershed. The elevation range varies between 258 to 429 meters as seen in Figure 6.

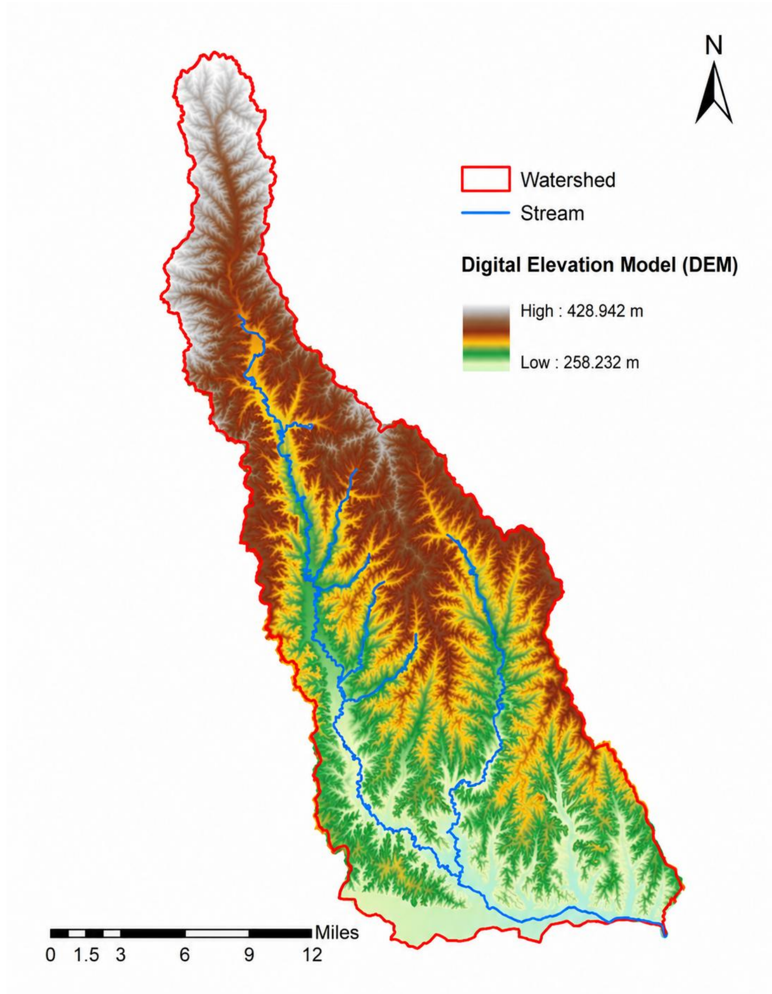

Figure 6: Digital Elevation Model (DEM) (10m) of Soldier Creek Watershed (Source: USGS)

Slope is another key input parameter in SWAT, used alongside land use and soil data to delineate HRUs, which are the smallest computational units within each sub-basin sharing similar hydrologic characteristics. The watershed has lower slopes and is relatively flat at the outlet where Solider creek outfalls to the Kansas River (0-2% slope). Figure 7 shows upstream areas have slopes mostly between 2-4% and with some areas having steep slopes above 15%. Slopes were classified into three classes to define slope ranges for HRU determination:0-4%, 4-8% and 8+%.

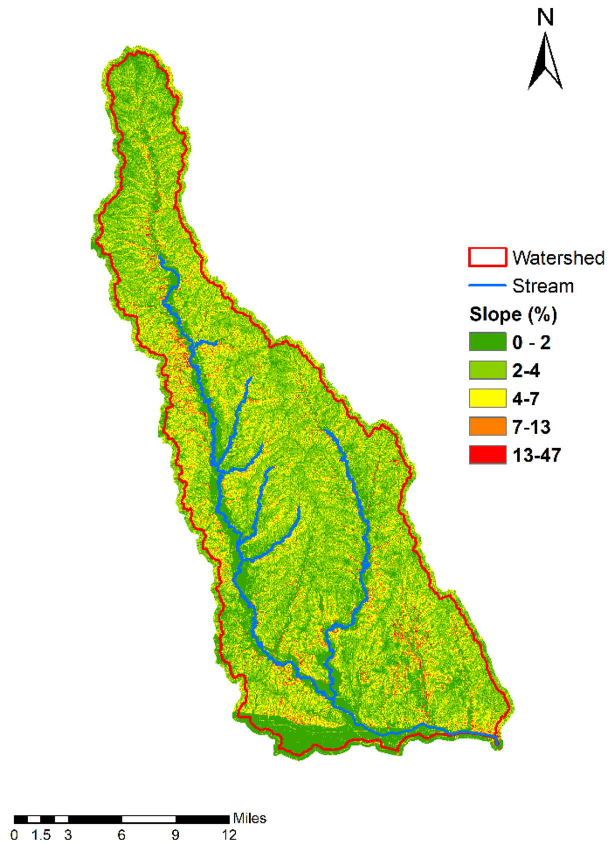

Figure 7: Slope Classification of Soldier Creek Watershed

3.5.2 Land Use and Soil Type

The 2020 crop data layer (CDL) was used to classify the watershed land use. Section 3.3 discusses the distribution of the land use within the watershed and PBPN study area. Soil data is an important input to the watershed model as it determines the runoff rate, infiltration, and percolation along with the land use and slope. Two soil datasets that are commonly used as SWAT inputs are the State Soil Geographic Database (STATSGO) and the Soil Survey Geographic Database (SSURGO). The primary distinction between the two is spatial resolution i.e. STATSGO assigns a single soil classification to areas that may contain multiple distinct soil types, whereas SSURGO captures finer spatial variability, generating significantly more HRUs and unique soil types within the same watershed. STATSGO is mapped at 1:250,000 while SSURGO ranges from 1:12,000 to 1:63,000, making SSURGO the preferred choice when higher accuracy in nutrient and sediment predictions is required (Geza & McCray, 2008). Figure 8 shows the soil distribution across the study area. Some of the major soils are Pawnee clay loam, Martin silty clay loam and Kennebec silt loam. Hydrologic Soil Group (HSG) analysis of soil (Table 4) across the watershed showed that around 60% of the soil type belonged to hydric soil group D followed by group C/D. Group D or C/D are characterized by clayey soil with low infiltration and high runoff potential.

Table 4: Hydrological Soil Groups Within the Prairie Band Pottawatomie Nation Boundaries

Hydrological Soil group	Percentage Coverage (%)
D	60.12
C/D	19.6
C	15.42
B	3.47
Un-defined	1.39

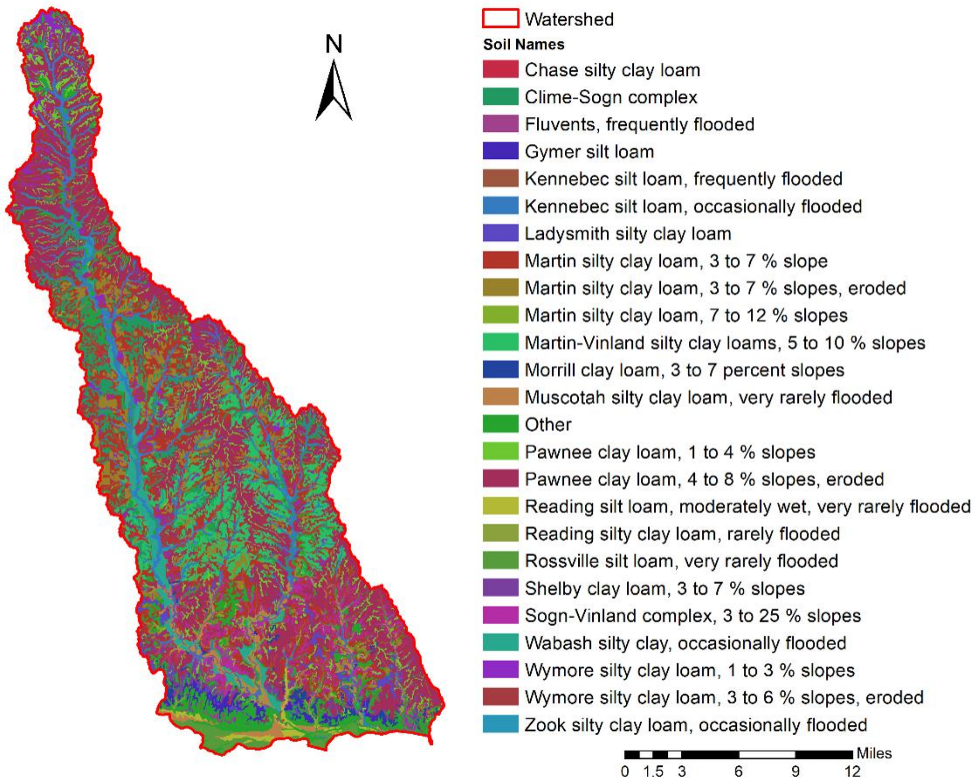

Figure 8: Major Soils SSURGO Map, Soldier Creek Watershed

3.5.3 Weather Data

Climate data for the study area was obtained for a daily time-step and analyzed from various local weather stations i.e. Circleville, KS (USC00141529), Holton, KS (USC00143759), Mayetta (US1KSJA0001) and Topeka, KS (USW00013996). The Topeka station had the most continuous complete data for both precipitation and temperature. In addition to local data, 1km*1km gridded data was obtained from Daymet (Daymet_Daily_V4R1). The location of the weather station data is shown in Figure 10. SWAT requires daily temperature, rainfall, wind speed, solar radiation and relative humidity as weather inputs. In the watershed the average monthly temperature ranges between –2°C to 26°C with average annual rainfall of 895 mm (Topeka Station, 1950-2020). May to August represents the wet season with higher temperatures being recorded during the months of July and August (Figure 9).

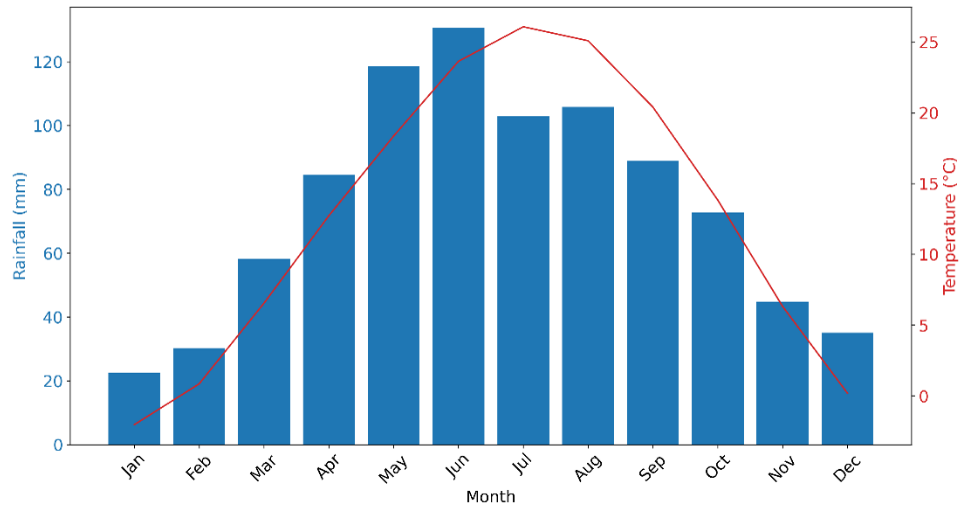

Figure 9: Average Monthly Precipitation and Temperature Plot (1950-2020) (Source: https://www.ncei.noaa.gov/cdo-web/datasets/GHCND/stations/GHCND:USW00013996/detail)

3.5.4 Discharge and Water Quality Data

Flow data was obtained from the existing active USGS gauges within the watershed (Figure 10). The Delia gauge (USGS station number 06889200) is on Big Soldier Creek and at the PBPN boundary. This gauge was primarily used for model calibration and validation purposes. The USGS also maintains a gauge near the outlet of the Big Soldier Creek watershed near Topeka (USGS station number 06889500). In addition to this there is a gauge at Circleville USGS station 006889110) upstream of Delia, though this gauge only provides discharge data from 1990 to 2001 and gauge height from 2021 onwards. Due to lack of discharge data for the study period this was not selected for model calibration and validation efforts. To understand the flow in and out of the PBPN reservation area, the mean monthly flows between the Circleville and Delia gages were analyzed from 1964 to 2001. Mean monthly flow between the two gauges increased by an average of 230%, with a maximum increase of 310% recorded in December between both gauges (Juracek, 2017). This signifies the contribution of flow into Soldier Creek by the reservation area.

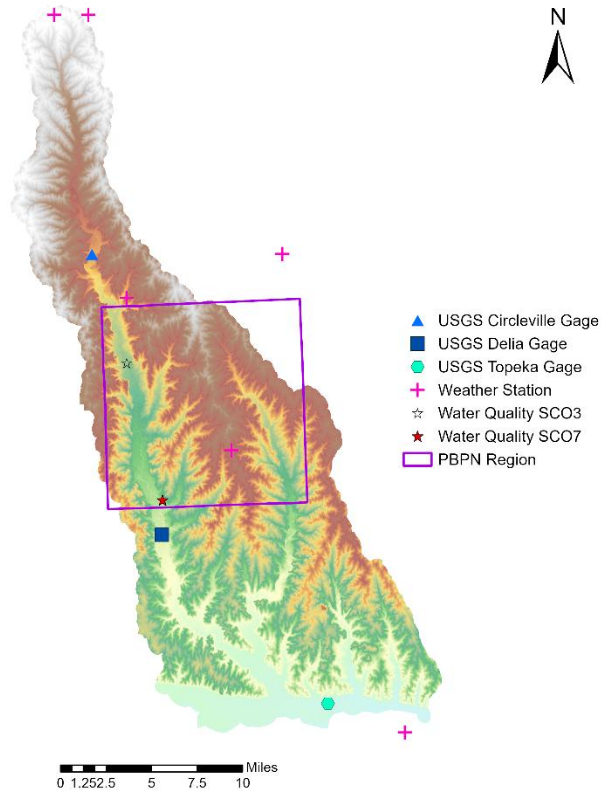

Figure 10: Locations of USGS Gauges, Water Quality Data Points, and Weather Stations Used for SWAT Model Creation

Figure 11 compares the flow response to rainfall at the Delia and Topeka USGS gauges for the study period (2000-2019). Both gauges show a similar hydrologic response to precipitation events throughout the record, with the Topeka gage recording slightly higher peak flows consistent with its position at the watershed outlet and larger contributing drainage area. A notable period of significantly reduced streamflow is observed at both gauges during the 2012 drought, with flows approaching zero, reflecting the severe dry conditions across the watershed during that period.

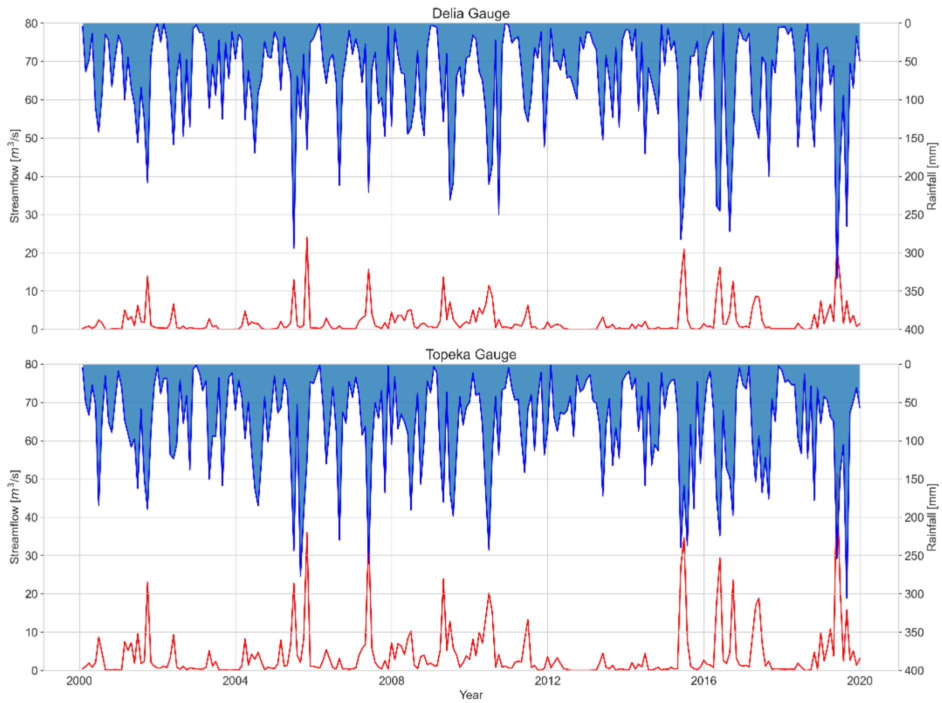

Figure 11: Flow Response (red line) to Precipitation Events (filled blue line) at Delia and Topeka Gauge (2000-2019)

Water quality data for the watershed collected by the PBPN for two locations along Big Soldier Creek (Figure 10) was used for analysis. Based on the availability of data between time period 2012 to 2021, total nitrogen and total phosphorus levels were above the acceptable range of 0.9 mg/l for nitrogen and 0.07 mg/l for phosphorus (Table 5), which are the nutrient water quality indicators in the watershed. There are also higher counts of the indicator bacteria *E. Coli* observed at both gauges in the watershed.

Table 5: Summary Statistics of Measured Total Nitrogen, Total Phosphorus concentrations (mg/L) and *E. coli* (MPN/100ml) at Two Water Quality Monitoring Stations on Big Soldier Creek (SC03 and SC07), based on Grab Samples Collected 2012 - 2019

Total Nitrogen (mg/l)				
Gage	Number of Observations	Average	Min	Max
Soldier Creek SC03	50	1.25	0.067	3.61
Soldier Creek SC07	50	1.31	0.23	3.4
Total Phosphorus (mg/l)				
Gage	Number of Observations	Average	Min	Max

Soldier Creek SC03	51	0.15	0.044	0.55
Soldier Creek SC07	51	0.17	0.073	0.79
E. Coli (MPN/100ml)				
Gage	Number of Observations	Average	Min	Max
Soldier Creek SC03	48	1077	20	12591
Soldier Creek SC07	49	827	4	19863

The sparse nature of water quality data, i.e. sediments, nutrients and phosphorus, makes it challenging to obtain continuous data comparable to streamflow. This sparse data needs to be transformed into continuous data so that it can be used to better support model calibration and validation. Continuous load development was done using a rating curve (HEC-RAS rating curve calculator) for sediments and load estimation tools (FLUX32) for nutrients. Further, to capture an additional source of sediment loading through unpaved roads, the Geomorphic Road Analysis and Inventory Package Lite (GRAIP Lite) was used to obtain a relative loading rate. The next chapter discusses these tools and their associated outputs in more detail.

3.6 Future Climate Model CIMP5

In this study, the output from 18 climate models from CMIP5 was extracted and statistically downscaled using the Multivariate Adaptative Constructed Analogs (MACAv2) methodology, which matches future large-scale weather patterns to those that occurred in the historical record (Abatzoglou and Brown, 2012). The primary advantages of this downscaling technique are strong performance compared to historical reanalysis and the conservation of the first principles of meteorology. For the future climate scenarios in SWAT, representative concentration pathways (RCP) 4.5 and 8.5 were selected. The RCP 4.5 scenario represents conditions in which carbon emissions peak in 2040 and declines thereafter while RCP 8.5 represents increasing emissions through 2100 (van Vuuren *et al*. 2011). The downscaled data were obtained for the study area from the MACA database (https://www.climatologylab.org/maca.html). For each climate model and emission scenario, daily maximum and minimum temperature, wind speed, precipitation, relative humidity, and solar radiation were aggregated from the 4 km downscaled resolution to the county level between 2006 and 2099. These inputs were used as forcing weather inputs to SWAT, creating a multi-model ensemble of 18 models to assess the uncertainty of future climate.

3.7 SWAT Model Setup

SWAT 2012 revision 681 was used for this study. The ArcSWAT tool interface was used to set up the model. HUC10 was defined as the watershed boundary. DEM delineation was done to match the SWAT sub basins to the HUC12 boundaries within the watershed. As seen in Figure 12, a total of 17 sub-basins were delineated and 9 sub-basins with a larger part of the basin intersecting with PBPN boundary were identified as PBPN sub-basins for analysis. Sub-basins within the PBPN region were more refined with an average area of 2,800 ha while areas outside the boundary had an average sub-basin area of 8,475 ha match the HUC-12 boundary. An additional subbasin was created to capture the model response at the USGS Delia gauge location. Because this outlet was placed to align with the gauge rather than a natural drainage divide, its contributing area is small relative to the cumulative upstream drainage area at that point.

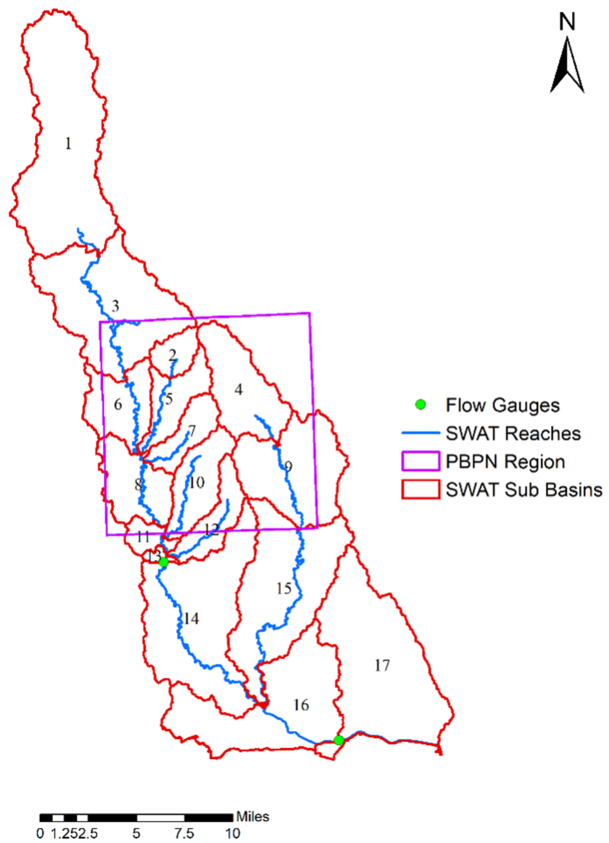

Figure 12: SWAT Model Sub-Basins

The initial HRU delineation produced a large number of HRUs, many of which represented small and fragmented landscape units. User-defined area thresholds for land use, soil, and slope are commonly applied in SWAT to improve computational efficiency, though applying these thresholds results in reapportionment of minor land use and soil types to dominant HRUs within each sub-basin (Her et al., 2015). A general percentage threshold of five percent of subbasin area is commonly used as optimal for maintaining model accuracy and efficiency; however, water quality estimates including sediment, nitrogen, and phosphorus have been found to be more sensitive to HRU aggregation than flow estimates, and more conservative thresholds are recommended for water quality focused applications (HAWQS, 2023; Her et al. 2015).

Conservative minimum area thresholds of 10 ha, 5 ha, and 5 ha were applied for land use, soil, and slope, respectively, which is well below the commonly used percentage-based defaults along with three slope classes. These thresholds resulted in a final count of 2,891 HRUs across 17 sub-basins. The relatively large number of HRUs reflects both the conservative thresholds applied and the high spatial detail captured by the SSURGO soil dataset.

3.7.1 Land Management Implementation

Baseline land management was defined at the HRU level through the SWAT management file (.mgt) operation scheduled, land use was further divided by coding the ownership (PBPN vs non tribal) to support targeted management and BMP scenario analysis. Cropland was represented as a two-year corn-soybean rotation implemented within each HRU's management file, rather than as an annual land-use reassignment. Corp data obtained through crop data layer (CDL) and added to the model. Corn was planted April 15 with fertilization initiated April 30, then harvested and killed September 15, followed by fall tillage (generic fall plowing) on September 30. Soybean was then planted May 15 with fertilization initiated May 30 and harvested and killed October 15 (USDA NASS, 2010). Corn and soybean phases vary across HRUs so that the watershed contains a mix of both crops in any given calendar year. Some farmlands had corn as the initial crop whereas other ones had soybean at the start of the crop rotation.

Grazing land was represented as a single continuous-season grazing operation on pasture/rangeland HRUs. Grazing begins late April and continues for 230 consecutive days, spanning roughly the full frost-free season through early December. The grazing consumption rate (BIO_EAT = 2.78 kg/ha/day) was derived from a stocking rate of one cow-calf pair per 8 acres (NRCS Kansas grazing guidance) and an assumed dry-matter intake of 20 lb/animal/day

(~9 kg/day, roughly 2% of a 1,000-lb animal unit's body weight. The manure deposition rate (MANURE_KG = 0.69 kg/ha/day) was derived from total-solids manure production of a finished animal over a 153-day finishing period (USDA AMS National Organic Program handbook, section 5017-1). Manure applied through the grazing operation is the primary mechanism representing bacterial loading from pastureland in the model.

Full management schedules, parameter values, and data sources for both cropland and grazing operations are provided in Appendix A.

3.8 Model Calibration and Validation

Evaluating the model's performance is required to understand if the model represents the field conditions. Calibration is the process of adjusting the model parameters by comparing model simulation with the observed values for the same set of conditions. Once the model parameters are adjusted, model simulation is compared against a different set of observed values to determine the accuracy of the model (Moriasi *et al*., 2007). For this SWAT model, calibration and validation were carried out using SWAT-CUP (Calibration and uncertainty program). SUFI-2 (Sequential Uncertainty Fitting) algorithm was used for calibration and validation. The program selects a different set of parameter values from a user-defined range for the parameter for each model run iteration and uses 95% probability distributions to account for the uncertainty in the model (K.C Abbaspour, 2015). As hydrology is the driving factor for sediments and nutrients in the SWAT model, flow is first calibrated followed by sediments. Finally, nutrients are calibrated with both sediments and flow parameters held fixed as both flow and sediments are impacting the nitrogen loading and routing. Since adjustment of sediment and nutrient parameters can alter model hydrological predictions, the calibration processes is iterative, with a return to each successive step of the calibration processes to verify that calibrated flow, sediment, and nutrients remain in line with observed values (Figure 13).

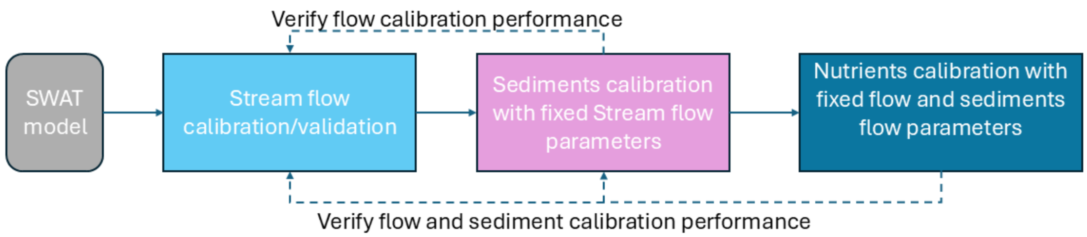

Figure 13: SWAT Calibration Workflow — Streamflow, Sediment, and Nutrient Calibration with Performance Verification

The sensitivity analysis found the model was sensitive to Curve number (CN2), Soil evaporation compensation factor (ESCO), available water capacity of the soil layer (SOL_AWC), hydraulic conductivity and Manning's n in the main channel (CH_N2 and CH_K2 parameters). These are the most common sensitive parameters found across various SWAT watershed models (Marin et al., 2020). The parameters and ranges used in calibration are summarized in Table 6 and grouped based on the physical process they represent as mentioned earlier in section 3.4. Parameters were selected based on their reported sensitivity in SWAT applications in Kansas and similar agricultural watersheds (Marin et al., 2020; Sinnathamby, 2014; Sheshukov et al., 2011; Arnold et al., 2012), with parameter ranges defined following SWAT model documentation and standard values reported in the literature.

Table 6: SWAT Calibration parameters and Ranges Used for Streamflow Calibration in this Study.

Parameter	Description	Range	Source
Surface Runoff			
CN2	SCS Curve Number	-0.2 to 0.2	a, b, c,d
SURLAG	Surface runoff lag time	0.05 to 10	a,b,c,d
OV_N	Manning's "n" value for overland flow	0.01 to 0.5	a,d
Soil Water / Evapotranspiration			

SOL_AWC	Available water capacity of the soil layer	-0.25 to 0.25	a,c,d
ESCO	Soil evaporation compensation factor	0 to 1	a,b,c,d
EPCO	Plant uptake compensation factor	0 to 1	a,b,c,d
Groundwater			
ALPHA_BF	Base flow alpha factor (1/days)	0 to 1	a, b, c,d
GW_DELAY	Groundwater delay time (days)	0 to 500	a, b, c,d
GWQMN	Threshold depth of water in shallow aquifer required for return flow to occur [mm]	0 to 5000	a, c,d
GW_REVAP	Groundwater ”revap” coefficient	0.02 to 0.2	a, c,d
REVAPMN	Threshold depth shallow aquifer water for ”revap” to occur [mm]	0 to 1000	a, c
RCHRG_DP	Deep aquifer percolation fraction	0 to 1	a,b,c,d
Channel Routing			
CH_N2	Manning’s ”n” value for the main channel	0 to 0.15	a,d
CH_K2	Effective hydraulic conductivity in main channel	0 to 150	a,d
ALPHA_BNK	Baseflow alpha factor for bank storage	0 to 1	a,d
Snowmelt			
SMFMN	Maximum melt rate for snow during year	0 to 10	a,c
SMTMP	Snow melt base temperature	-5 to 5	c,d
SMFMX	Maximum melt rate for snow during year	0 to 10	a,c
TIMP	Snowpack temperature lag factor	0 to 1	c

a Marin et al., 2020; b Sinnathamby, 2014; c Sheshukov et al., 2011; d Arnold et al., 2012

In Table 6, A through D indicates studies reporting use of this parameter in SWAT calibration for Kansas or similar agricultural watersheds.

The calibration requires sets of objective functions which can be used to evaluate the performance of the simulation against the observed data. In the case of SWAT-CUP there are various calibration algorithms used like SUFI- 2 (Sequential Uncertainty Fitting version 2), PSO (Particle Swarm Optimization), GLUE (Generalized Likelihood Uncertainty Estimation) and others. SUFI-2 is one of the most used algorithms (K.C Abbaspour, 2015). There are various model evaluation statistics, such as i.e. Coefficient of Determination (R^2), Pearson Correlation

Coefficient (r), Nash-Sutcliffe efficiency (NSE), Percent bias (PBIAS), Percent Model Error (PME) and Percent Error ($P_{e)}$. In this study, the NSE was used as the main objective function to evaluate the model performance. In addition, the error index Percent bias (PBIAS) and R^2 were used to support the calibration process. The main objective NSE (eq 9) has a range of -∞ to 1, where Q_{i_obs} is the ith observation, and Q_{i_sim} is the corresponding simulated observation, and Q_{mean} is the mean of the observed data. An NSE of 1 depicts the best fit, though an NSE of around 0.5 or higher is considered satisfactory and greater than 0.75 as very good (Moriasi *et al.* 2007). PBIAS (eq. 10) was used to determine the tendency of the simulated data to be lower or higher as compared to observed and has an acceptable range of within ±10% for very good and within ±25% is considered satisfactory for streamflow.

$$NSE = 1 - \frac{\sum_{i=1}^{n}\left(Q_{i_{obs}} - Q_{i_{sim}}\right)^2}{\sum_{i=1}^{n}\left(Q_{i_{obs}} - Q_{mean}\right)^2} \tag{9}$$

$$PBIAS = \frac{\sum_{i=1}^{n}\left(Q_{i\_obs} - Q_{i\_sim}\right) * 100}{\sum_{i=1}^{n}(Q_{i\_obs})} \tag{10}$$

In addition to calibration against streamflow, sediment, and nutrient observations simulated crop yield was compared against independent county level data on HRU level to determine the model behavior. Average annual yield value for corn and soybean HRUs were obtained from the model and compared, on an area-weighted basis, against county yield statistics from USDA NASS Quick Stats (Jackson County, 2005-2019). This comparison evaluates the internal, land-use-specific representation of the model in addition to the hydrology and nutrients.

3.9 Model Scenarios

Once the SWAT existing condition model was developed, the model was run for different scenarios to determine the response of the system for various BMP and climate conditions. This study focused on reducing the impact of water quality impediments and understanding the resiliency of the system. In consultation with the Tribe and Vireo, the following BMPs were considered.

Filter Strips- These are narrow bands of grasses, legumes and forbs used to limit sediments and nutrients flowing into the stream or water bodies. They act on sheet flow slowing down the velocities of flow. They are located immediately next to the croplands or parallel to the streams. These are one of the most efficient measures used in agriculture and pasture dominated land use areas (Liu et al.,2017; Ramiao et al.,2022; Parajuli et al.,2008).

No Till - The agricultural land is not tilled before planting using specialized equipment to sow the seeds to minimize the soil disturbance (USDA Climate Hubs).

Regenerative Farming- This is an emerging approach towards land management where all aspects of agriculture are connected through a web of networks requiring a holistic and sustainable approach. The SWAT model has no module to apply regenerative farming as a BMP. A reduction in CN by 10% was assumed for farmlands where regenerative agriculture is undertaken as studies have shown regenerative practices to improve infiltration and hydraulic conductivity (Smith, 2016; Sittig and Sur, 2024). This assumption is a single parameter adjustment of CN, and it does not capture other parameters associated with RA, such as change in soil organic matter, soil structure development, or surface roughness associated with vegetation cover in between cash crops. The results from this scenario shows the modeled effects of 10% CN reduction, rather than the complete representation of regenerative agriculture hydrologic and water quality impacts.

A total of 12 scenarios (Table 7) were developed which consisted of BMPs and an area of application, i.e. on land maintained by PBPN and non-PBPN farmers within the PBPN region. Additional details describing scenario implementation in SWAT are provided in Appendix X.

Table 7: Scenarios Developed for Analysis

Scenarios	Description
S1	Filter strips applied only to crop lands in the PBPN reservation area.
S2	Filter Strips applied to crops and rangeland/pasture in the PBPN reservation area.
S3	Filter strips applied only to crop lands held by the tribal community.
S4	All the conditions of S1 i.e. filter strips and no till operation
S5	All the conditions of S2 i.e. filter strips for crop and range land along with no till operation.
S6	Only no till with no filter strips or other BMPs
S7	Only no till applied to crop lands owned by PBPN
S8	Regenerative Agriculture applied to all crop land in study area along the creek
S9	Regenerative Agriculture practice along with filter strip added to PBPN owned land only
S10	Regenerative Agriculture and no till practice applied to PBPN owned lands
S11	All the crop lands undertook regenerative and no till practices.
S12	All the PBPN owned land had regenerative agriculture and no till applied and only part of non PBPN owned land (with Corn landuse) had filter strip added as BMP.
B1	Filter strips added to rangeland and pastureland owned by the tribal community
B2	Filter strips added to all rangeland and pastureland in the PBPN reservation area
R1	Reservoir supplying only the domestic water demand.
R2	Reservoir supplying irrigation water for corn and soybean production.
R3	Reservoir supplying 50% of the irrigation demand for corn and soybean production.

Stream reaches delineated in the SWAT model that fell primarily within the PBPN boundaries were identified for assessing existing baseline conditions and watershed scenarios S1 through S12. Since some reaches were not within the PBPN boundaries, an assumption was made that reaches which had more than 50% of its respective sub-basins within the PBPN region would be representative of hydrologic and water quality responses to watershed scenarios and were selected for the analysis. As a result, nine basins (2, 4, 5, 6, 7, 8, 9, 10 and 12) were selected as shown in Figure 14.

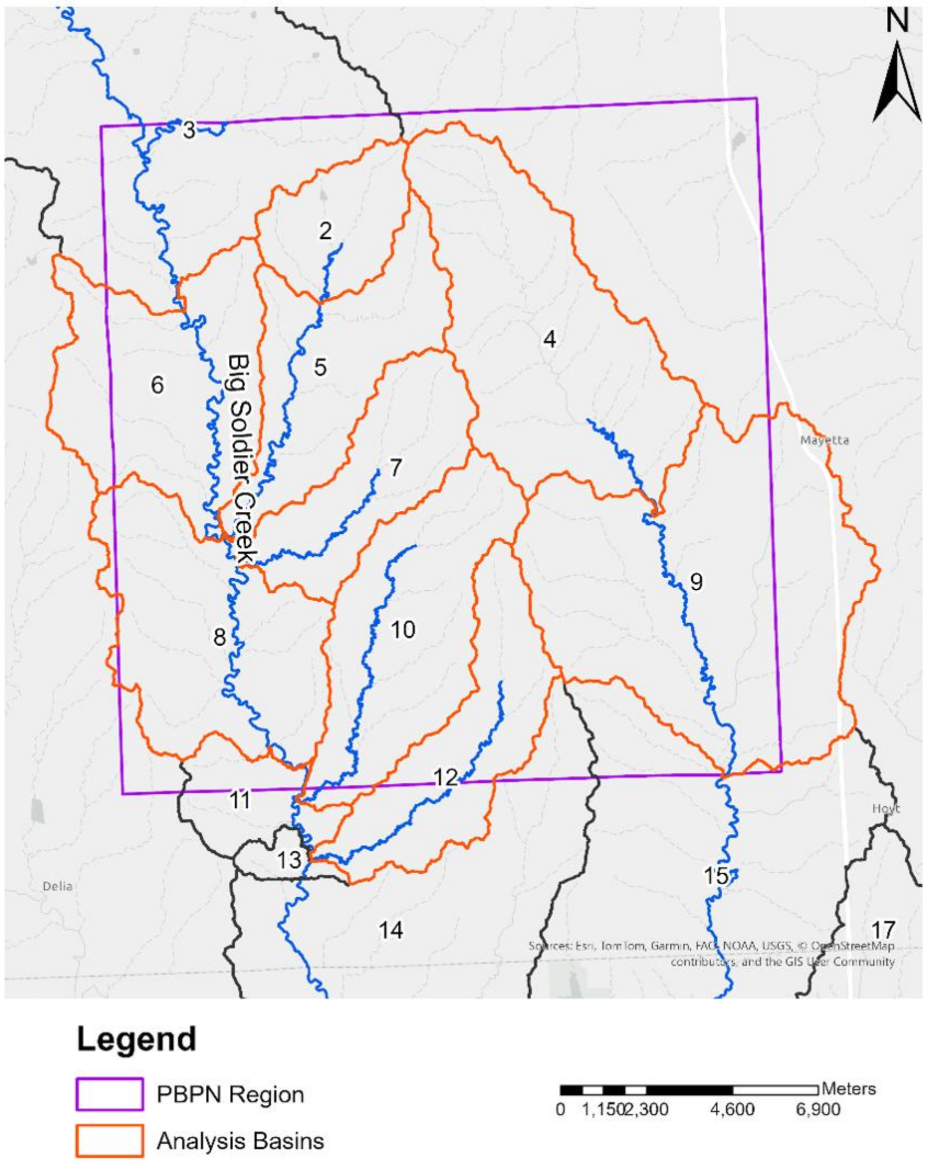

Figure 14: Focus Sub Watersheds Within PBPN

Chapter 4 - Results and Discussion

4.1 Calibration and Validation

The uncalibrated model had a low NSE of 0.22 for monthly streamflow at the Topeka USGS gauge for the simulated period between 2000-2019, before any parameter adjustment or changes. On analysis, it was determined that the usage of one weather gage located south of the watershed near Topeka was a major factor impacting the performance of the model. Similar studies have shown that model performance improves significantly when spatially distributed rainfall data are used instead of relying on a single gage. Because SWAT is a semi-distributed model that aggregates processes within sub-basins and HRUs, its streamflow simulations are highly sensitive to how precipitation inputs are represented in space; consistent with this, Xue et al. (2018) and Chordia et al. (2022) both show that different spatially distributed precipitation datasets and interpolation approaches lead to substantial differences in SWAT runoff performance, particularly in basins with heterogeneous rainfall. Their findings emphasized that incorporating more spatially representative precipitation inputs can enhance the accuracy of hydrological simulations, particularly in regions with heterogeneous rainfall patterns. To incorporate the spatial variability in rainfall the Daymet dataset, which is continuous gridded rainfall product at 1 km*1 km, was used. These data are derived from ground-based observations using statistical interpolation and are widely used in ecological, agricultural, and climate modeling (Thorton et al.,2020). Gridded data was downloaded for each sub-basin based on the centroid of each sub-basin spatially. These gridded precipitation data were used in addition to local weather gage data in the model. Muche et al. (2020) had found that a combination of gridded precipitation sources with local gauge measured data improved hydrological performance in agricultural watersheds in Kansas. The PBPN SWAT model was run using the combination of gridded dataset and local gauge station, followed by hydrologic calibration.

SWAT-CUP was used to calibrate and validate the model. The calibration period was taken from 1/1/2005 to 12/31/2012 and the validation period covered 1/1/2013 to 12/31/2019. The calibration period encompassed a range of hydrologic conditions, including relatively wet period from 2007 to 2009 and the extreme drought year of 2012 (Line et al., 2017). A monthly step was used for calibration. To better represent the model, calibration was carried out at both the Delia gage, which is downstream of PBPN, and the Topeka gage, which is near the outlet of the Soldier Creek watershed. The parameter ranges were defined as shown in table 6, and model was run for 1000 iterations in SWAT CUP. Once the best fit parameters were identified, the model was run for the validation period. NSE was used as a single objective function to calibrate the model. Table 8 shows that post calibration the NSE was above 0.7 for the gages.

Table 8: Model performance indicator for flow for the calibration period (2005 to 2012)

Objective Parameter	Calibration		Validation	
	Delia Location	Topeka Location	Delia Location	Topeka Location
NSE	0.7	0.8	0.89	0.81
R^2	0.71	0.81	0.91	0.85
PBIAS (%)	1.1	9.8	18.2	24.9
KGE	0.68	0.82	0.71	0.62

The objective function performance improved for validation period, which is further discussed later in this section.

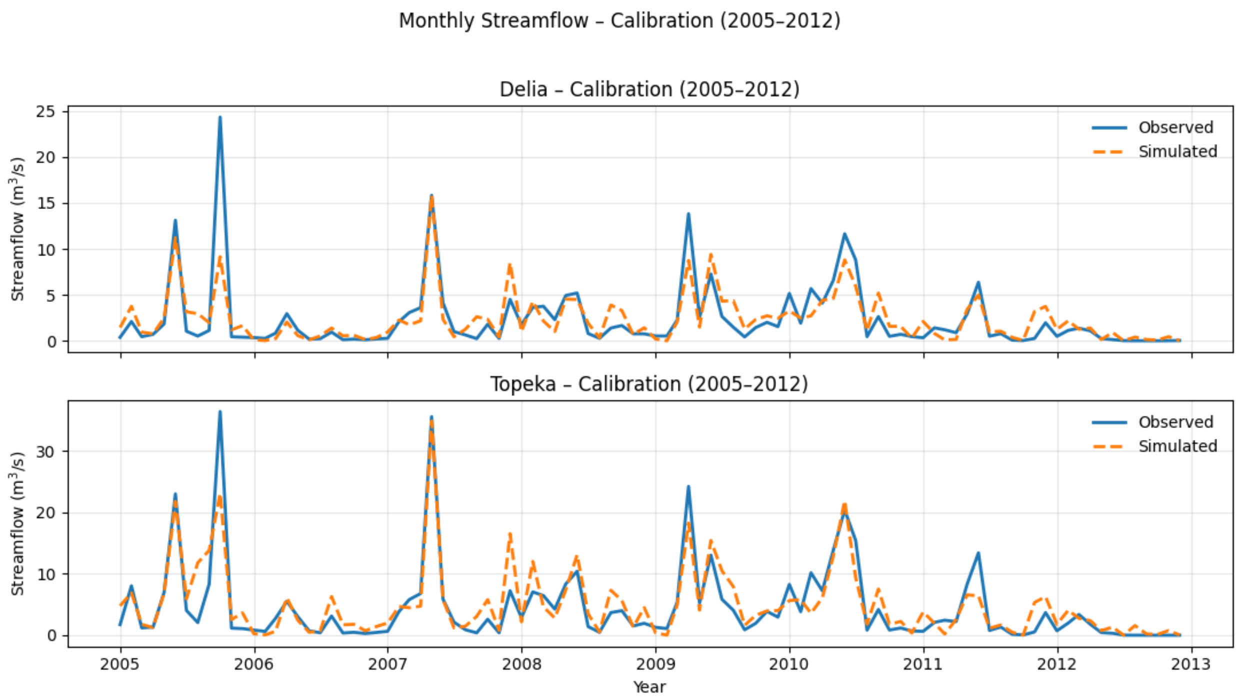

Figure 15: Observed and simulated discharges for Calibration period.

Figure 15 shows the comparison between the observed and simulated monthly flows for the calibration period at both Delia and Topeka locations. Some of the peaks during the wetter years of 2005 are underestimated but the model can better capture the high flow events in 2007. Post 2011, we can see the reduction in monthly flow caused by the drought. Overall, the model reliably represents the seasonal dynamics across a range of hydrologic conditions.

Calibrated models were validated for the period from 2013 to 2019. As seen in figure 16, the validation period was hydrologically wetter compared to the calibration period. Most of the peak flows were captured by the model though we see some overestimation of flows during 2013-2015. In terms of objective function, NSE was approximately 0.89 at Delia and 0.81 at Topeka, which is better than the calibration event. One of the reasons for better performance maybe the hydrologically smoother (that is, less variable) time period compared to the calibration period. In later years, including 2018 and 2019, which contain a mix of high flow and recession periods, the model tracked the observed trends. This shows the calibrated parameters that can be adopted into the model and are suitable for subsequent Best Management Practices (BMP) and climate resilience analysis.

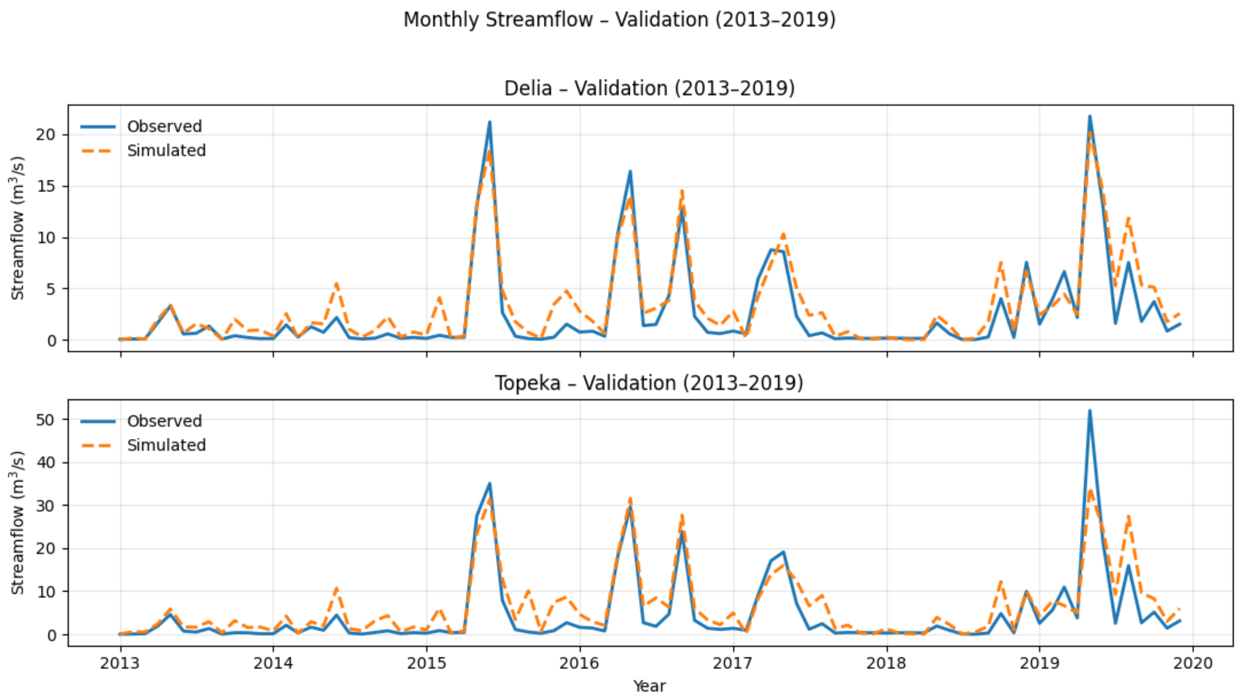

Figure 16: Observed and simulated discharge for Validation Period

The fitted parameters are provided in table 9. Curve Number (CN2) was the most sensitive parameter followed by Baseflow alpha factor for bank storage (ALPHA_BNK), soil evaporation compensation factor (ESCO), available water capacity (SOL_AWC), and channel hydraulic conductivity (CH_K2). These five parameters showed high t-stat values (>10) and statistically significant p-values (<0.05).

Table 9: Fitted parameters post Calibration and Validation applied to all sub-basins in the model.

Parameter No.	Parameters	Fitted Value
Surface Runoff		
1	CN2.mgt (relative)	0.0498
2	OV_N.hru	0.0377
3	SURLAG.bsn	2.781
Soil Water / Evapotranspiration		
4	SOL_AWC.sol (relative)	−0.2268

5	ESCO.hru	0.7955
6	EPCO.hru	0.8025
Groundwater		
7	ALPHA_BF.gw	0.5525
8	GW_DELAY.gw (days)	10.25
9	RCHRG_DP.gw	0.4635
10	REVAPMN.gw (mm)	187.75
11	GW_REVAP.gw	0.0338
12	GWQMN.gw (mm)	637.5
Channel Routing		
13	ALPHA_BNK.rte	0.2575
14	CH_N2.rte	0.1045
15	CH_K2.rte (mm/hr)	6.075
Snowmelt		
16	SFTMP.bsn (°C)	0.825
17	SMFMX.bsn	3.49
18	TIMP.bsn	0.1205
19	SMFMN.bsn	4.44

Sheshukov et al. (2011) calibrated a SWAT model for the same Soldier Creek watershed against daily streamflow at the watershed outlet near Topeka (USGS 06889500) for a 16-year period (1983–1999). Their reported statistics were R^2 = 0.56, NSE = 0.56, and PBIAS = 5.7% at the daily time step; R^2 = 0.74, NSE = 0.73, and PBIAS = 5.8% at the monthly time step; and R^2 = 0.88, NSE = 0.84, and PBIAS = 5.7% at the annual time step. The present model calibrated (2005–2012) and validated (2013–2019) at a monthly time step at the same Topeka location, produced comparable results: NSE = 0.8, R^2 = 0.81, and PBIAS = 9.8% during calibration, and NSE = 0.81, R^2 = 0.85, and PBIAS = 24.9% during validation. The outlet of PBPN boundary i.e. Delia gauge, an additional calibration/validation location in present model, was not included in the 2011 study. These results support that the model's performance is in line with prior SWAT applications in this watershed.

The model was next calibrated for water quality parameters. Sediment data in Soldier Creek was sparse, highly variable, and few samples were collected over the period. To address the lack of continuous measurement a sediment rating curve was developed using the best-practice methodology mentioned in HEC-RAS Sediment Transport User Manual (USACE_HEC, 2023). Discrete sediment samples were paired with concurrent streamflow measurements to establish the relationship between discharge and sediment concentration. Piecewise linear interpolation was applied between the observed sample in logarithmic space to avoid overfitting the sparse dataset and reduce bias associated with log-transformed regression models. Sediment calibration was performed at monitoring station locations SC03 and SC07 (Figure 10) using the rating curve method. Because the continuous flow was not available at the measurement location, the discharge was estimated using drainage-area ratio method i.e. measured flow from Delia gage was scaled to the SC03 and SC07 locations based on contributing drainage area.

Discrete sediment observations at each location were used to develop bias corrected sediment rating curve using Equation 11.

$$Q_s = E \cdot a \cdot Q^b \tag{11}$$

Where Q_s is the sediment load in tons, Q is the stream discharge in cfs, E is the bias correction factor and a, and b are the power exponential coefficient of the rating curve. The bias correction factor E was calculated using the smearing estimator (Duan, 1983), defined as the mean of the antilogged residuals from the log-space regression. Calculated value of E was 1.19 for SC03 and 1.4 SC07. Values for the coefficients a and b are shown in figure 17. The sediment loads derived from the rating curve were aggregated to monthly totals and used to calibrate the simulated loads in SWAT-CUP.

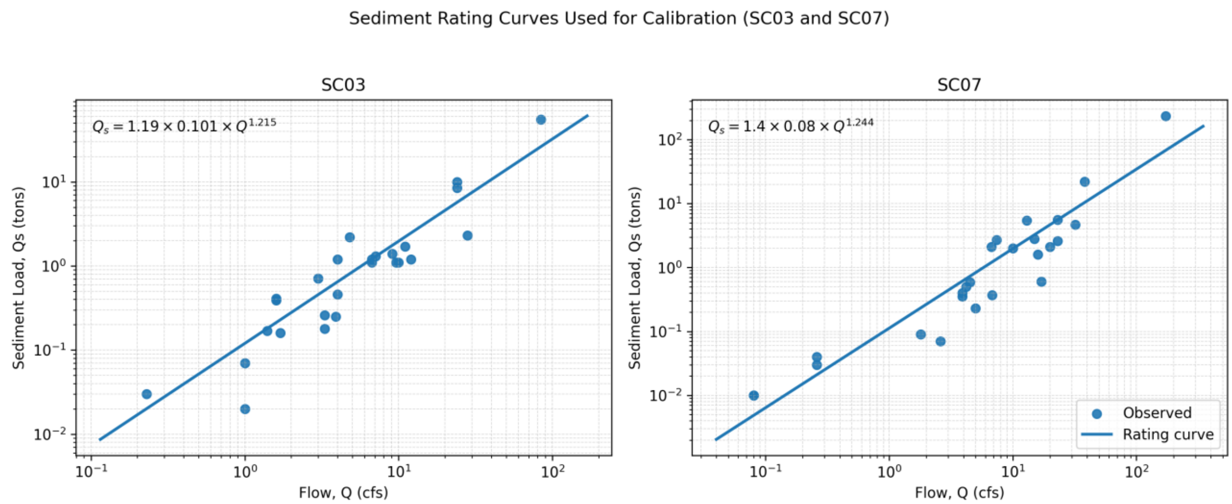

Figure 17: Observed sediment loads and fitted power-law sediment rating curves for SC03 and SC07

The calibration and validation were done for sediments with 500 iterations over a defined range of parameter values in SWAT CUP. Figure 18 shows the comparison between the observed and simulated monthly sediment loads. At SC03, the model had an NSE of 0.47 and R^2 of 0.49 for calibration and NSE of 0.52 with R^2 of 0.68, showing moderate agreement with simulated and observed monthly loads. However, PBIAS was around 4.31% for calibration and 30.17% for validation, indicating overestimation of loads. In the case of SC07, NSE was 0.77 and R^2 was 0.82 in the calibration period, which shows a good fit between the observed and simulated values. PBIAS was -14.8% showing slight underprediction. Validation at SC07 showed a slightly lower NSE of 0.63 and R^2 of 0.6 with PBIAS of 13.06%. This may be due to better representation of flows in the rating curve-derived sediment load calculation as the SC07 monitoring station location is nearer to the Delia streamflow gage.

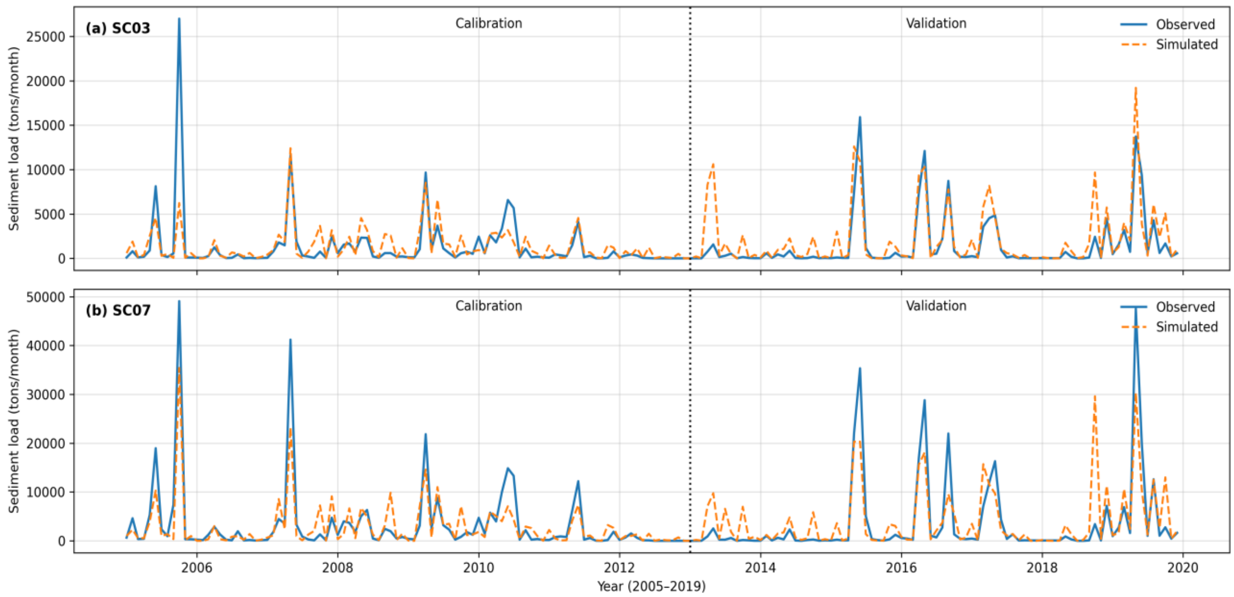

Figure 18: Comparison of observed and model simulate sediment loads.

The range of parameters used for calibration and best fitted parameter is provided in Table 10 which were obtained from SWAT manual and literature (Brighenti et al.,2018; Abbaspour et al.,2015) and grouped into different physical processes they represent (Section 3.4). Values which were changed on a relative basis are noted with the parameter name. Some of the critical parameters adjusted were channel erosion, sediment routing and USLE based parameters reflecting the importance of channel and in-stream processes in controlling sediment transport within the watershed.

Table 10: Parameters used in sediments calibration and best fit values.

No.	Parameter (Change Type)	Min	Max	Best Fit
Erosion-MUSLE based				
1	HRU_SLP.hru (relative)	−0.20	0.2	−0.1476
2	USLE_P.mgt	0.2	0.7	0.6125
3	SLSUBBSN.hru (relative)	−0.20	0.2	−0.0476
4	USLE_K.sol (relative)	−0.20	0.2	−0.1516
5	USLE_P.mgt	0.1	0.5	0.102
6	USLE_C.plant.dat (relative)	−0.20	0.2	−0.0180

Channel Erosion / Geometry				
7	CH_COV1.rte	0	1	0.407
8	CH_COV2.rte	0	1	0.207
9	CH_W2.rte (relative)	−0.20	0.2	−0.0716
10	CH_S2.rte (relative)	−0.20	0.2	−0.0324
11	CH_ERODMO.rte	0	0.6	0.2982
Sediment Routing / Transport				
12	ADJ_PKR.bsn	0.5	2	0.9845
13	SPCON.bsn	0.0001	0.01	0.001021
14	SPEXP.bsn	1	1.5	1.3715
15	PRF.bsn	0	2	0.062

The observed grab samples for Total Phosphorus (TP) and Total Nitrogen (TN) obtained at SC03 and SC07 were converted to monthly loads using FLUX32 tool (Dipesh et al., 2022, Lencha et al., 2022, Minnesota Pollution Control Agency, 2013). A regression relationship was developed between the observed flow and concentration from the observed sample. Here, the observed values for location SC03 and SC07 were correlated with area-scaled daily flows from the Delia gage. Based on data availability, daily estimated monthly loads were developed from 2012-2019. The calibration was carried out in RSWAT (Nguyen et al,2022). A total of 700 simulations were run for both gages with the calibration period from 2012-2017 and validation from 2018-2019. In the case of TN, the average NSE for monthly calibration and validation across the two water quality monitoring stations was 0.62 and 0.65, respectively. TP had an average calibration NSE of 0.68 and validation NSE of 0.4. Some extreme events had a higher scaled observed loading value as seen in figure 19 caused by the higher flows and uncertainty in the regression model. With the data gaps and constraints, these simulated results and parameters were retained as the representation of existing condition. Table 11 provides the parameters used in calibrating the TN and TP at the SC03 and SC07 locations. The Phosphorus-related parameters considered in the TP load uncertainty analysis included those governing soil–water partitioning, plant uptake, sediment attachment, and fertilizer placement, namely PPERCO, PHOSKD, PSP, P_UPDIS and ERORGP. Nitrogen-related parameters included those controlling nitrate movement, uptake, denitrification, sediment association, initial soil and groundwater concentrations, and fertilizer placement, specifically NPERCO, N_UPDIS, SDNCO, CDN and ERORGN. Parameter sampling ranges were selected based on SWAT model documentation and values reported in previous SWAT-based watershed studies (Wallace et al, 2018;Abdullah et al, 2019).

Table 11: Parameters used in Total Nitrogen and Total Phosphorus calibration and best fit values.

No.	Parameter (absolute change)	Min	Max	Best Fit
Nitrogen				
1	SDNCO.bsn	0.5	1	0.98
2	CDN.bsn	0	3	0.2
3	CMN.bsn	0.0001	0.003	0.0009
4	ERORGN.hru	1	3	1.77
5	NPERCO.bsn	0	1	0.23
6	N_UPDIS.bsn	0	100	95.3
Phosphorus				
7	PPERCO.bsn	10	17.5	16.38
8	PHOSKD.bsn	100	200	101.31
9	PSP.bsn	0	0.7	0.16
10	P_UPDIS.bsn	0	100	85.03
11	ERORGP.hru	1	3	1.2

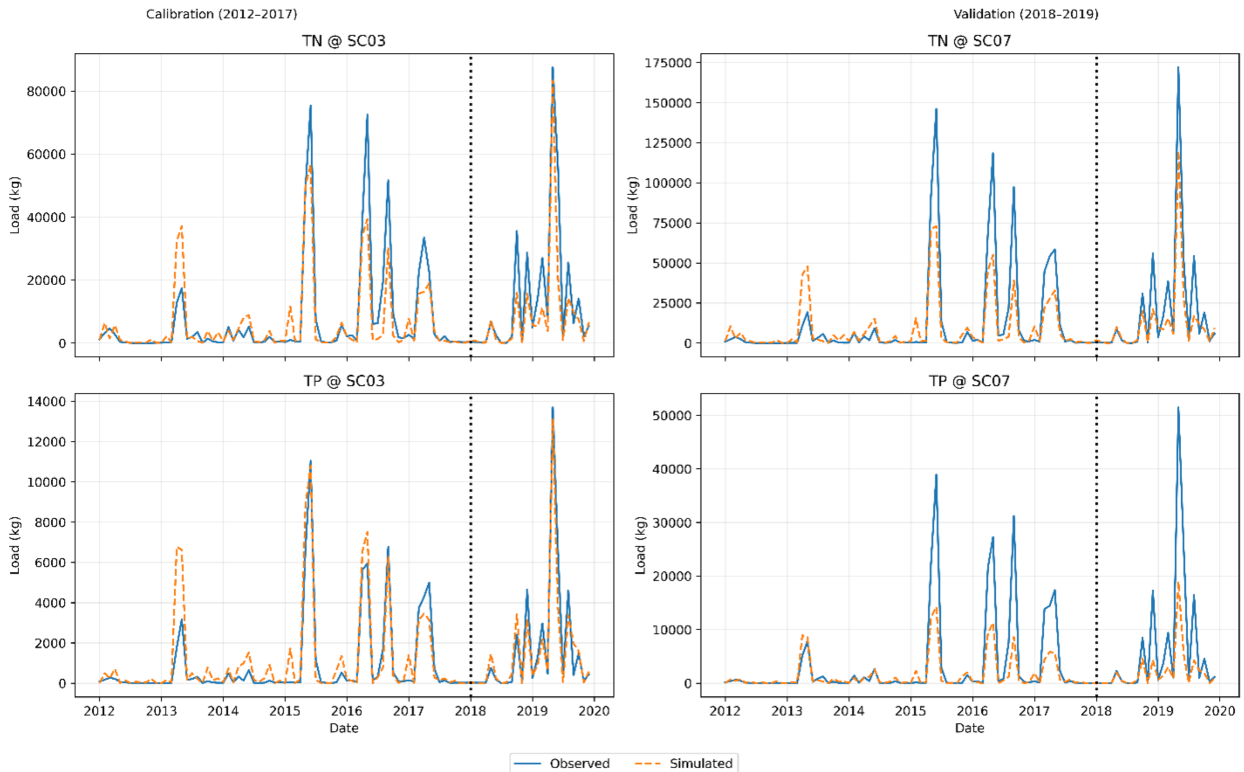

Figure 19: Calibration and validation for the monthly Total Nitrogen and Total Phosphorus loads.

The sediment and nutrient (TN/TP) calibration results have more uncertainty associated with them relative to streamflow calibration due to the limited amount of observed water quality data available in the watershed. A small number of grab samples for water quality data were collected over the study period and converted to continuous data using fitted rating curves (sediment) and flow concentration regression (TN/TP). This introduces two compounding sources of uncertainty, first by the sparsity of grab samples itself and additional uncertainty introduced by transforming those samples into continuous loads. This pattern is consistent with other SWAT water quality studies that derive their calibration targets from limited monitoring data and streamflow-dependent transformations (Wellen et al. 2014).

An additional spot check was undertaken to evaluate the land use specific output at HRU level against the regional productivity. Average annual crop yield and biomass were extracted from the model and compared against USDA NASS Jackson County yield statistics for cropland, and the USFS Rangeland Productivity dataset (USDA Forest Service) for rangeland. Both crop yield and rangeland productivity data were averaged over the period from 2005–2019. Simulated corn yield averaged 9.63 t/ha, which was within 10% of the NASS county average of 10.68 t/ha during wet years, indicating the model reasonably represents corn productivity despite plant growth parameters not being a calibration target. Simulated soybean yield averaged 1.96 t/ha, approximately 29% below the NASS average of 2.76 t/h. Both corn and soybean were modeled as non-irrigated, which can explain the reduction in yield. Simulated rangeland biomass averaged 7.06 t/ha, which was above the USFS Rangeland Productivity estimate of 4.14 t/ha (2005–2019 average). This over prediction in biomass for the rangeland growth parameters in the model is most likely caused by the rangeland growth parameters in the SWAT plant growth database

4.2 Best Management Practices Analysis

The aim of this study was to understand the impact of various BMPs on the water quality within the Tribal nation. As mentioned in the previous section three major mitigation pathways were chosen, i.e. addition of riparian buffer/filter strips along the areas near to the creek, no-till agriculture and regenerative agriculture. A relative reduction analysis was carried out to understand the impact of various BMPs on the project area.

4.2.1 Filter strips

In the model, filter strips were used to simulate the buffer strips along the farmland. The filter strips act a filter before the runoff leaves the field and trap sediments, nutrients and organic materials (Appendix B). In addition to this the flow velocity of the runoff is reduced, helping to reduce erosion downstream. If these strips are located along the river, they act like riparian buffer strips by treating the sheet flow into the Soldier Creek. Vegetative filter strips are represented in SWAT through the scheduled management operations (ops) file and are widely reported in the literature to significantly reduce sediment and nutrient transport from agricultural landscapes (White & Arnold, 2009[4-16]; Vigiak et al., 2016). Three scenarios were developed which varied from applying filter strips to all the croplands in the study area to specific tribal owned lands in the project region. Sediment loading reduction was predicted by 3-70%, with scenario S3 (filter strips added only to Tribal community owned crop lands), seeing a lower reduction in sediments. Scenario S2, that modeled filter strip added to both rangeland plus cropland, had more than 50% reduction on average for sediments. Figures 20 and 21 show the average annual loading reduction across the 12 reaches, identified with much of their drainage area in the PBPN boundaries.

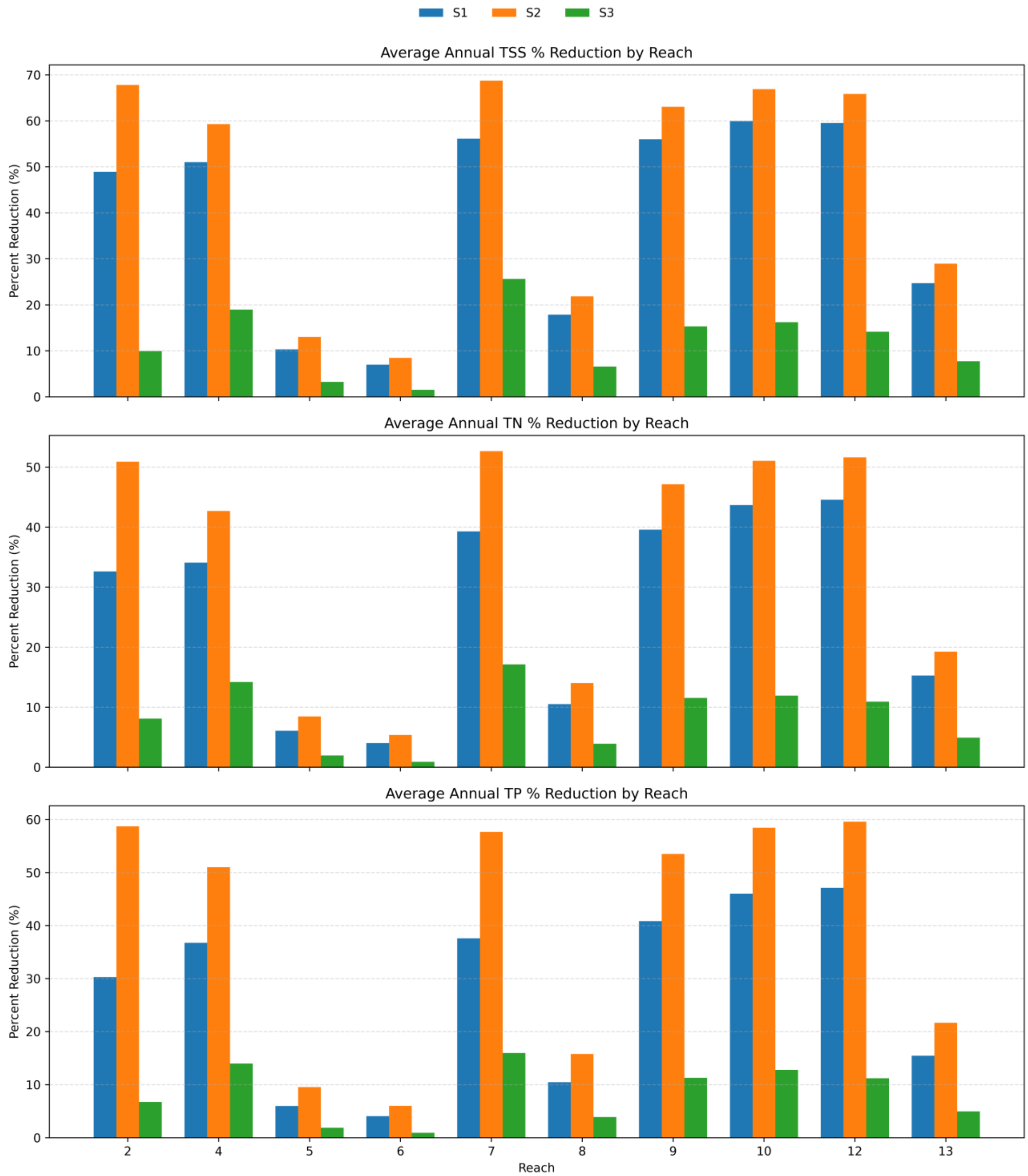

Figure 20: Reach level Simulated Sediment (top panel), TN (middle panel), and TP (bottom panel) load reduction with Filter Strips

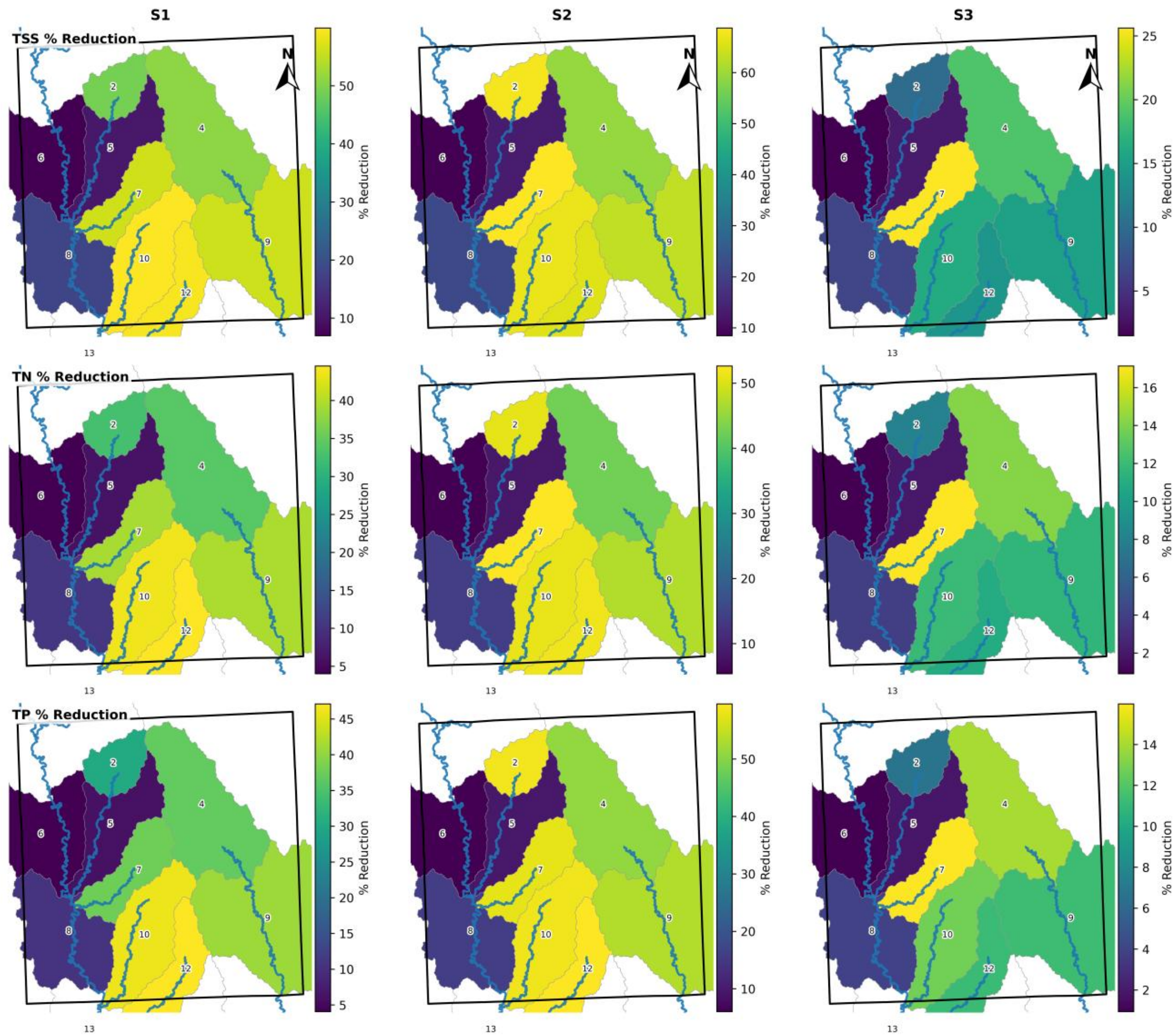

Figure 21: Basin level reduction in loading for total suspended sediments (top row), total nitrogen (middle row) and total phosphorus (bottom row)

The reduction in TSS, TN and TP loadings was relatively low in basins 5, 6, and 8 as these basins are impacted by incoming load from upstream basins limiting the benefit potential. The effective reduction at the outlet downstream of PBPN boundary on Big Soldier Creek, which is reach 13, includes the loading from upstream basins 2, 6, 5, 8, 10, 11 and 12, while Little Solider Creek is reach 9, which includes basins 4 and 9 contributing to it. The reduction for TSS at reach 13 was in the range of 7-24%, while TN and TP had a reduction between 4-15%. Out of three scenarios S2 had the most benefits as the filter strips were added to all the crops and range land (i.e., Tribal and non-tribal). We can see the overall impact reducing to less than 10% when BMPs are only included in farming areas owned by the tribe. In scenario S1, in which all crop lands in the study area had filter strips applied, had a higher reduction in sediments and nutrients, though its slightly lower than S2.

The overall reduction is similar to what other studies have recorded. At the field scale, sediment (TSS) reductions typically range between 40–85%, while total phosphorus (TP) reductions range from 30–70%, and total nitrogen (TN) reductions range from 20–60%, depending on strip width, slope, and vegetation density (Yuan et al, 2022, Kroll et al, 2019). However, at the watershed scale, overall load reductions were generally lower than predicted in previous studies (commonly 5–30%) due to partial implementation across HRUs and hydrologic connectivity effects (Gassman et al., 2007; White & Arnold, 2009).

4.2.2 Filter strips and No-Till operation

Tillage operations are usually carried out in the fall or early spring. Based on field data, cropping in the PBPN primarily follows the maize-soybean cropping cycles. Tillage operations and crop rotation were added to the management practices in the baseline SWAT model, and this was removed to simulate no-till farming. This reduced the sheet and wind erosion, improving the soil organic matter content. Scenarios S4 to S7 represent various combinations of no-till and filter strip operations. Combined BMPs, i.e. adding both filter strips with no-till operation for crop land and range lands, are represented by S4 and S5. Both these scenarios were predicted to have a higher reduction with TSS with a maximum reduction up to 75%, while TN and TP had an average reduction of approximately 33-38% across all reaches. This increase in percentage load reduction compared to previous scenarios S1 and S2 (filter strips only) can be explained by addition of no-till operations. To determine the impact of only no-Till operations, scenarios S6 and S7 were developed to represent conditions if only no-till was added to all the crop lands in the study area (S6) or only adopted in PBPN owned crop lands (S7). There was a limited reduction achieved: S6 achieved TSS reductions in the range of 3-20%, TN loading reduced by 1-12% and TP reduced by 1-15%. A further decline in load reductions was observed when no-till was applied only to PBPN owned land, where sediment was reduced by an average of 4% and nutrients loading reduced by 1-2%. This relatively small reduction in nutrient loads under no-till may reflect the lower adoption of the practice and effectiveness of no-till for reducing soil displacement and sediment-bound nutrient transport but not for capturing dissolved nutrients flowing through sheet flow (Merriman et al., 2019; Wu et al., 2022).

The relatively low sediment load reduction achieved by no-till only may reflect the influence of land slope on modeled sediment delivery. As discussed further in Section 4.2.4, sediment yield in Soldier Creek is slope-driven (lower slopes have lower yield compared to higher slopes);, and SWAT's no-till parameterization improves infiltration but does not change the slope-length-steepness factor in MUSLE, which remains one of the dominant erosion controls on steeper cropland. A study by Wu et al. (2022) found no till was least effective (3.18% reduction) in a slope-driven, highly erodible watershed, and Özcan et al. (2017), also reported negligible sediment reduction by no-till. In contrast, Ricci et al. (2020) found no till had better reduction in a setting controlled more by tillage condition than slope. The checkerboard pattern of land ownership further limits S7, since untreated non-PBPN cropland continues to deliver sediment to the same reaches. Finally, the gain in sediment reduction is diluted at the reach outlet by untreated upstream contributions and in-stream routing, for example, at the outlets of Subbasins 6 and 8.

Overall, no-till performed well when combined with other BMPs like filter strip in the watershed for load reduction as observed with other studies (Li et al., 2018; Parajuli et al., 2016).

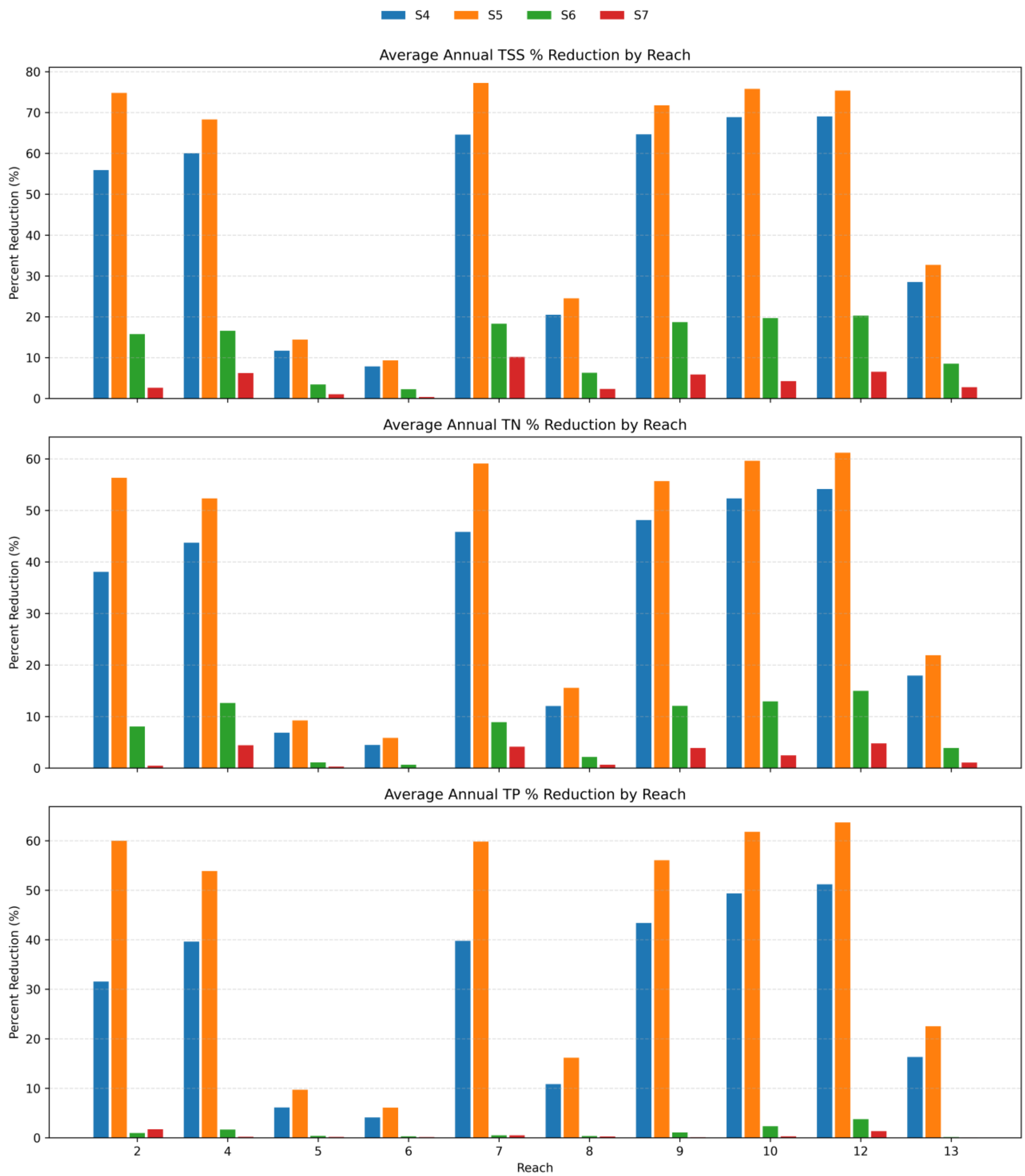

Figure 22: Reach level Simulated load reduction with Scenarios S4, S5, S6 and S7

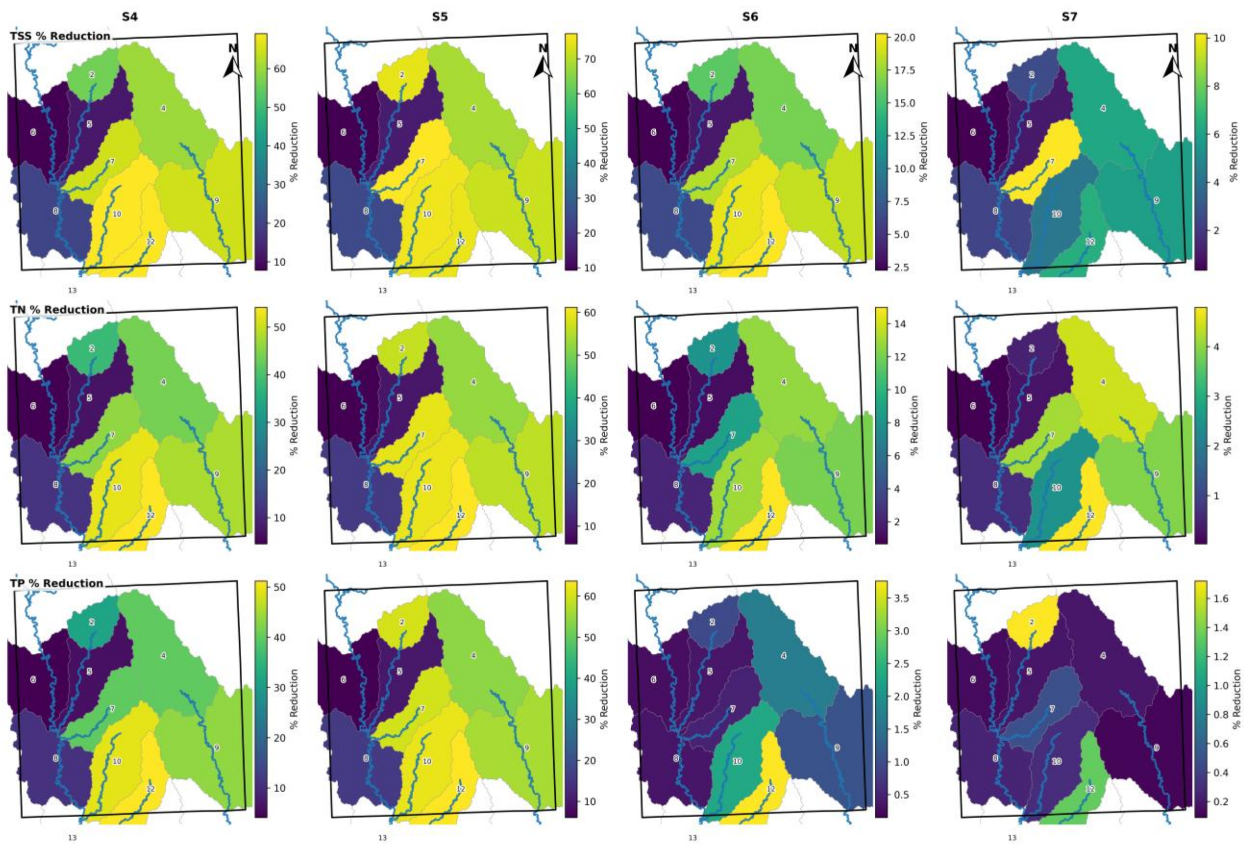

Figure 23: Relative percentage total suspended solids (top row), total nitrogen (middle row) and total phosphorus (bottom row) load reductions predicted with the combined No-Till and Filter Strop (S4 and S5) or No-Till only (S6 and S7) scenarios.

4.2.3 Regenerative Agriculture

Regenerative agriculture (RA) is an approach that's focused on improving soil health to improve ecosystem services and sustainable food production. RA is part of a strategy to help regenerate environmental, social and economic systems in agroecosystems (Schreeefel et al. 2020). There has been recent research showing the relationship between RA and reduction in runoff, with one study finding an increase in soil infiltration rate by 86-198% compared to their respective controls (Panta, 2025). In the case of the SWAT model, there is no module to replicate the RA; hence it was assumed that implementation of RA would reduce the CN by 10%, which in turn will reduce the runoff from agricultural lands. This reduction in CN was applied only to crop landuse in the study area. Because this single-parameter adjustment does not capture the full range of mechanisms associated with RA, the scenario results discussed below (S8-S12) should be interpreted as the modeled effects of this 10% CN reduction rather than a general characterization of regenerative agriculture's hydrologic impacts. The initial three RA scenarios represented RA applied to crop lands along the creek (S8), RA combined with filter strips added to PBPN owned land (S9), and RA combined with no-till practice for PBPN managed land (S10). To implement S8 in SWAT, a buffer of 500m was added around Solider and Little Soldier Creeks and crop land ownership in that area was analyzed (Figure 23). Only 40% of the floodplain cropping area is owned by the PBPN and around 60% of the cropping area is owned by non-tribal members.

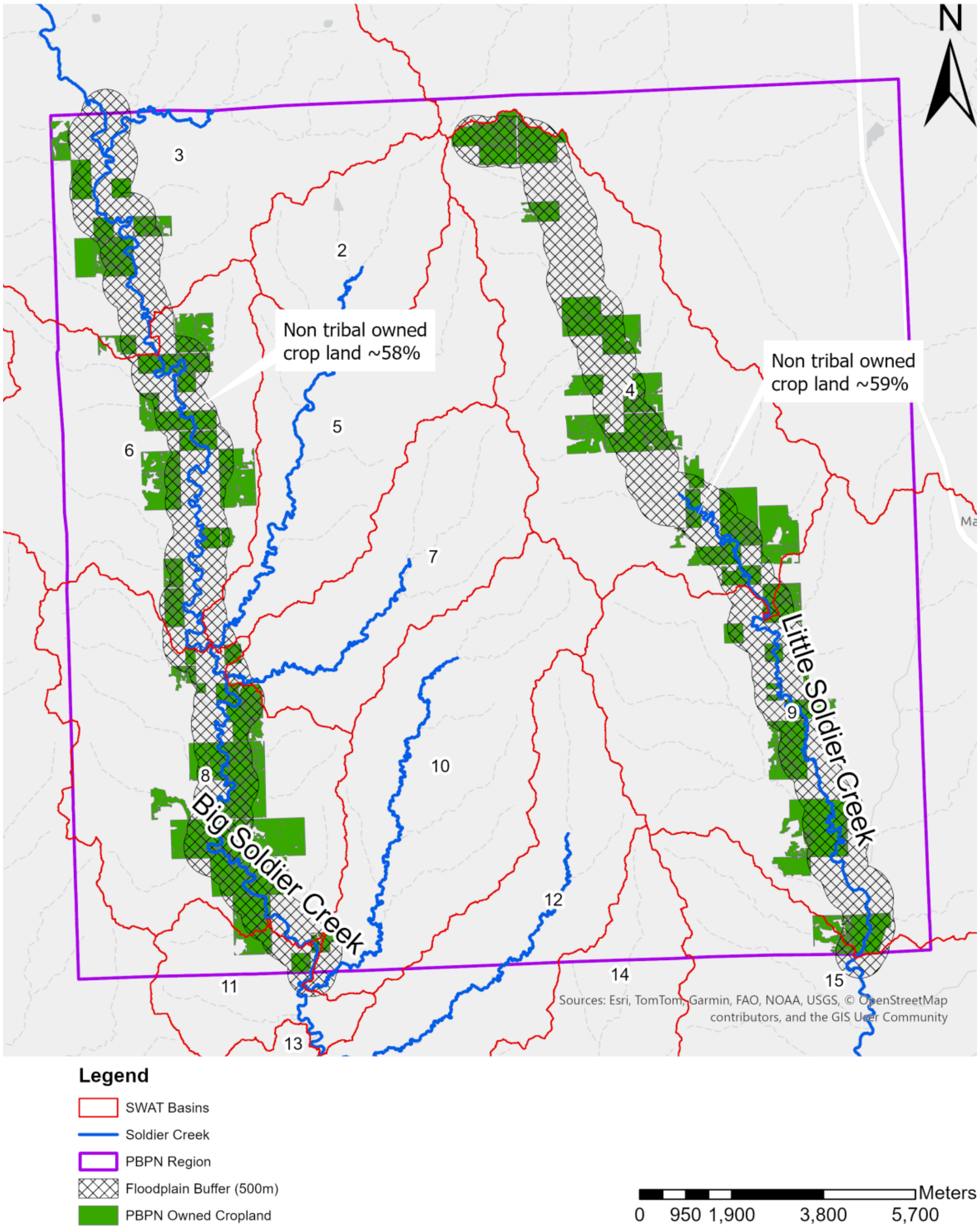

Figure 24: PBPN owned cropland in a 500-m riparian buffer area around Soldier and Little Soldier Creeks.

These scenarios were more conservative in nature by limiting the RA application to smaller areas in the study area. Comparing the scenarios, S8 and S9 had similar reduction benefits for sediments with an average reduction between 2-26%, while S8 had slightly higher reduction for TN and TP as compared to S9 (Figure 25). Applying RA across all cropping areas along the creek had a higher impact on nutrient reduction as a larger area cropland was covered in S8. The limited reduction seen in nutrients for S9 is due to limited area of BMP coverage in the tribal owned land. The combination of RA and no-Till applied to only PBPN owned lands resulted in the lowest reduction in sediments and nutrients. In a way, RA incorporates the no-till practice and benefits are mostly controlled by the runoff reduction from those basins.

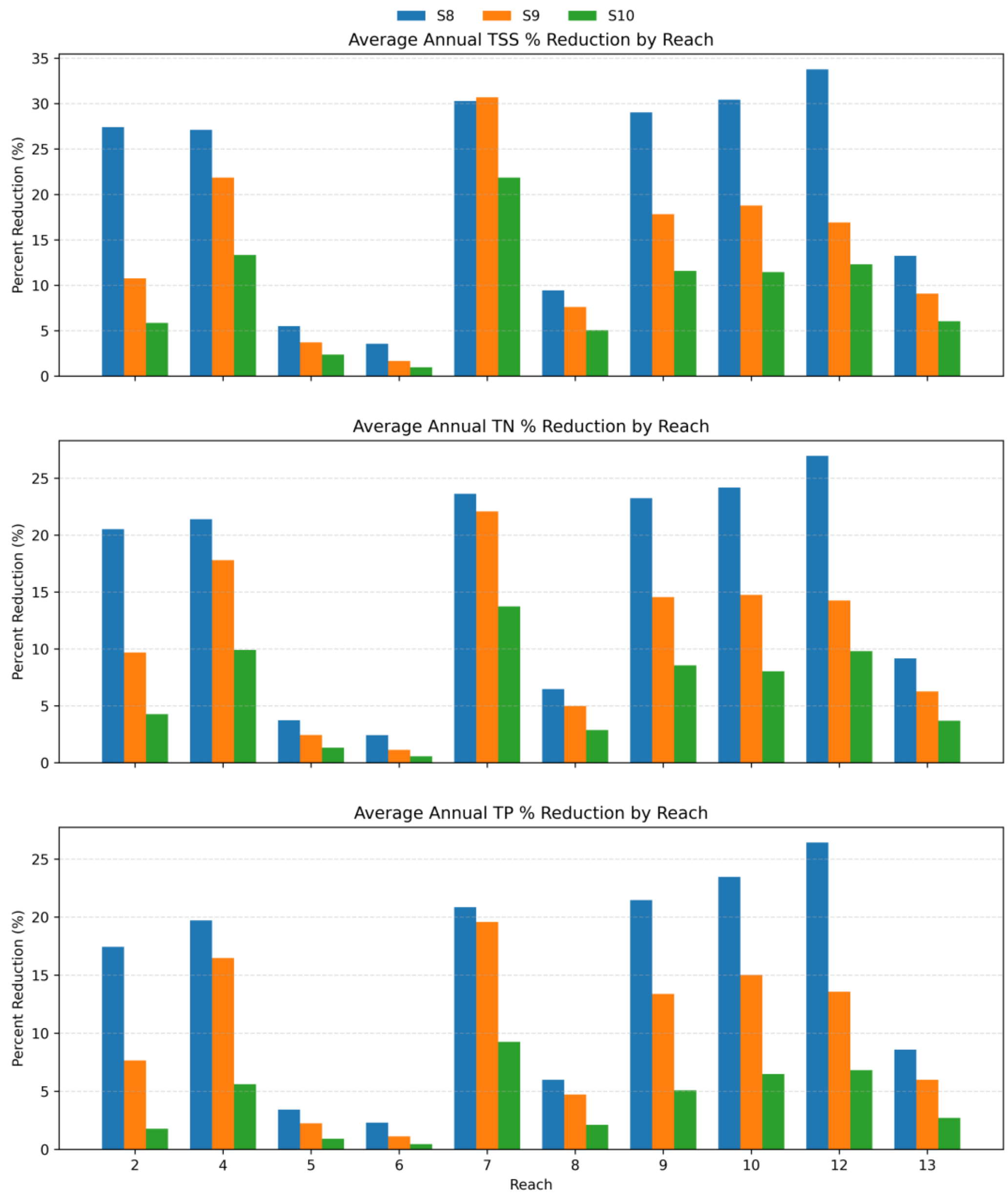

Figure 25: Average annual Load reductions in total suspended solids (top panel), total nitrogen (middle panel) and total phosphorus (bottom panel) for regenerative agricultural (RA) scenarios S8, S9, and S10.

Scenario S11 included RA across all the crop lands (tribal and non-tribal) in combination with no till practice. S12 was a hybrid approach with RA and no-till applied to PBPN owned cropland and filter strips applied to approximately 35% of privately owned cropland. Comparing these two scenarios as shown in Figure 26, S11 had an overall better reduction in loading for sediments (up to 46% versus 36% for S12), followed by TN, for which the maximum reduction was 34% for S11 (compared to 28% for S12), and TP for which loading reduced up to 27% in S11 and 24% in S12 This was expected due to a larger area adopting RA in S11 while the hybrid approach (S12) had more moderate reduction. Along Soldier Creek the sediment reduction was around 14% while nutrients were reduced by 7-10%. By contrast, Little Soldier Creek (reach 9) reductions of 25% for sediments and 15-20% for nutrients were achieved. One of the main factors for this difference was no upstream loading from other basins into the Little Soldier Creek basin.

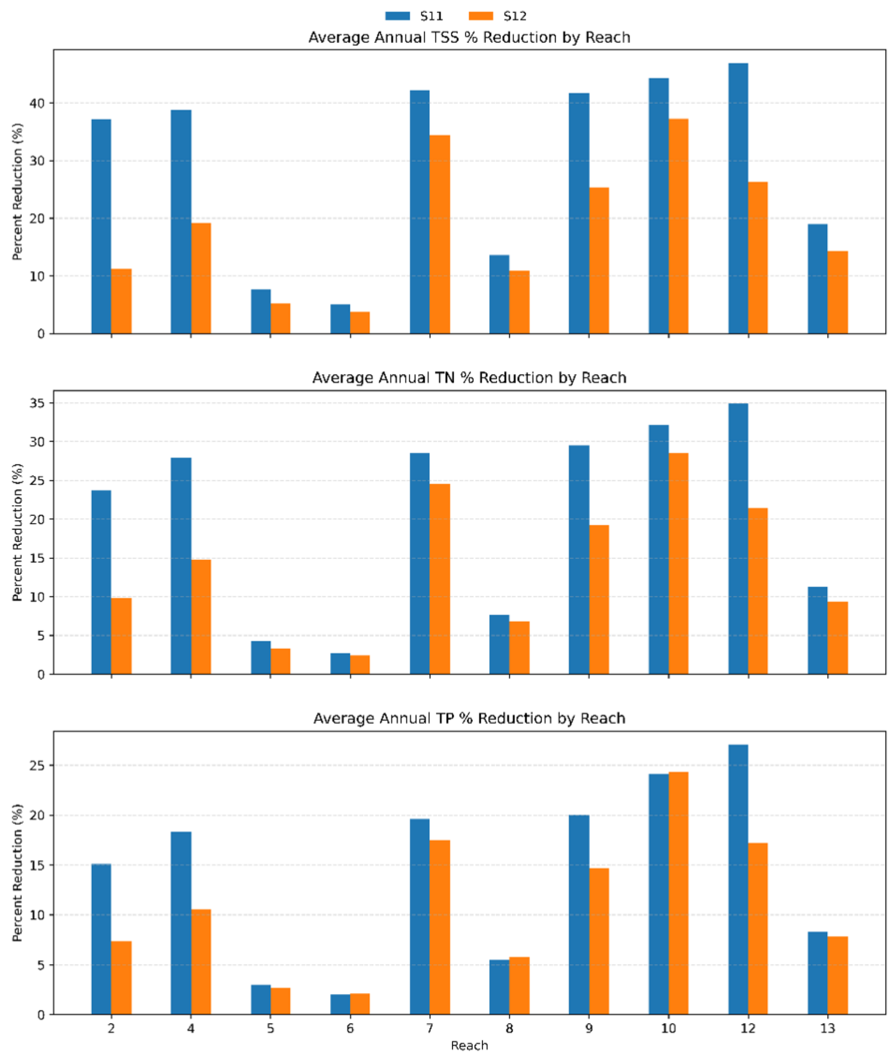

Figure 26: Reduction in sediments and nutrient loading for scenarios S11 and S12

Table 12 provides a summary of average annual loading for all scenarios at the outlet of PBPN boundary area for Soldier Creek (reach 13) and Little Soldier Creek (reach 9). Across three BMP approaches, filter strips resulted in the greatest reduction at the outlet for scenarios S2 and S3 with 15-28% reduction at reach 13 and 50-60% in reach 9. The higher reduction for Little Soldier Creek (reach 9) is likely due to its smaller watershed area, and the headwaters are completely within the PBPN area with no upstream loading present. For the scenarios where the application of BMPs were limited just to the cropland owned by the tribal community (Scenarios S3, S7, S9 and S10) the reduction effectiveness was much lower. The hybrid approach represented by S12 in which part of non-tribal landowners adopted BMPs along with all the PBPN owned land resulted in a reduction in pollutant loading in the range of around 8-15% at reach 13 and 15-25% at reach 9. Compounding impact of BMPs can be better realized when 30-40% of non-tribal owned cropland also incorporated the filter strips or RA in addition to all the PBPN owned crop land.

Table 12: Average Annual Sediment and Nutrient loading at Soldier Creek outlet (13) and Little Soldier Creek outlet (9) at PBPN

Reach	**9**	**13**	**9**	**13**	**9**	**13**
Scenario	**TSS (tons)**		**TN (kg)**		**TP (kg)**	
Existing	14242	40607	35479	131297	8432	31250
S1	6270	30572	21441	111237	4989	26418
S2	5260	28861	18759	106020	3921	24476
S3	12063	37468	31389	124834	7480	29697
S4	5031	29037	18409	107743	4773	26153
S5	4021	27327	15726	102537	3704	24212
S6	11582	37147	31194	126194	8341	31203
S7	13406	39492	34092	129887	8423	31279
S8	10107	35226	27235	119268	6621	28565
S9	11702	36920	30317	123066	7303	29376
S10	12592	38155	32444	126457	8002	30401
S11	8306	32916	24999	116462	6742	28657
S12	10631	34820	28649	118971	7190	28810

4.2.4 HRU Level Analysis

In SWAT, the loading is calculated at a Hydrologic Response Unit (HRU) level and aggregated to sub-basin level. In the WRAPS program for the Soldier Creek watershed, sediments were identified as a targeted impediment; therefore, additional analysis was undertaken at the HRU level to further understand sediment loading dynamics. An erosion rate of 5 tons/ha/year was considered as baseline based on the NRCS soil loss tolerance values (T-Values) (NRCS, 2017). In SWAT, sediment loading is determined using the Modified Universal Soil Loss Equation (MUSLE; Williams 1975). Slope length and steepness as well as surface runoff rates are among the factors that contribute to predicted sediment loads, with higher slopes resulting in quicker runoff and, in turn, higher sediment yields. Accordingly, slope was a determining factor in predicted sediment loads at the HRU level across the Soldier Creek watershed, with lower sloped fields (0-4%) producing an average annual sediment load of 4.47 tons/ha and fields with higher slopes (> 4%) producing up to 13.37 tons/ha/yr. Figure 27 shows the baseline annual average sediment yield below and above the 5 tons/ha baseline value at the HRU level for all crop lands and PBPN owned crop lands in the study region.

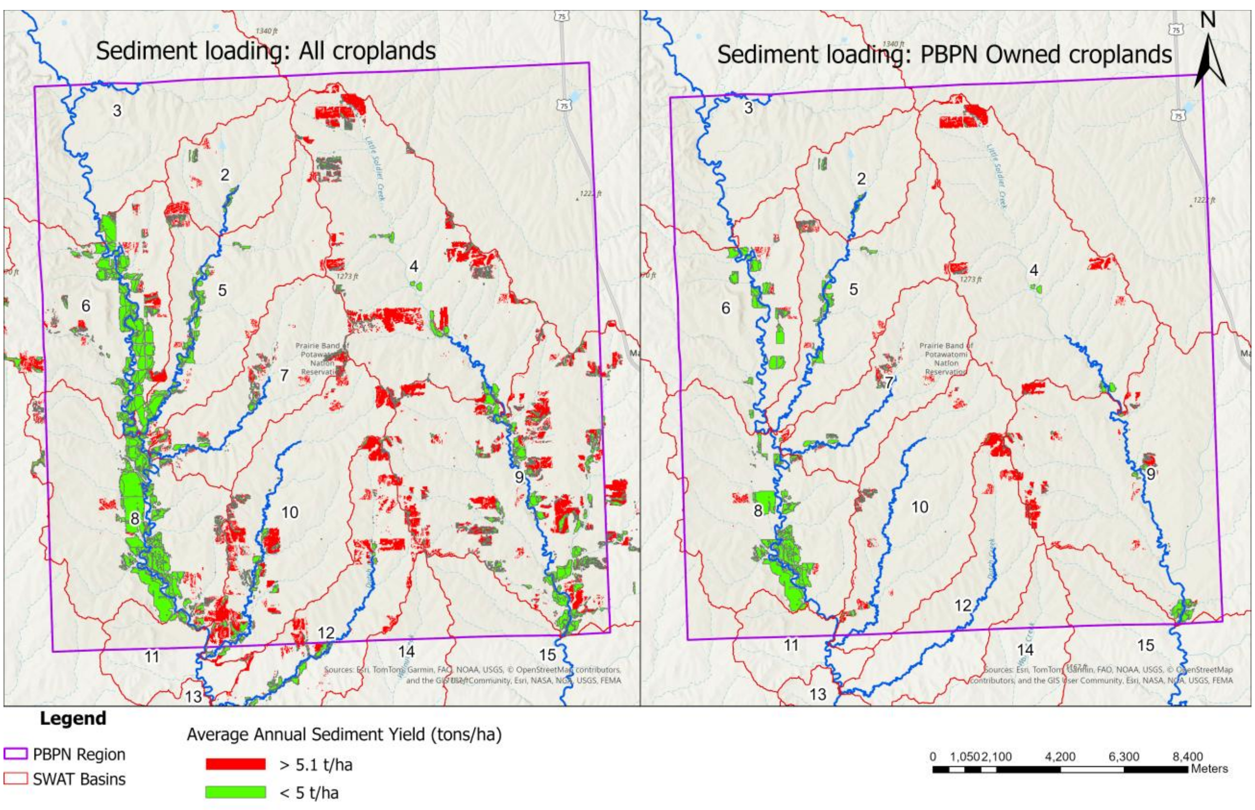

Figure 27: Baseline Average annual sediment yield from crop lands across study area.

The sediment yield from cropland HRU was reduced under the various management scenarios. The combination of filter strips and no till represented in scenarios S4 and S5 had the highest reduction, with predicted sediment yields from 97% of HRUs falling below 5tons/ha. Scenarios S1-S3, which used filter strips as BMPs at the field level, were the next most effective for mitigating sediment losses, with predicted sediment yield reduced below 5 tons/ha in approximately 82% of HRUs. In the case of scenarios S6 and S7, which applied no till management practices, a modest reduction in sediment yield was predicted compared to baseline/existing conditions. Applying regenerative agriculture practices as represented by scenarios S9-S12 resulted in a varying level of sediment yield reductions. Scenario S11, which represented adoption of RA in all croplands in the PBPN reservation area, resulted in 65% of HRUs with sediment yields below 5 tons/ha, while the hybrid approach represented by S12, in which RA practices were applied in all PBPN-owned cropland and corn only in non-tribal cropland, resulted in 52% of HRUs producing less than 5 tons/ha. Figure 28 represents this variation in sediment yield over various BMP scenarios.

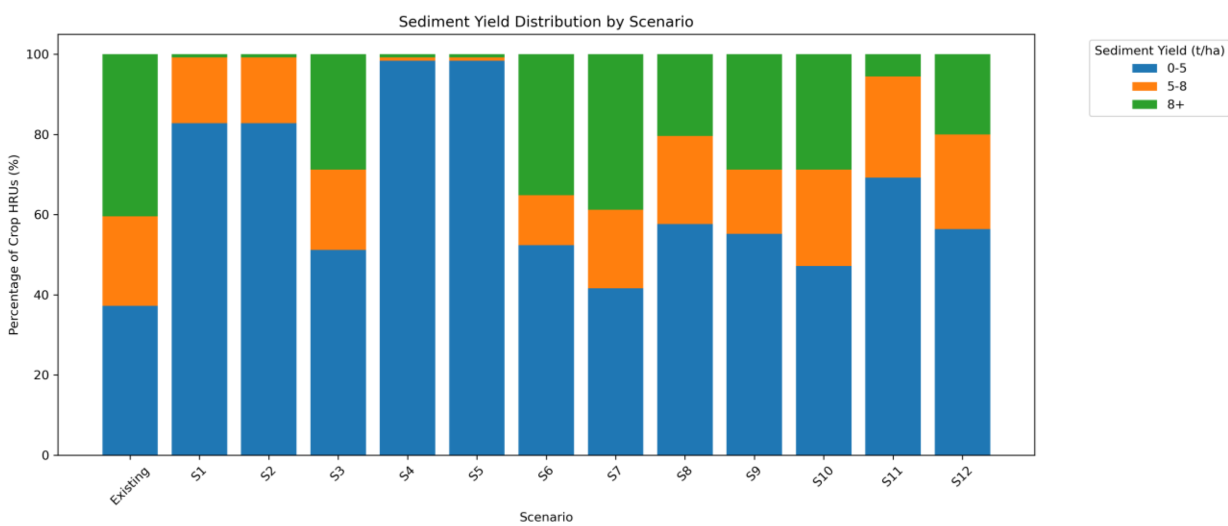

Figure 28: Distribution of Sediment Yield at the farmland level for various scenarios.

4.2.5 Bacteria Loading

A few historical water quality samplings done at Soldier Creek within the PBPN reservation area showed an elevated level of *E. coli* bacteria, with a median value of 260

MPN/100ml which was higher than EPA limit of 126 MPN/100ml. One of the contributors of bacterial loading is cattle grazing in the project area. Fecal deposition by the cattle on the pastureland will run off as sheet flow during precipitation events into the creek and introduce bacteria in the riparian ecosystem. Around 54% of the PBPN region is identified as either Grassland/Pasture based on NLCD data. Of this, roughly 45% is owned by the Tribe. To determine the potential reduction in the bacterial loading, grazing with cattle was simulated in the SWAT model and water treatment interventions were included. Two scenarios were developed, one with filter strips for the pasture region held by Tribal communities which is B1. The next scenario included filter strips applied for both tribal and non-tribal owned lands, B2. As expected, the reduction in B2 was higher than B1: reductions of up to 25% were predicted for reach 12 under B2 whereas the maximum reduction for scenario B1 was 12% in reach 10 (figure 29). This variation can be explained by the distribution of pastureland owned by tribal community and private land ownership across different reaches. Reach 9, which is the outlet for Little Soldier Creek, had predicted reductions of 7% and 20% for scenarios B1 and B2, respectively. So, in bacteria loading, the effectiveness of filter strips as a BMP is related to upstream loading into the watershed and distribution of pastureland within the reach.

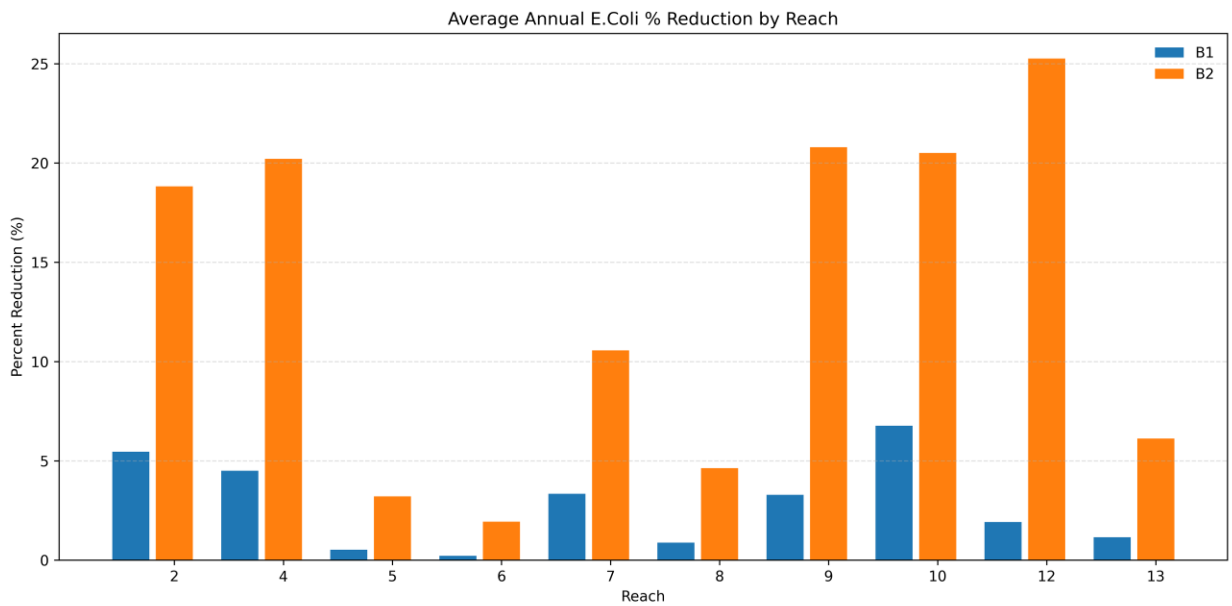

Figure 29: Average annual bacteria load reduction across reaches.

4.2.6 Reservoir

The primary source of drinking water for the PBPN is from the Banner Creek Reservoir which is located outside the reservation boundary. Currently, PBPN is exploring options for an emergency water supply lake, as identified by a Surface Water Management Study commissioned by PBPN in 2020 (PBP Surface Water Management Report, 2020). This report analyzed the current domestic water needs and provided the total annual demand for current and future conditions. Total domestic water demand was projected to increase from 1.08 ac-ft/day 1.33 ac-ft/day in 2040. An estimation on irrigation requirements for corn, soybean and grassland was also determined as shown in table 13.

Table 13: Irrigation Water Requirement (data from the PBP Surface Water Management Report, 2020)

Crop Type	Total seasonal water requirement (ac-ft)
Grassland	30069
Corn	4757
Soybean	2733

Two locations were identified along Big Soldier Creek as possible reservoir location. One location, which was 116 acers in size, had a smaller upstream catchment and required diverting the water from Soldier Creek to support the lake. The second location was a 144-acre storage area which had a larger catchment area draining into the lake. In this study, the second location with 144-ac storage was selected for modelling purposes. Reach 2 of the watershed contains the potential location of the reservoir as seen in figure 30.

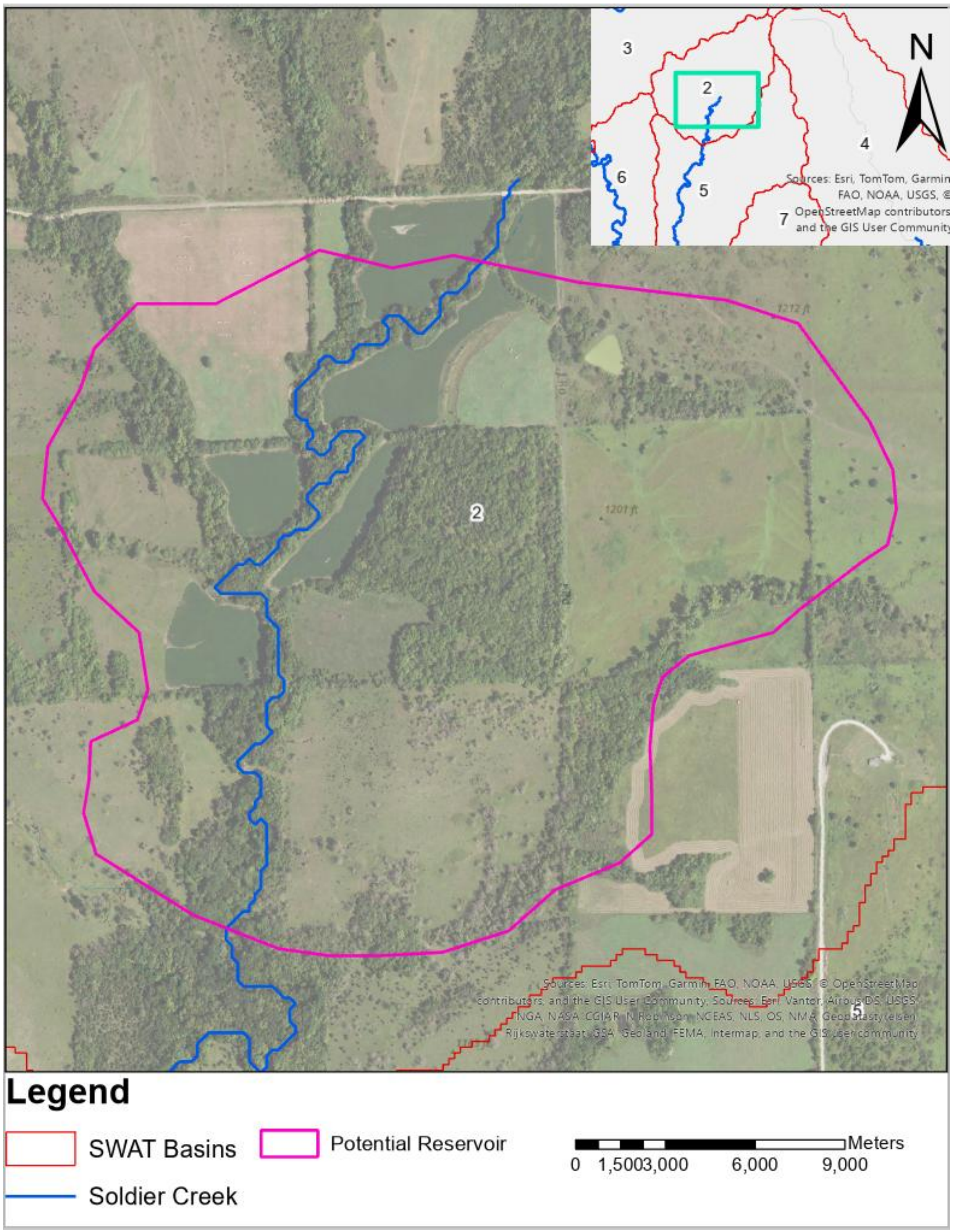

Figure 30: Potential Reservoir Location

SWAT's Reservoir module was activated in the model over the simulation period for three different scenarios: R1, R2 and R3. The initial scenario R1 assumed that the consumption requirement from the storage was only for domestic needs. The R2 and R3 scenarios both considered irrigation demands that could be met by the reservoir, with R2 incorporating all the irrigation needs for Corn/Soybean and R3 assuming approximately 50% of the irrigation needs for corn and soybean were met from the reservoir. Irrigation applications are seasonal with the demand peaking during the summer between June and August. The reservoir module in SWAT was set up with the reservoir surface area of 58.2ha, average depth of 30ft and 3:1 slope. Additional details regarding implementation of the reservoir and water use scenarios in SWAT are provided in Section C of the Appendix.

As mentioned earlier, domestic water requirement was taken from the Water Resources Solutions (2020) study for the projected water supply demand in 2040. The report further provided the estimated total seasonal crop water demand of 4,757 ac-ft for corn and 1,594 ac-ft for Soybean which was distributed as the monthly water requirement across months from May to September with July having the peak demand in the SWAT reservoir module in addition to water supply demand. In case of scenario R3, the total seasonal crop water demand was reduced by 50% for both crops i.e. 2,379 ac-ft for corn and 797 ac-ft for soybean.

In the case of drinking water, the reservoir had the capacity to meet the existing demand and even the future demand of 1.33 ac-ft/day through the drought period of 2012-2014. The water level went to a critical level in that period between 2012-2015 as seen with scenario R1 in figure 31. Irrigation of crops was more challenging, as the total demand for corn and soybean couldn’t be met completely with the reservoir capacity. All the months when irrigation was applied the reservoir went dry with complete drawdown depicted by red dots in the figure 31. Comparing R2 and R3, there was slightly better availability for R3, which was simulated by applying half the total irrigation demand. During the irrigation demand period of June through August both scenarios R2 and R3 had completely drawn down. In the wet period post 2015, there was a reduction in the number of months with complete water draw down for R3 whereas R2 irrigation needs still couldn't be met by the reservoir.

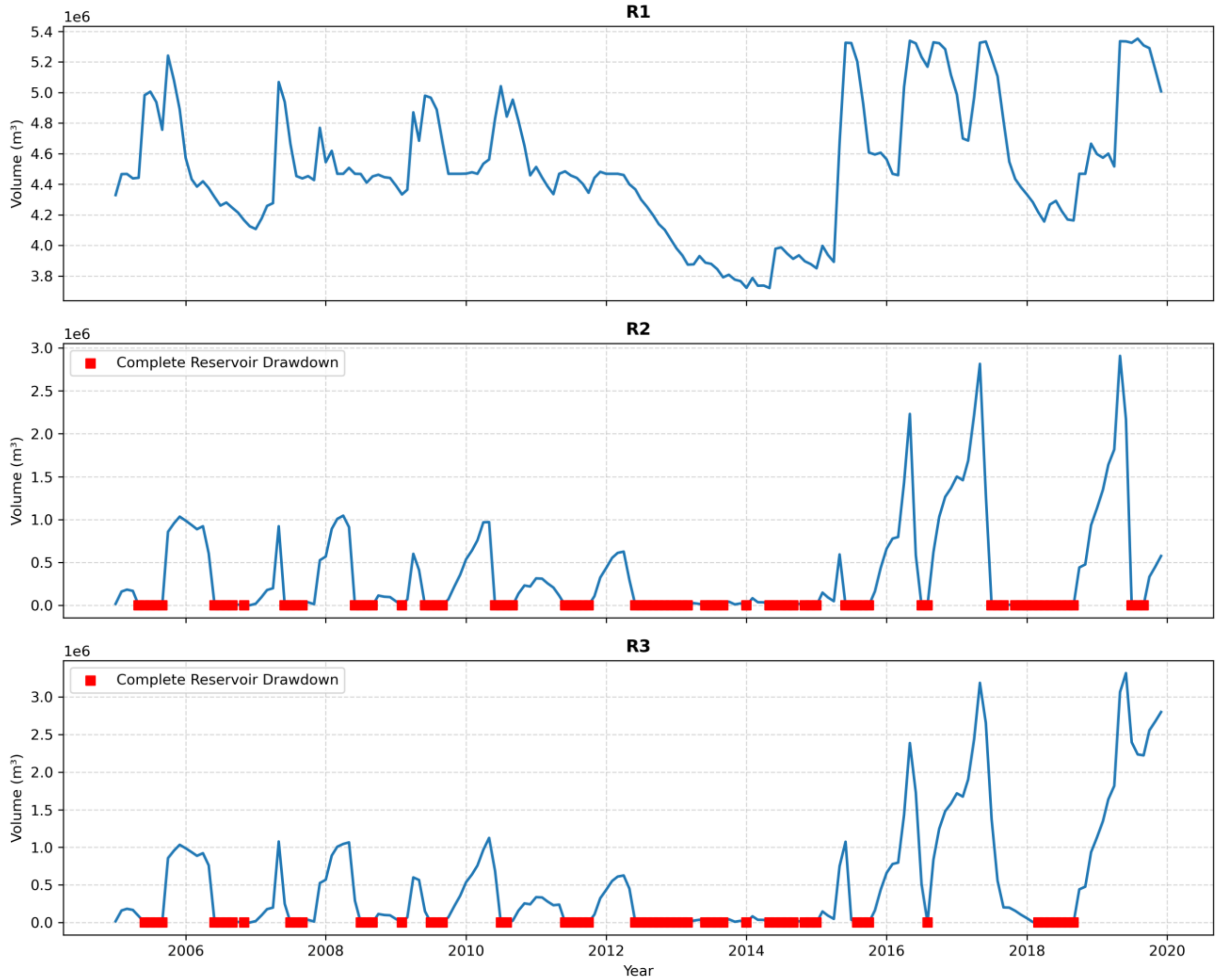

Figure 31: Reservoir Volume Time Series for different Scenarios.

The current 144 ac storage area can meet the domestic water needs of the PBPN region and can act as backup reservoir during the extended drought period. Though PBPN does not currently irrigate any of its land, further analysis would be required to determine an operation schedule that can be developed to support minimum critical irrigation if not the complete irrigation needs during dry spells.

4.2.7 Sediment Loading through Unpaved Roads

Unpaved and gravel roads can be source of sediment in rural watersheds. The vehicle traffic and weathering can loosen the surface of these roads which will be carried to the nearest stream through roadway ditches during precipitation events. The rate of erosion can increase when there are intense storms associated with extreme weather. Most of the roads in PBPN are unpaved and modeling these in SWAT can be challenging due to input landuse data resolution and density of roadway network in each sub-basin.

To evaluate the potential contribution of sediments from these roads, the Geomorphic Road Analysis and Inventory Package Lite (GRAIP Lite) tool was used (Nelson et al.,2019). This is a GIS based tool package developed by the U.S. Forest Service to estimate the sediment loading from the road network. This tool analyzes the road segment in relation to slope, drainage pathways and proximity to streams while estimating the sediment loading and transport. In this study, a preliminary analysis was carried out using GRAIP Lite tool. Due to limited availability of detailed road inventory information, the basic run option under the GRAIP Lite was used. Hence the model outputs are a relative indicator of sediment loading rather than an actual estimate of sediment load.

Basic run utilizes two inputs: the road network and DEM layer. The tool uses a base rate to determine the amount of sediment generated per unit road length per unit change in elevation and by default 1 kg/yr/m is used; this default value was adopted for this study as no field calculated base rate was available for this study. Sediment production considers the base rate along with surface type with traffic to determine the loading i.e. native roads will have higher loading multiplication factors as compared to paved roads. Along Big Soldier Creek, the tributaries with relatively higher estimates for sediment loading derived from gravel roads were spread across multiple subbasins as shown in figure 32. The stream network highlighted with red indicates relatively higher loading rate and green lines, which indicate lower loading rates. Stream segments for which the highest sediment loads included upstream reaches of Big Soldier Creek and its tributaries in the northern section of the PBPN reservation area between 182nd Rd and 190th Rd. Similarly, the tributary between 158th and 150th Rd along J Rd also had a relatively high predicted loading rate. Several tributaries to Little Soldier Creek were also predicted to have relatively high sediment loadings from gravel roads, namely the tributary running between 150th Rd, and 142nd Rd. Near the outlet of Little Soldier Creek, the GRAIP tool indicated relatively high loadings from the Q Rd between the 126th Rd and 118th Rd. Most of these loading can be mitigated by paving with asphalt to prevent sediment runoff during rainfall events. GRAIP tool estimated the loading rate of 25-76 tons/year for the highly erosive unpaved roads, while average land-based sediment erosion from crop land was around 718 tons/year for the smallest basin in the study area and 40,604 tons/year at the PBPN outlet. Though the loading rate from unpaved road is small as compared to land erosion it must be noted that a default base rate value of 1kg/yr/m was used in the GRAIP tool. Actual base rate can be much higher which may result in larger magnitude of sediment loading from these unpaved roads and needs to be analyzed in future studies.

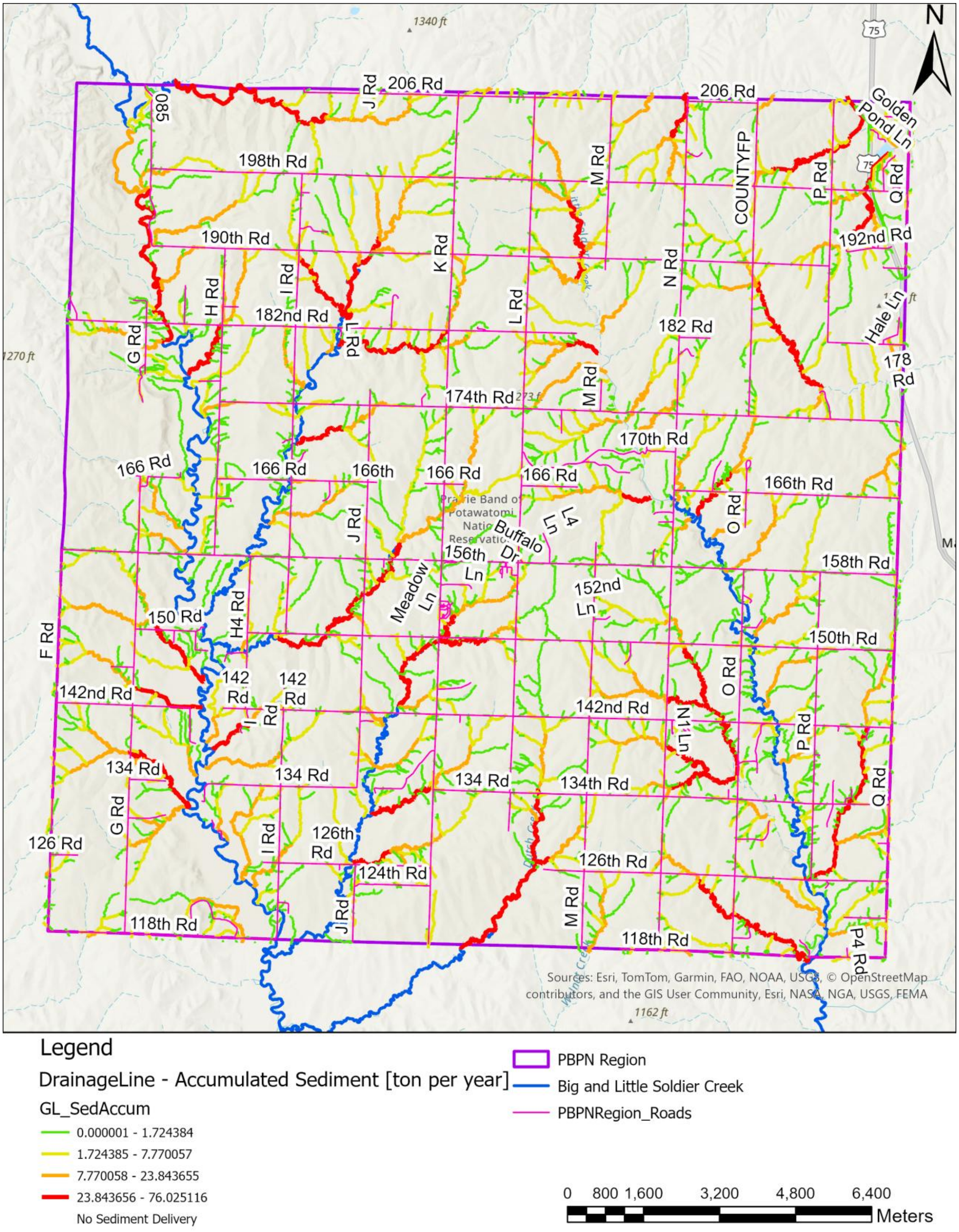

Figure 32: Relative Sediment loading due to Unpaved Road

4.2.8 Climate Change Analysis

Over the last decade, there have been increasing heat waves, flooding and drought due to climate change impacts caused by anthropogenic activities. These are impacting water bodies and streams with reduced flow and increased nutrient loading (Michalak, et al. 2012). One of the objectives of this thesis was to understand the potential effects of future climate change on hydrology in the Soldier Creek watershed; thus, an analysis was carried out to understand the trend of climate change and the impact on the flow through Soldier Creek at the outlet of PBPN area. An ensemble of 18 models from CIMP5 was used for two pathways, i.e. RCP4.5 and RCP8.5 representing moderate and high emission conditions, respectively. Two future time periods, mid-term from 2040-2070 and long term from 2071-2099 were chosen for the analysis. Future climate data were downscaled using Multivariate Adaptive Constructed Analogs (MACA) and the SWAT model was run individually for each climate model. The results from the runs were aggregated and averaged across the ensemble of models. To determine the trend, the non-parametric Mann-Kendall (MK) test was used for most hydrological time series to identify the direction of trend while Sen's slope was used to determine the magnitude of the trend. There was no trend observed in total annual rainfall for both mid- and long-term periods under both RCP4.5 and RCP8.5 with precipitation averaging around 932 mm/year (figure 33). It should be noted that extreme precipitation is included in the model simulations but may not be fully reflected in annual aggregate values. Additionally, climate models may have limited ability to accurately capture localized extreme rainfall events which could further contribute to apparent lack of trend in annual totals.

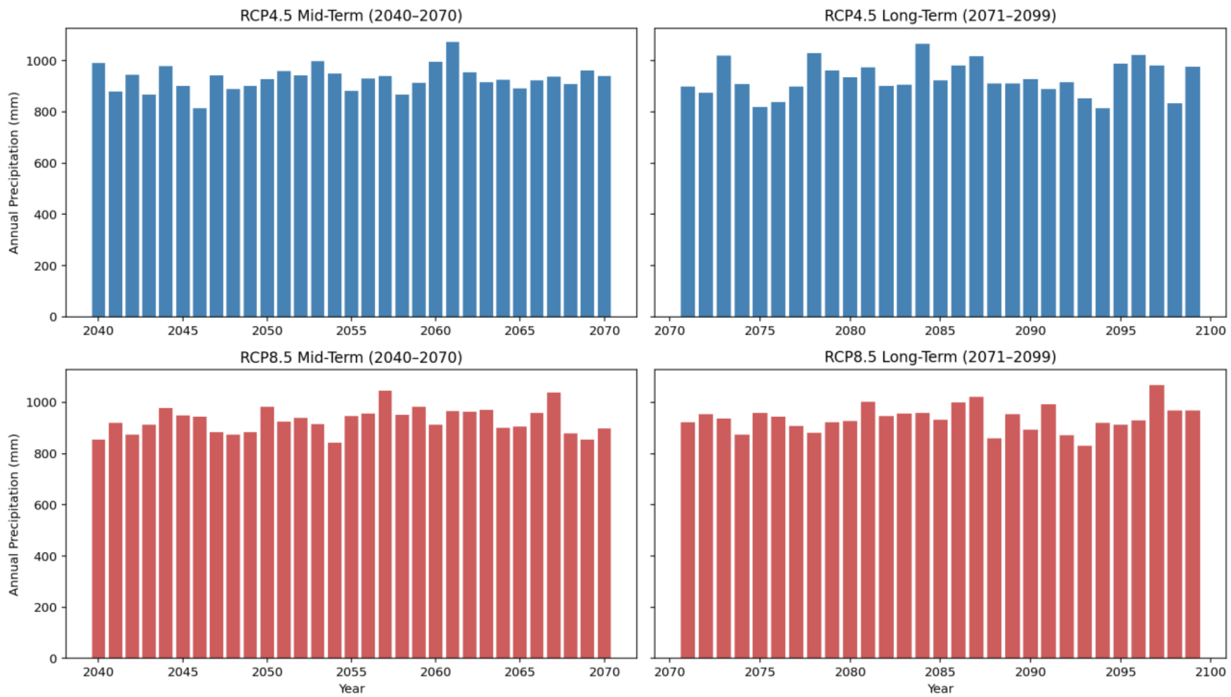

Figure 33: Future Annual Precipitation in Soldier Creek Watershed

For future maximum and minimum temperatures, there is a noticeable increasing trend in both RCP4.5 and RCP8.5 scenarios. The rate of increase was moderate for RCP4.5 with Sen's slope of mean temperature around 0.025°C/year for mid-term and 0.017°C/year for long-term. In comparison, RCP8.5 exhibited a stronger warming trend for both mid- and long-term having a Sen's slope of 0.071°C/year and 0.064°C/year, respectively (Table 14).

Table 14: Trend analysis for average temperature for future period

Scenario	**Period**	**Sen's Slope (°C/year)**	**p-value**
RCP 4.5	2040-2070	0.025	<0.001
RCP 4.5	2071-2099	0.017	0.0155
RCP 8.5	2040-2070	0.071	<0.001
RCP 8.5	2071-2099	0.064	<0.001

Comparing the mean monthly runoff at the outlet of PBPN as shown in figure 34 provides the variation in flow rate over the season for the mid- and long-term horizon with the baseline (1980-2020). Both the pathways show a reduction in flow for most of the year. The reduction is relatively high during the wet months of May and June. While both RCP 4.5 and

RCP 8.5 project a long-term (2071-2099) reduction of around 32-35% in average flows for the wet months, RCP 4.5 saw a reduction in annual mean flow by 28% as compared to 34% in RCP 8.5 for the same duration. These projections indicated a slight increase in runoff for the month of November and nearly similar flows for the month of December compared to the baseline. In the case of RCP 8.5 there is a slight increase in flows relative to RCP 4.5 for the initial months of February, March, April and May followed by a sharp drop in June for both mid- and long-term projections (Figure 34).

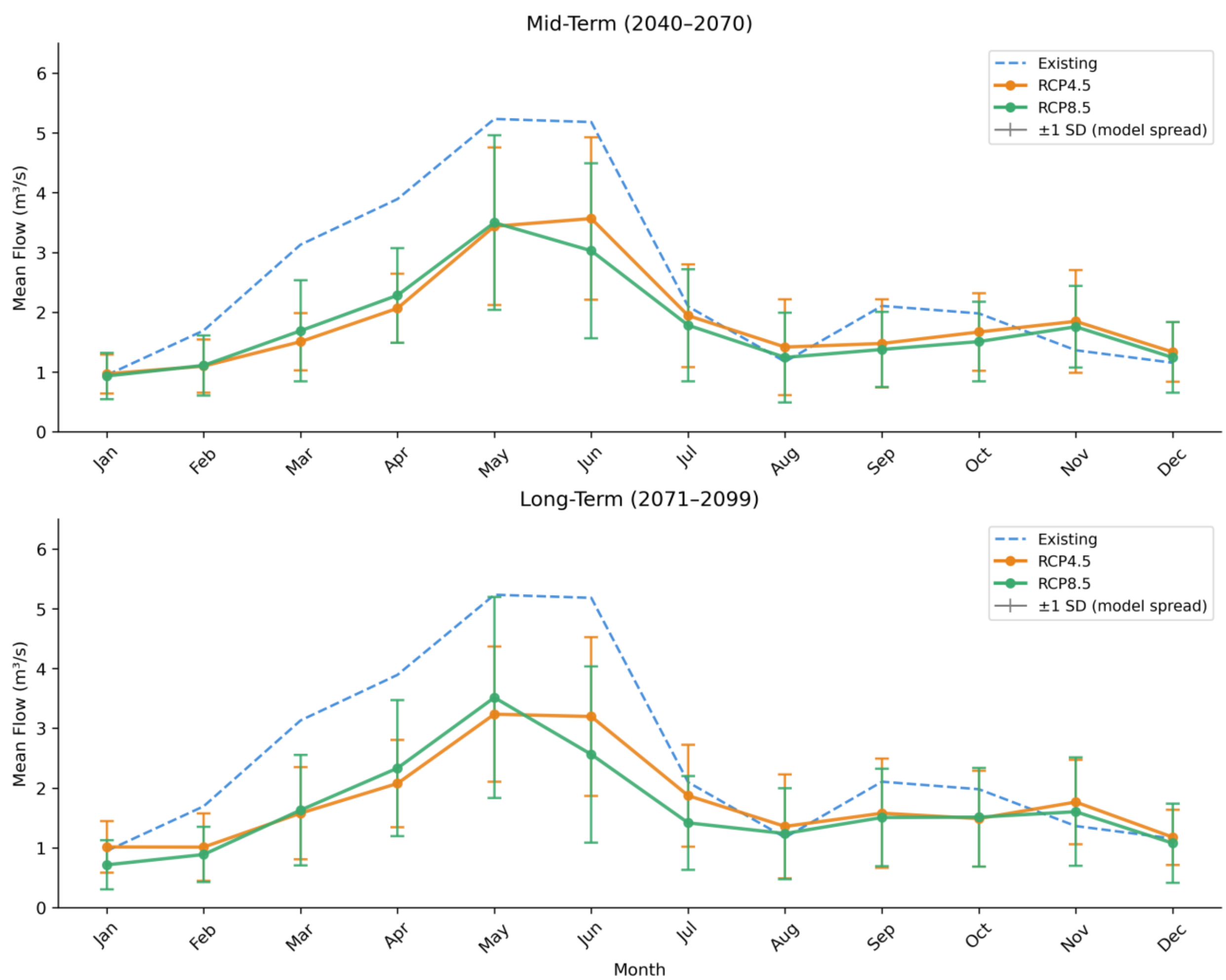

Figure 34: Mean monthly discharge for mid and long-term time period consider adding error bars to show variation in monthly means. For example, you could add error bars representing 1 standard deviation of the mean monthly values across each time period.

To analyze the impact of extreme weather, the Standardized Precipitation Evapotranspiration Index (SPEI) was used. The index quantifies drought with consideration for drought and temperature effects, by computing a water balance by taking a difference between precipitation and potential evapotranspiration (PET): The climatic water balance at each time step i is computed as:

$$D_i = P_i - PET_i \tag{12}$$

where P is precipitation and PET is potential evapotranspiration estimated using the Thornthwaite method. Future predictions of daily precipitation data and PET were then aggregated to a mean monthly timestep. The water balance series was aggregated over a 3-month time scale to capture the seasonal variability and standardized using a z-score approach to obtain SPEI values (Vicente-Serrano et. Al, 2010). A simplified standardized anomaly approach was adopted to quantify drought conditions. Drought severity was classified based on a standard threshold with values lower than -1, -1.5 and -2 representing moderate, severe and extreme drought conditions, respectively. Baseline or historical data were obtained from the Topeka climate station (USW00013996), which had recorded data from August 1947 onwards for precipitation, minimum and maximum temperature. The SPEI was calculated using a fixed reference approach where a fixed reference period was taken for baseline and future climate to estimate distribution parameters (Stagge et al., 2015). Table 15 shows the cumulative percentages of months at or below the SPEI threshold i.e. severe drought months are also considered within moderate drought category. RCP 4.5 shows severe drought increase to 30.42% while in RCP 8.5 scenario it increases further to 46.25%. Extreme drought with SPEI values smaller than -2 increases from 5.82% in baseline to around 41.25% for RCP 8.5 pathway. Climate change shows a shift towards extreme drought and gets worse during late century triggered by the temperature driven increase of potential evapotranspiration for both emission pathways.

Table 15: Projected changes in drought frequency under RCP 4.5 and RCP 8.5 scenarios relative to the historical baseline

Scenario	Time Period	Moderate Drought (SPEI<-1), %	Severe Drought (SPEI<-1.5), %	Extreme Drought (SPEI<-2), %
Baseline	1980-2020	13.7	8.02	5.82
RCP 4.5	2040-2099	38.47	30.42	25.83
RCP 8.5	2040-2099	55.42	46.25	41.25

BMP practices like RA will help develop resilience with increasing temperature resulting in increased evapotranspiration and reduced runoff (Rhodes, 2017; Lal, 2020). Climate change will impact the agricultural activities in the region (Barkley et al.,2013; Obembe et al., 2021; Araya et al.,2017). Field level management practices which improve infiltration, soil moisture and lower runoff will be able to mitigate the increased frequency of extreme events in the future.

Chapter 5 - Summary and Conclusion

The study developed a hydrologic and water quality model to evaluate the Soldier Creek watershed particularly the region which is under the stewardship of the Prairie Band Potawatomi Nation (PBPN). This model was used to understand watershed conditions, identify water quality challenges, assess BMPs and simulate the long-term climate impact on creek hydrology. Using the calibrated and validated SWAT model, the study provides a dynamic of sediment, nutrient and hydrology while considering the influence of land ownership, climate variability and management practices across both tribal and non-tribal lands.

The SWAT model's performance for streamflow prediction was assessed at two locations along Soldier Creek (at the outlet near the southern PBPN reservation border and the Soldier Creek watershed outlet near Topeka) and achieved an NSE greater than 0.5, indicating a reliable representation of watershed hydrology. There was a moderate agreement between modeled and observed data for sediment, total nitrogen and total phosphorus loads on the backdrop of sparse sampling data and inherent uncertainties. The validated SWAT model formed the basis for BMP scenario testing and climate projection analysis.

Across all the BMP types examined (i.e. filter strips, no-till agriculture, regenerative agriculture (RA) and hybrid strategies), SWAT model results demonstrated that landscape scale adoption resulted in water quality improvements. Filter strips provided the highest reduction on a watershed scale i.e. HUC-12 level implementation with sediment reduction up to around 70% in headwater tributaries and around 15-28% at the PBPN outlet. This reduction was muted when the filter strip application was confined to PBPN owned agricultural parcels. This was due to limited areas of BMP application and underscored the influence of non-tribal areas and upstream loading from areas outside PBPN on water quality within the Tribal Nation.

No-till agriculture alone had limited benefits but enhanced performance when combined with filter strips. RA was modeled as a 10% reduction in curve number, a simplification that does not capture the full range of mechanisms associated with regenerative agriculture; the results below should therefore be read as the effects of this CN reduction rather than RA in general. This modeled reduction produced moderate water quality improvement when applied across all the crop lands in the region but lower benefits when restricted to PBPN owned land due to less than 50% of crop land owned by the tribe. The most effective scenario was S11, which was RA plus no till across all croplands in the reservation boundary and yielded the highest combined reduction for sediments (approximately 46%) and nutrients (TN approx. 34% and TP approx. 27%). The hybrid approach, which represented a portion of non-tribal farmers adopting RA practices along with the tribally owned farms achieved reductions in sediment and nutrients ranging from 10-25% near the Soldier Creek and Little Soldier Creek outlets near the PBPN boundary.

The bacteria loading analysis highlighted grazing lands as one of the contributors to *E.coli* impairment and filter strips provided up to a 25% reduction depending on the reach and ownership pattern of pasture lands. Reservoir analysis showed that the proposed 144-acre storage site could reliably support domestic needs even under extreme conditions like drought but cannot fully meet the crop irrigation requirements unless withdrawals are significantly limited or managed seasonally.

Climate change simulations using CIMP5 MACA v2 downscaled data suggested no significant trend in long term annual precipitation but showed a warming trend under both RCP

4.5 and RCP 8.5 pathways. Rising temperatures will increase evapotranspiration leading to reduction in runoff which can potentially decrease the average monthly runoff by 30-40% in the historically wet season by late century. A simple drought analysis using the SPEI index showed more frequent moderate and severe drought in the future, with RCP 8.5 projecting more extreme drought events late in the century. These changes highlight increasing hydroclimatic stress on water availability, aquatic ecosystems, and agricultural productivity.

Overall, the study reinforces that PBPN's watershed resiliency depends strongly on both the spatial extent and cooperative adoption of BMPs, especially given the checkerboard pattern of land ownership. Improvements on tribal land alone are insufficient, and meaningful watershed-scale change requires participation from surrounding non-tribal landowners. The SWAT model developed here can support further studies for watershed level planning, prioritization of mitigation strategies, and long-term adaptation to climate stressors. This work serves as a base for future modeling efforts, continued monitoring, expansion of BMP adoption, and development of climate-resilient watershed management strategies tailored to the needs and values of the Prairie Band Potawatomi Nation.

5.1 Future Research

Future research to further understand the watershed level dynamics, contributing factors and resiliency is needed, including:

1. This study focused on watershed scale modeling and does not specifically focus on the Soldier Creek stream routing or overbank condition. 2D modeling incorporating the stream topology and current condition can help better understand the sediment routing, channel erosion and the role of riparian buffers along the stream.

2. Future water quality monitoring efforts could be coupled with water quality-based sensors and low-cost data collection system to collect and monitor real time data along the creek.
3. This study focused on the trend of climate change. Further analysis of climate change projections using CIMP6 with changing landuse and management practices can give better insights into possible vulnerabilities and help in building resiliency into the watershed management practices.
4. Only a couple of hybrid management practices involving both PBPN and non PBPN owned crop land were tested. Further analysis of this combined approach including cropping pattern, management practices, and grazing cycles can be explored to figure out the optimum solution.
5. A socio-economic study to understand the barriers and challenges to adopt various BMPs can be undertaken to help the tribe develop targeted outreach or cooperative agreement to expand BMP coverage.

This study introduced the challenges involved in developing watershed level interventions to improve the water quality, adopt climate resiliency and mitigation strategies within the area governed by the PBPN. It is hoped that this can support other studies focused on further understanding and analyzing the watershed within the PBPN reservation.

References

Abbaspour, K. C. 2015. *SWAT-CUP 2012: SWAT Calibration and Uncertainty Programs—A User Manual.* Dübendorf, Switzerland: Swiss Federal Institute of Aquatic Science and Technology, Eawag.

Abbaspour, K. C., E. Rouholahnejad, S. Vaghefi, R. Srinivasan, H. Yang, and B. Kløve. 2015. "A Continental-Scale Hydrology and Water Quality Model for Europe: Calibration and Uncertainty of a High-Resolution Large-Scale SWAT Model." *Journal of Hydrology* 524:733–752. doi:10.1016/j.jhydrol.2015.03.027.

Abatzoglou, J. T., and T. J. Brown. 2012. "A Comparison of Statistical Downscaling Methods Suited for Wildfire Applications." *International Journal of Climatology* 32(5):772–780. doi:10.1002/joc.2312.

Ad Astra Collaborative, LLC. 2021. *Prairie Band of Potawatomi Land and Water Management Plan.* Prepared for the Prairie Band Potawatomi Nation, Division of Planning and Environmental Protection, Mayetta, Kansas, with planning assistance from Norman Ecological.

Afolabi, E. O., R. S. Quilliam, and D. M. Oliver. 2023. "Persistence of *E. coli* in Streambed Sediment Contaminated with Faeces from Dairy Cows, Geese, and Deer: Legacy Risks to Environment and Health." *International Journal of Environmental Research and Public Health* 20(7):5375. doi:10.3390/ijerph20075375.

Alamdari, N., D. J. Sample, A. C. Ross, and Z. M. Easton. 2020. "Evaluating the Impact of Climate Change on Water Quality and Quantity in an Urban Watershed Using an Ensemble Approach." *Estuaries and Coasts* 43(1):56–72. doi:10.1007/s12237-019-00649-4.

Araya, A., I. Kisekka, X. Lin, P. V. Vara Prasad, P. H. Gowda, C. Rice, and A. Andales. 2017. "Evaluating the Impact of Future Climate Change on Irrigated Maize Production in Kansas." *Climate Risk Management* 17:139–154. doi:10.1016/j.crm.2017.08.001.

Arnold, J. G., D. N. Moriasi, P. W. Gassman, K. C. Abbaspour, M. J. White, R. Srinivasan, C. Santhi, R. D. Harmel, A. van Griensven, M. W. Van Liew, N. Kannan, and M. K. Jha. 2012. "SWAT: Model Use, Calibration, and Validation." *Transactions of the ASABE* 55(4):1491–1508. doi:10.13031/2013.42256.

Barkley, A., J. Tack, L. L. Nalley, J. Bergtold, R. Bowden, and A. Fritz. 2013. *The Impact of Climate, Disease, and Wheat Breeding on Wheat Variety Yields in Kansas, 1985–2011.* Kansas State University Agricultural Experiment Station and Cooperative Extension Service Bulletin SB665.

Berberian, A. G., D. J. X. Gonzalez, and L. J. Cushing. 2022. "Racial Disparities in Climate Change-Related Health Effects in the United States." *Current Environmental Health Reports* 9(3):451–464. doi:10.1007/s40572-022-00360-w.

Biswas, A. K. 2008. "Integrated Water Resources Management: Is It Working?" *International Journal of Water Resources Development* 24(1):5–22. doi:10.1080/07900620701871718.

Borah, D. K., and M. Bera. 2003. "Watershed-Scale Hydrologic and Nonpoint-Source Pollution Models: Review of Mathematical Bases." *Transactions of the ASAE* 46(6):1553–1566. doi:10.13031/2013.15644.

Brauman, K. A., G. C. Daily, T. K. Duarte, and H. A. Mooney. 2007. "The Nature and Value of Ecosystem Services: An Overview Highlighting Hydrologic Services." *Annual Review of Environment and Resources* 32(1):67–98. doi:10.1146/annurev.energy.32.031306.102758.

Brighenti, T. M., N. B. Bonumá, F. Grison, A. de Almeida Mota, M. Kobiyama, and P. L. B. Chaffe. 2019. "Two Calibration Methods for Modeling Streamflow and Suspended Sediment with the SWAT Model." *Ecological Engineering* 127:103–113. doi:10.1016/j.ecoleng.2018.11.007.

Carpenter, S. R., N. F. Caraco, D. L. Correll, R. W. Howarth, A. N. Sharpley, and V. H. Smith. 1998. "Nonpoint Pollution of Surface Waters with Phosphorus and Nitrogen." *Ecological Applications* 8(3):559–568. doi:10.2307/2641247.

Chaubey, I., L. Chiang, M. W. Gitau, and S. Mohamed. 2010. "Effectiveness of Best Management Practices in Improving Water Quality in a Pasture-Dominated Watershed." *Journal of Soil and Water Conservation* 65(6):424–437. doi:10.2489/jswc.65.6.424.

Chordia, J., U. R. Panikkar, R. Srivastav, and R. U. Shaik. 2022. "Uncertainties in Prediction of Streamflows Using SWAT Model—Role of Remote Sensing and Precipitation Sources." *Remote Sensing* 14(21):5385. doi:10.3390/rs14215385.

Cibin, R., I. Chaubey, M. J. Helmers, K. P. Sudheer, M. J. White, and J. G. Arnold. 2018. "An Improved Representation of Vegetative Filter Strips in SWAT." *Transactions of the ASABE* 61(3):1017–1024. doi:10.13031/trans.12661.

Cozzetto, K., K. Chief, K. Dittmer, M. Brubaker, R. Gough, K. Souza, F. Ettawageshik, S. Wotkyns, S. Opitz-Stapleton, S. Duren, and P. Chavan. 2013. "Climate Change Impacts on the Water Resources of American Indians and Alaska Natives in the U.S." *Climatic Change* 120(3):569–584. doi:10.1007/s10584-013-0852-y.

Dagnew, A., D. Scavia, Y.-C. Wang, R. Muenich, C. Long, and M. Kalcic. 2019. "Modeling Flow, Nutrient, and Sediment Delivery from a Large International Watershed Using a Field-Scale SWAT Model." *JAWRA Journal of the American Water Resources Association* 55(5):1288–1305. doi:10.1111/1752-1688.12779.

Dakhlalla, A. O., and P. B. Parajuli. 2019. "Assessing Model Parameters Sensitivity and Uncertainty of Streamflow, Sediment, and Nutrient Transport Using SWAT." *Information Processing in Agriculture* 6(1):61–72. doi:10.1016/j.inpa.2018.08.007.

Devia, G. K., B. P. Ganasri, and G. S. Dwarakish. 2015. "A Review on Hydrological Models." *Aquatic Procedia* 4:1001–1007. doi:10.1016/j.aqpro.2015.02.126.

Dodds, W. K., and R. M. Oakes. 2008. "Headwater Influences on Downstream Water Quality." *Environmental Management* 41(3):367–377. doi:10.1007/s00267-007-9033-y.

Dodds, W. K., and V. H. Smith. 2016. "Nitrogen, Phosphorus, and Eutrophication in Streams." *Inland Waters* 6(2):155–164. doi:10.5268/IW-6.2.909.

Douglas-Mankin, K. R., R. Srinivasan, and J. G. Arnold. 2010. "Soil and Water Assessment Tool (SWAT) Model: Current Developments and Applications." *Transactions of the ASABE* 53(5):1423–1431. doi:10.13031/2013.34915.

Duan, N. 1983. "Smearing Estimate: A Nonparametric Retransformation Method." *Journal of the American Statistical Association* 78(383):605–610. doi:10.2307/2288126.

Elçi, A. 2017. "Evaluation of Nutrient Retention in Vegetated Filter Strips Using the SWAT Model." *Water Science and Technology* 76(10):2742–2752. doi:10.2166/wst.2017.448.

Garzio-Hadzick, A., D. R. Shelton, R. L. Hill, Y. A. Pachepsky, A. K. Guber, and R. Rowland. 2010. "Survival of Manure-Borne *E. coli* in Streambed Sediment: Effects of Temperature and Sediment Properties." *Water Research* 44(9):2753–2762. doi:10.1016/j.watres.2010.02.011.

Gassman, P. W., M. R. Reyes, C. H. Green, and J. G. Arnold. 2007. "The Soil and Water Assessment Tool: Historical Development, Applications, and Future Research Directions." *Transactions of the ASABE* 50(4):1211–1250. doi:10.13031/2013.23637.

Geza, M., and J. E. McCray. 2008. "Effects of Soil Data Resolution on SWAT Model Stream Flow and Water Quality Predictions." *Journal of Environmental Management* 88(3):393–406. doi:10.1016/j.jenvman.2007.03.016.

Golmohammadi, G., S. Prasher, A. Madani, and R. Rudra. 2014. "Evaluating Three Hydrological Distributed Watershed Models: MIKE-SHE, APEX, SWAT." *Hydrology* 1(1):20–39. doi:10.3390/hydrology1010020.

Grizzetti, B., D. Lanzanova, C. Liquete, A. Reynaud, and A. C. Cardoso. 2016. "Assessing Water Ecosystem Services for Water Resource Management." *Environmental Science & Policy* 61:194–203. doi:10.1016/j.envsci.2016.04.008.

Hargett, E. G., D. Konecek, C. Stiles, and T. Zey. 2005. "Developing and Implementing Locally Led Watershed Restoration and Protection Strategies." *WIT Transactions on Ecology and the Environment* 83. doi:10.2495/WRM050411.

HAWQS 2.0. 2023. *HAWQS System 2.0 and Data to Model the Lower 48 Conterminous U.S. Using the SWAT Model.* Version 2. Texas Data Repository. doi:10.18738/T8/GDOPBA.

He, C., and L. A. James. 2021. "Watershed Science: Linking Hydrological Science with Sustainable Management of River Basins." *Science China Earth Sciences* 64(5):677–690. doi:10.1007/s11430-020-9723-4.

Her, Y., J. Frankenberger, I. Chaubey, and R. Srinivasan. 2015. "Threshold Effects in HRU Definition of the Soil and Water Assessment Tool." *Transactions of the ASABE* 58(2):367–378. doi:10.13031/trans.58.10805.

Hoekema, D. J., and V. Sridhar. 2011. "Relating Climatic Attributes and Water Resources Allocation: A Study Using Surface Water Supply and Soil Moisture Indices in the Snake River Basin, Idaho." *Water Resources Research* 47(7). doi:10.1029/2010WR009697.

Intergovernmental Panel on Climate Change. 2014. *Climate Change 2014: Synthesis Report. Contribution of Working Groups I, II and III to the Fifth Assessment Report.* Edited by R. K. Pachauri and L. A. Meyer. Geneva, Switzerland: IPCC.

Intergovernmental Panel on Climate Change. 2021. *Climate Change 2021: The Physical Science Basis. Contribution of Working Group I to the Sixth Assessment Report.* Cambridge University Press. doi:10.1017/9781009157896.

Jabbar, F. K., and K. Grote. 2019. "Statistical Assessment of Nonpoint Source Pollution in Agricultural Watersheds in the Lower Grand River Watershed, MO, USA." *Environmental Science and Pollution Research* 26(2):1487–1506. doi:10.1007/s11356-018-3682-7.

Jaiswal, R. K., S. Ali, and B. Bharti. 2020. "Comparative Evaluation of Conceptual and Physical Rainfall–Runoff Models." *Applied Water Science* 10(1):48. doi:10.1007/s13201-019-1122-6.

Jajarmizadeh, M., S. Harun, and M. Salarpour. 2012. "A Review on Theoretical Consideration and Types of Models in Hydrology." *Journal of Environmental Science and Technology* 5(5):249–261. doi:10.3923/jest.2012.249.261.

Jantarasami, L., R. Novak, R. Delgado, C. Narducci, E. Marino, S. McNeeley, J. Raymond-Yakoubian, L. Singletary, and K. P. Whyte. 2018. "Chapter 15: Tribal and Indigenous Communities." In *Impacts, Risks, and Adaptation in the United States: The Fourth National Climate Assessment, Volume II.* U.S. Global Change Research Program. doi:10.7930/NCA4.2018.CH15.

Jha, M. K., P. W. Gassman, and Y. Panagopoulos. 2015. "Regional Changes in Nitrate Loadings in the Upper Mississippi River Basin under Predicted Mid-Century Climate." *Regional Environmental Change* 15(3):449–460. doi:10.1007/s10113-013-0539-y.

Juracek, K. E. 2017. *Streamflow Characteristics and Trends Along Soldier Creek, Northeast Kansas.* Scientific Investigations Report 2017–5061. U.S. Geological Survey. doi:10.3133/sir20175061.

Kamrath, B., and Y. Yuan. 2023. "Streamflow Duration Curve to Explain Nutrient Export in Midwestern USA Watersheds: Implication for Water Quality Achievements." *Journal of Environmental Management* 336:117598. doi:10.1016/j.jenvman.2023.117598.

Kansas Watershed Restoration and Protection Strategy (WRAPS). n.d. Retrieved June 10, 2026, from https://kswraps.org/.

Keller, A. A., K. Garner, N. Rao, E. Knipping, and J. Thomas. 2023. "Hydrological Models for Climate-Based Assessments at the Watershed Scale: A Critical Review of Existing Hydrologic and Water Quality Models." *Science of the Total Environment* 867:161209. doi:10.1016/j.scitotenv.2022.161209.

Kroll, S. A., and H. C. Oakland. 2019. "A Review of Studies Documenting the Effects of Agricultural Best Management Practices on Physiochemical and Biological Measures of Stream Ecosystem Integrity." *Natural Areas Journal* 39(1):58–77. doi:10.3375/043.039.0105.

Krysanova, V., and R. Srinivasan. 2015. "Assessment of Climate and Land Use Change Impacts with SWAT." *Regional Environmental Change* 15(3):431–434. doi:10.1007/s10113-014-0742-5.

Krysanova, V., and M. White. 2015. "Advances in Water Resources Assessment with SWAT—An Overview." *Hydrological Sciences Journal* 60(5):771–783. doi:10.1080/02626667.2015.1029482.

Kujawa, H., M. Kalcic, J. Martin, A. Apostel, J. Kast, A. Murumkar, G. Evenson, N. Aloysius, R. Becker, C. Boles, R. Confesor, A. Dagnew, T. Guo, R. L. Muenich, T. Redder, Y.-C. Wang, and D. Scavia. 2022. "Using a Multi-Institutional Ensemble of Watershed Models to Assess Agricultural Conservation Effectiveness in a Future Climate." *JAWRA Journal of the American Water Resources Association* 58(6):1326–1341. doi:10.1111/1752-1688.13023.

Lal, R. 2020. "Regenerative Agriculture for Food and Climate." *Journal of Soil and Water Conservation* 75(5):123A–124A. doi:10.2489/jswc.2020.0620A.

Leh, M. D. K., A. N. Sharpley, G. Singh, and M. D. Matlock. 2018. "Assessing the Impact of the MRBI Program in a Data Limited Arkansas Watershed Using the SWAT Model." *Agricultural Water Management* 202:202–219. doi:10.1016/j.agwat.2018.02.012.

Lencha, S. M., M. D. Ulsido, and J. Tränckner. 2022. "Estimating Point and Nonpoint Source Pollutant Flux by Integrating Various Models, a Case Study of the Lake Hawassa Watershed in Ethiopia's Rift Valley Basin." *Water* 14(10):1569. doi:10.3390/w14101569.

Li, P., R. L. Muenich, I. Chaubey, and X. Wei. 2019. "Evaluating Agricultural BMP Effectiveness in Improving Freshwater Provisioning under Changing Climate." *Water Resources Management* 33(2):453–473. doi:10.1007/s11269-018-2098-y.

Li, X., G. Cheng, H. Lin, X. Cai, M. Fang, Y. Ge, X. Hu, M. Chen, and W. Li. 2018. "Watershed System Model: The Essentials to Model Complex Human–Nature Systems at the River Basin Scale." *Journal of Geophysical Research: Atmospheres* 123(6):3019–3034. doi:10.1002/2017JD028154.

Lin, X., J. Harrington, I. Ciampitti, P. Gowda, D. Brown, and I. Kisekka. 2017. "Kansas Trends and Changes in Temperature, Precipitation, Drought, and Frost-Free Days from the 1890s to 2015." *Journal of Contemporary Water Research & Education* 162(1):18–30. doi:10.1111/j.1936-704X.2017.03257.x.

Liu, Y., B. A. Engel, D. C. Flanagan, M. W. Gitau, S. K. McMillan, and I. Chaubey. 2017. "A Review on Effectiveness of Best Management Practices in Improving Hydrology and Water Quality: Needs and Opportunities." *Science of the Total Environment* 601–602:580–593. doi:10.1016/j.scitotenv.2017.05.212.

Mantey, E. P., L. Liu, and C. R. Rehmann. 2025. "Disparities in Potential Nitrate Exposures within Iowa Public Water Systems." *Environmental Science: Water Research & Technology* 11(4):959–971. doi:10.1039/D4EW00907J.

Marin, M., I. Clinciu, N. C. Tudose, C. Ungurean, A. Adorjani, A. L. Mihalache, A. A. Davidescu, Ș. O. Davidescu, L. Dinca, and H. Cacovean. 2020. "Assessing the Vulnerability of Water Resources in the Context of Climate Changes in a Small Forested Watershed Using SWAT: A Review." *Environmental Research* 184:109330. doi:10.1016/j.envres.2020.109330.

Mehl, H., D. Restrepo-Osorio, M. Howard, and C. Annett. 2022. "An Analysis of Community-Based Values Informing Land Management on the Midwestern Prairie Band Potawatomi Nation of Kansas, USA." *International Grassland Congress Proceedings.* https://uknowledge.uky.edu/igc/24/6-2/2.

Merriman, K. R., P. Daggupati, R. Srinivasan, and B. Hayhurst. 2019. "Assessment of Site-Specific Agricultural Best Management Practices in the Upper East River Watershed, Wisconsin, Using a Field-Scale SWAT Model." *Journal of Great Lakes Research* 45(3):619–641. doi:10.1016/j.jglr.2019.02.004.

Michalak, A. M., E. J. Anderson, D. Beletsky, S. Boland, N. S. Bosch, T. B. Bridgeman, J. D. Chaffin, K. Cho, R. Confesor, I. Daloğlu, J. V. DePinto, M. A. Evans, G. L. Fahnenstiel, L. He, J. C. Ho, L. Jenkins, T. H. Johengen, K. C. Kuo, E. LaPorte, X. Liu, M. R. McWilliams, M. R. Moore, D. J. Posselt, R. P. Richards, D. Scavia, A. L. Steiner, E. Verhamme, D. M. Wright, and M. A. Zagorski. 2013. "Record-Setting Algal Bloom in Lake Erie Caused by Agricultural and Meteorological Trends Consistent with Expected Future Conditions." *Proceedings of the National Academy of Sciences* 110(16):6448–6452. doi:10.1073/pnas.1216006110.

Moriasi, D. N., J. G. Arnold, M. W. Van Liew, R. L. Bingner, R. D. Harmel, and T. L. Veith. 2007. "Model Evaluation Guidelines for Systematic Quantification of Accuracy in Watershed Simulations." *Transactions of the ASABE* 50(3):885–900. doi:10.13031/2013.23153.

Moss, B. 2008. "Water Pollution by Agriculture." *Philosophical Transactions of the Royal Society B: Biological Sciences* 363(1491):659–666. doi:10.1098/rstb.2007.2176.

Muche, M. E., S. Sinnathamby, R. Parmar, C. D. Knightes, J. M. Johnston, K. Wolfe, S. T. Purucker, M. J. Cyterski, and D. Smith. 2020. "Comparison and Evaluation of Gridded Precipitation Datasets in a Kansas Agricultural Watershed Using SWAT." *JAWRA Journal of the American Water Resources Association* 56(3):486–506. doi:10.1111/1752-1688.12819.

Mueller-Warrant, G. W., C. L. Phillips, and K. M. Trippe. 2019. "Use of SWAT to Model Impact of Climate Change on Sediment Yield and Agricultural Productivity in Western Oregon, USA." *Open Journal of Modern Hydrology* 9(2):54–88. doi:10.4236/ojmh.2019.92004.

Najjar, R. G., C. R. Pyke, M. B. Adams, D. Breitburg, C. Hershner, M. Kemp, R. Howarth, M. R. Mulholland, M. Paolisso, D. Secor, K. Sellner, D. Wardrop, and R. Wood. 2010. "Potential Climate-Change Impacts on the Chesapeake Bay." *Estuarine, Coastal and Shelf Science* 86(1):1–20. doi:10.1016/j.ecss.2009.09.026.

Neitsch, S. L., J. G. Arnold, J. R. Kiniry, and J. R. Williams. 2011. *Soil and Water Assessment Tool Theoretical Documentation Version 2009.* Texas Water Resources Institute Technical Report No. 406. College Station, TX: Texas Water Resources Institute.

Nelson, N., C. Luce, and T. Black. 2019. *GRAIP_Lite: A System for Road Impact Assessment.* USDA Forest Service, Rocky Mountain Research Station.

Nepal, D., and P. B. Parajuli. 2022. "Assessment of Best Management Practices on Hydrology and Sediment Yield at Watershed Scale in Mississippi Using SWAT." *Agriculture* 12(4):518. doi:10.3390/agriculture12040518.

Newton, P., N. Civita, L. Frankel-Goldwater, K. Bartel, and C. Johns. 2020. "What Is Regenerative Agriculture? A Review of Scholar and Practitioner Definitions Based on Processes and Outcomes." *Frontiers in Sustainable Food Systems* 4. doi:10.3389/fsufs.2020.577723.

Nguyen, T. V., J. Dietrich, T. D. Dang, D. A. Tran, B. V. Doan, F. J. Sarrazin, K. Abbaspour, and R. Srinivasan. 2022. "An Interactive Graphical Interface Tool for Parameter Calibration, Sensitivity Analysis, Uncertainty Analysis, and Visualization for the Soil and Water Assessment Tool." *Environmental Modelling & Software* 156:105497. doi:10.1016/j.envsoft.2022.105497.

Obembe, O. S., N. P. Hendricks, and J. Tack. 2021. "Decreased Wheat Production in the USA from Climate Change Driven by Yield Losses Rather than Crop Abandonment." *PLoS ONE* 16(6):e0252067. doi:10.1371/journal.pone.0252067.

Okiria, E., H. Okazawa, K. Noda, Y. Kobayashi, S. Suzuki, and Y. Yamazaki. 2022. "A Comparative Evaluation of Lumped and Semi-Distributed Conceptual Hydrological

Models: Does Model Complexity Enhance Hydrograph Prediction?" *Hydrology* 9(5):89. doi:10.3390/hydrology9050089.

Osmond, D., D. Meals, D. Hoag, M. Arabi, A. Luloff, G. Jennings, M. McFarland, J. Spooner, A. Sharpley, and D. Line. 2012. "Improving Conservation Practices Programming to Protect Water Quality in Agricultural Watersheds: Lessons Learned from the National Institute of Food and Agriculture–Conservation Effects Assessment Project." *Journal of Soil and Water Conservation* 67(5):122A–127A. doi:10.2489/jswc.67.5.122A.

Otto, I. M., D. Reckien, C. P. O. Reyer, R. Marcus, V. Le Masson, L. Jones, A. Norton, and O. Serdeczny. 2017. "Social Vulnerability to Climate Change: A Review of Concepts and Evidence." *Regional Environmental Change* 17(6):1651–1662. doi:10.1007/s10113-017-1105-9.

Özcan, Z., E. Kentel, and E. Alp. 2017. "Evaluation of the Best Management Practices in a Semi-Arid Region with High Agricultural Activity." *Agricultural Water Management* 194:160–171. doi:10.1016/j.agwat.2017.09.007.

Pahl-Wostl, C., M. Craps, A. Dewulf, E. Mostert, D. Tabara, and T. Taillieu. 2007. "Social Learning and Water Resources Management." *Ecology and Society* 12(2):Article 5.

Panta, S. 2025. "Regenerative Farming Systems to Improve Soil Water Infiltration and Soil Health in Semi-Arid Environments." M.S. thesis, New Mexico State University.

Parajuli, P. B., P. Jayakody, G. F. Sassenrath, and Y. Ouyang. 2016. "Assessing the Impacts of Climate Change and Tillage Practices on Stream Flow, Crop and Sediment Yields from the Mississippi River Basin." *Agricultural Water Management* 168:112–124. doi:10.1016/j.agwat.2016.02.005.

Parajuli, P. B., K. R. Mankin, and P. L. Barnes. 2008. "Applicability of Targeting Vegetative Filter Strips to Abate Fecal Bacteria and Sediment Yield Using SWAT." *Agricultural Water Management* 95(10):1189–1200. doi:10.1016/j.agwat.2008.05.006.

Prairie Band Potawatomi Nation. n.d. "Prairie Band Potawatomi Nation." Accessed June 24, 2021. https://www.pbpindiantribe.com/

Rabalais, N. N., and R. E. Turner. 2019. "Gulf of Mexico Hypoxia: Past, Present, and Future." *Limnology and Oceanography Bulletin* 28(4):117–124. doi:10.1002/lob.10351.

Ramião, J. P., C. Carvalho-Santos, R. Pinto, and C. Pascoal. 2022. "Modeling the Effectiveness of Sustainable Agricultural Practices in Reducing Sediments and Nutrient Export from a River Basin." *Water* 14(23):3962. doi:10.3390/w14233962.

Rasoulzadeh Gharibdousti, S., G. Kharel, R. B. Miller, E. Linde, and A. Stoecker. 2019. "Projected Climate Could Increase Water Yield and Cotton Yield but Decrease Winter Wheat and Sorghum Yield in an Agricultural Watershed in Oklahoma." *Water* 11(1):105. doi:10.3390/w11010105.

Reid, W. V., D. Chen, L. Goldfarb, H. Hackmann, Y. T. Lee, K. Mokhele, E. Ostrom, K. Raivio, J. Rockström, H. J. Schellnhuber, and A. Whyte. 2010. "Earth System Science for Global Sustainability: Grand Challenges." *Science* 330(6006):916–917. doi:10.1126/science.1196263.

Reidmiller, D. R., C. W. Avery, D. R. Easterling, K. E. Kunkel, K. L. M. Lewis, T. K. Maycock, and B. C. Stewart, eds. 2018. *Impacts, Risks, and Adaptation in the United States: Fourth National Climate Assessment, Volume II.* Washington, DC: U.S. Global Change Research Program. doi:10.7930/NCA4.2018.

Rhodes, C. J. 2017. "The Imperative for Regenerative Agriculture." *Science Progress* 100(1):80–129. doi:10.3184/003685017X14876775256165.

Ricci, G. F., J. Jeong, A. M. De Girolamo, and F. Gentile. 2020. "Effectiveness and Feasibility of Different Management Practices to Reduce Soil Erosion in an Agricultural Watershed." *Land Use Policy* 90:104306. doi:10.1016/j.landusepol.2019.104306.

Samavati, A., O. Babamiri, Y. Rezai, and M. Heidarimozaffar. 2023. "Investigating the Effects of Climate Change on Future Hydrological Drought in Mountainous Basins Using SWAT Model Based on CMIP5 Model." *Stochastic Environmental Research and Risk Assessment* 37(3):849–875. doi:10.1007/s00477-022-02319-7.

Schreefel, L., R. P. O. Schulte, I. J. M. de Boer, A. Pas Schrijver, and H. H. E. van Zanten. 2020. "Regenerative Agriculture—The Soil Is the Base." *Global Food Security* 26:100404. doi:10.1016/j.gfs.2020.100404.

Sheshukov, A. Y., C. B. Siebenmorgen, and K. R. Douglas-Mankin. 2011. "Seasonal and Annual Impacts of Climate Change on Watershed Response Using an Ensemble of Global Climate Models." *Transactions of the ASABE* 54(6):2209–2218. doi:10.13031/2013.40660.

Sheshukov, A. Y., K. R. Douglas-Mankin, S. Sinnathamby, and P. Daggupati. 2016. "Pasture BMP Effectiveness Using an HRU-Based Subarea Approach in SWAT." *Journal of Environmental Management* 166:276–284. doi:10.1016/j.jenvman.2015.10.023.

Singh, V. P., and D. A. Woolhiser. 2002. "Mathematical Modeling of Watershed Hydrology." *Journal of Hydrologic Engineering* 7(4):270–292. doi:10.1061/(ASCE)1084-0699(2002)7:4(270).

Sinnathamby, S. 2014. "Modeling Tools for Ecohydrological Characterization." Ph.D. dissertation, Kansas State University, Manhattan, KS.

Sittig, S., and R. Sur. 2024. "Runoff and Erosion Mitigation via Conservation Tillage and Cover Crops—Derivation of Model Input Parameters from Literature." *Environmental Challenges* 17:101015. doi:10.1016/j.envc.2024.101015.

Sivapalan, M., H. H. G. Savenije, and G. Blöschl. 2012. "Socio-Hydrology: A New Science of People and Water." *Hydrological Processes* 26(8):1270–1276. doi:10.1002/hyp.8426.

Smith, C. W. 2016. *Effects of Implementation of Soil Health Management Practices on Infiltration, Saturated Hydraulic Conductivity (Ksat), and Runoff.* USDA Natural Resources Conservation Service, National Soil Survey Center.

Stagge, J. H., L. M. Tallaksen, L. Gudmundsson, A. F. Van Loon, and K. Stahl. 2015. "Candidate Distributions for Climatological Drought Indices (SPI and SPEI)." *International Journal of Climatology* 35(13):4027–4040. doi:10.1002/joc.4267.

Tan, M. L., D. L. Ficklin, B. Dixon, A. L. Ibrahim, Z. Yusop, and V. Chaplot. 2015. "Impacts of DEM Resolution, Source, and Resampling Technique on SWAT-Simulated Streamflow." *Applied Geography* 63:357–368. doi:10.1016/j.apgeog.2015.07.014.

Tan, M. L., P. W. Gassman, X. Yang, and J. Haywood. 2020. "A Review of SWAT Applications, Performance and Future Needs for Simulation of Hydro-Climatic Extremes." *Advances in Water Resources* 143:103662. doi:10.1016/j.advwatres.2020.103662.

Thornton, M. M., R. Shrestha, Y. Wei, P. E. Thornton, and S.-C. Kao. 2022. *Daymet: Daily Surface Weather Data on a 1-km Grid for North America, Version 4 R1.* Version 4.1. ORNL Distributed Active Archive Center. doi:10.3334/ORNLDAAC/2129.

Thornton, P. E., R. Shrestha, M. Thornton, S.-C. Kao, Y. Wei, and B. E. Wilson. 2021. "Gridded Daily Weather Data for North America with Comprehensive Uncertainty Quantification." *Scientific Data* 8(1):190. doi:10.1038/s41597-021-00973-0.

U.S. Department of Agriculture Climate Hubs. n.d. "Northwest No-Till Farming for Climate Resilience." USDA Climate Hubs. Accessed June 27, 2026.

U.S. Environmental Protection Agency. 2003. *National Management Measures to Control Nonpoint Source Pollution from Agriculture.* EPA 841-B-03-004. Washington, DC: U.S. Environmental Protection Agency, Office of Water.

USDA NASS. 2010. *Field Crops Usual Planting and Harvesting Dates*. Agricultural Handbook Number 628. Washington, DC: U.S. Department of Agriculture, National Agricultural Statistics Service.

van Vuuren, D. P., J. Edmonds, M. Kainuma, K. Riahi, A. Thomson, K. Hibbard, G. C. Hurtt, T. Kram, V. Krey, J.-F. Lamarque, T. Masui, M. Meinshausen, N. Nakicenovic, S. J. Smith, and S. K. Rose. 2011. "The Representative Concentration Pathways: An Overview." *Climatic Change* 109(1):5–31. doi:10.1007/s10584-011-0148-z.

Venishetty, V., P. B. Parajuli, and D. Nepal. 2023. "Spatial Variability of Best Management Practices Effectiveness on Water Quality within the Yazoo River Watershed." *Hydrology* 10(4):92. doi:10.3390/hydrology10040092.

Vicente-Serrano, S. M., S. Beguería, and J. I. López-Moreno. 2010. "A Multiscalar Drought Index Sensitive to Global Warming: The Standardized Precipitation Evapotranspiration Index." *Journal of Climate* 23(7):1696–1718. doi:10.1175/2009JCLI2909.1.

Vigiak, O., A. Malagó, F. Bouraoui, B. Grizzetti, C. J. Weissteiner, and M. Pastori. 2016. "Impact of Current Riparian Land on Sediment Retention in the Danube River Basin." *Sustainability of Water Quality and Ecology* 8:30–49. doi:10.1016/j.swaqe.2016.08.001.

Wallace, C. W., D. C. Flanagan, and B. A. Engel. 2018. "Evaluating the Effects of Watershed Size on SWAT Calibration." *Water* 10(7):898. doi:10.3390/w10070898.

Wang, G., M. E. Barber, S. Chen, and J. Q. Wu. 2014. "SWAT Modeling with Uncertainty and Cluster Analyses of Tillage Impacts on Hydrological Processes." *Stochastic Environmental Research and Risk Assessment* 28(2):225–238. doi:10.1007/s00477-013-0743-9.

Wang, S., T. Stiles, T. Flynn, A. J. Stahl, J. L. Gutierrez, R. T. Angelo, and L. Frees. 2009. "A Modeling Approach to Water Quality Management of an Agriculturally Dominated Watershed, Kansas, USA." *Water, Air, and Soil Pollution* 203(1):193–206. doi:10.1007/s11270-009-0003-2.

Water Resources Solutions, LLC. 2020. *Prairie Band Potawatomi Nation Surface Water Management Report.* Prepared for the Prairie Band Potawatomi Nation. February 13, 2020.

Wellen, C., G. B. Arhonditsis, T. Long, and D. Boyd. 2014. "Quantifying the Uncertainty of Nonpoint Source Attribution in Distributed Water Quality Models: A Bayesian Assessment of SWAT's Sediment Export Predictions." *Journal of Hydrology* 519:3353–3368

White, M. J., and J. G. Arnold. 2009. "Development of a Simplistic Vegetative Filter Strip Model for Sediment and Nutrient Retention at the Field Scale." *Hydrological Processes* 23(11):1602–1616. doi:10.1002/hyp.7291.

Wilkison, D. H., D. J. Armstrong, and S. A. Hampton. 2009. *Character and Trends of Water Quality in the Blue River Basin, Kansas City Metropolitan Area, Missouri and Kansas, 1998 through 2007.* Scientific Investigations Report 2009–5169. U.S. Geological Survey. doi:10.3133/sir20095169.

Williams, J. R. 1975. "Sediment-Yield Prediction with Universal Equation Using Runoff Energy Factor." In *Present and Prospective Technology for Predicting Sediment Yield and Sources,* ARS-S-40, 244–252. Washington, DC: U.S. Department of Agriculture, Agricultural Research Service.

Wischmeier, W. H., and D. D. Smith. 1978. *Predicting Rainfall Erosion Losses: A Guide to Conservation Planning.* Agriculture Handbook No. 537. Washington, DC: U.S. Department of Agriculture.

Wu, L., X. Liu, J. Chen, J. Li, Y. Yu, and X. Ma. 2022. "Efficiency Assessment of Best Management Practices in Sediment Reduction by Investigating Cost-Effective Tradeoffs." *Agricultural Water Management* 265:107546. doi:10.1016/j.agwat.2022.107546.

Xue, F., P. Shi, S. Qu, J. Wang, and Y. Zhou. 2019. "Evaluating the Impact of Spatial Variability of Precipitation on Streamflow Simulation Using a SWAT Model." *Water Policy* 21(1):178–196. doi:10.2166/wp.2018.118.

Yasarer, L. M. W., S. Sinnathamby, and B. S. M. Sturm. 2016. "Impacts of Biofuel-Based Land-Use Change on Water Quality and Sustainability in a Kansas Watershed." *Agricultural Water Management* 175:4–14. doi:10.1016/j.agwat.2016.05.002.

Yuan, Y., R. S. Book, K. R. Mankin, L. Koropeckyj-Cox, L. Christianson, T. Messer, and R. Christianson. 2022. "An Overview of the Effectiveness of Agricultural Conservation Practices for Water Quality Improvement." *Journal of the ASABE* 65(2):419–426. doi:10.13031/ja.14503.

Appendix A - SWAT Model Implementation

A Baseline Model Setup

Landuse was intersected with parcel-level PBPN ownership data and reclassified based on ownership. This supports the targeted implementation of management and BMP operations. Non-tribal cropland was coded CORN (corn) and SOYB (soybean) and tribal owned cropland was coded COPB (corn) and SOPB (soybean). The "PB" ownership suffix appears on other landuse classes in HRU like BRPB (brome), RNPB (rangeland) etc. The corn-soybean rotation was implemented as a two-year cycle within a single HRU's management file (Year 1 / Year 2, via "Add Year"), not as an annual land-use reassignment. For example, the tribal-owned HRU in Table A.1 plants corn in Year 1 and soybean in Year 2; while a non-tribal HRU elsewhere in the watershed has the opposite cycle (soybean first; Figure A.1), so the watershed contains a mix of corn and soybean in any given calendar year. This was done to approximate the total acreage of corn or soybean in any given year as provided by the USDA Crop Data Layer (CDL).

Appendix Table A.1: Management schedule used for corn

Year	Month	Day	Operation	Crop
1	4	15	Plant/begin growing season	COPB (Corn PBPN)
1	4	30	Auto fertilization initialize	—
1	9	15	Harvest and kill	—
1	9	30	Tillage operation (Generic Fall Plowing, CNOP=0)	—
2	5	15	Plant/begin growing season	SOPB (Soybean PBPN)
2	5	30	Auto fertilization initialize	—
2	10	15	Harvest and kill	—

Current Management Operations

Year	Month	Day	Operation	Crop
1	5	15	Plant/begin. growing se	SOYB
1	5	30	Auto fertilization initializ	(null)
1	10	15	Harvest and kill operati	(null)
1	10	30	Tillage operation	(null)
2	4	15	Plant/begin. growing se	CORN
2	4	25	Auto fertilization initializ	(null)
2	9	15	Harvest and kill operati	(null)

Appendix Figure A.1: Operation Schedule for a cropland HRU with first year as Soybean followed by Corn next year

Grazing was implemented as a single continuous season grazing operation (MGT_OP = 9) on pasture/rangeland HRUs, not as a series of shorter rotational/paddock events. In the example presented in Table A.2, grazing was set to begin April 20 and run for GRZ_DAYS = 230 consecutive days i.e., roughly April through early December, essentially the full frost-free season. This grazing timeframe was set to reflect common practices in the watershed, particularly in grazing land managed or leased by the PBPN (personal communication, Michael Boswell).

BIO_EAT (grazing consumption rate) was derived from a stocking rate of 1 cow-calf pair per 8 acres (source: NRCS Kansas grazing guidance) and an assumed dry-matter intake of 20 lb/animal/day (~9 kg/day, roughly 2% of a 1,000-lb animal unit's body weight).

MANURE_KG (manure deposition rate) was derived separately, from total-solids manure production of a finished animal (source: USDA AMS National Organic Program handbook, section 5017-1) over an assumed 153-day finishing period. Loading rates for nutrients and bacteria assumed for the model are presented in Figure A.2.

Appendix Table A.2: Grazing Schedule

Parameter	**Value**	**Parameter**	**Value**
Schedule	By date, April 20	MANURE_ID	Beef-Fresh Manure
GRZ_DAYS	230 consecutive days	BIO_EAT	2.78 (kg/ha)/day
BIO_TRMP	0 (trampling not simulated)	MANURE_KG	0.69 (kg/ha)/day

Manure enters the model through the grazing operation and accounted as a source of bacteria loading.

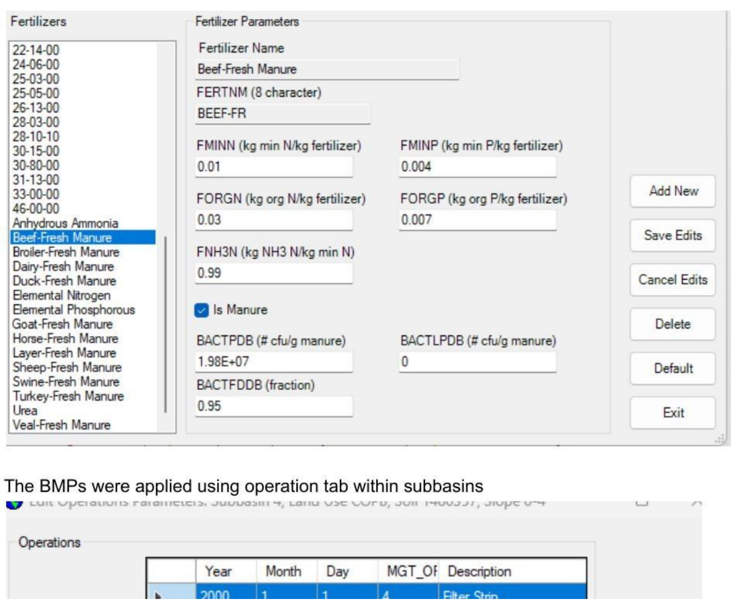

Appendix Figure A.2: Fertilizer database entry for manure showing nutrient fractions and bacteria concentrations used to compute loading rates.

B. BMP Scenario and Future Climate Scenario Implementation

BMPs were applied through the Operations tab under subbasin options for a specifically targeted HRU (identified by subbasin, ownership-coded land use, soil & slope), not at the watershed or subbasin level. Table A.3 shows the parameter input values for filter strips.

Appendix Table A.3: Filter strip input parameters

Parameter	Meaning	Value
VFSI	Filter strip simulation flag	1 (on)
VFSRATIO	Field-to-filter-strip area ratio	40
VFSCON	Fraction of flow entering the most concentrated 10% of the strip	0.5
VFSCH	Fraction of flow entirely bypassing the strip (channelized)	0

No-Till was implemented by deleting the Tillage operation row from the baseline schedule shown in section A of management practices (Table A.1; Figure A.1). The Regenerative Agriculture scenario was applied through "Manual calibration" editor in ArcSWAT where the CN for crop lands in the PBPN region were reduced by 10%. The snapshot in Figure A.3 gives one example of the application.

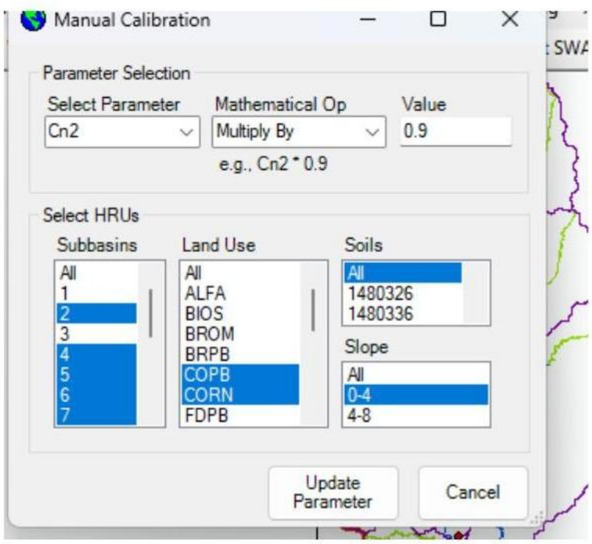

Appendix Figure A.3: RA implementation in the model

For future climate, 18 climate input files for precipitation (.pcp), temperature (.tmp), wind (.wnd), and solar radiation (.slr) were generated for the 2006–2099 period for RCP 4.5 and RCP 8.5. The model was provided each climate model input and simulated for the time period. A total of 36 runs were completed; the extracted result was aggregated to get the hydrological response of the watershed with future climate.

C. Reservoir Scenario Implementation

Reservoir parameters were entered at the reach/subbasin level — dialog title "Edit Reservoir Parameters, Subbasin 2, Reservoir ID 1". The snapshot presented in Figure A.4 shows the parameters populated to represent the reservoir module in the model.

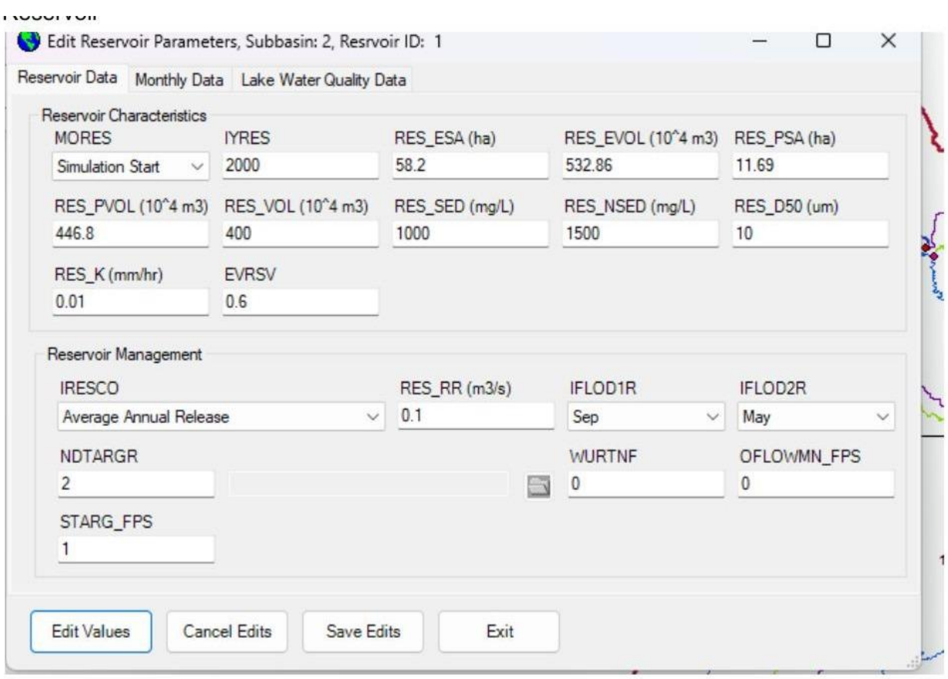

Appendix Figure A.4: Input parameters for Reservoir

Monthly consumptive-use withdrawal (WURESN, in 10^4 m^3 withdrawn per day during the month) is the mechanism for removing domestic and irrigation demand from storage. The table below shows the monthly consumptive use for model scenario R2.

Appendix Table A.4: Monthly water demand application to the model

Month	Monthly Use (10^4 m^3)
Jan	0.16
Feb	0.16
Mar	0.16
Apr	0.16
May	1.11
Jun	6.68
Jul	9.63
Aug	6.48
Sep	2.45
Oct	0.16
Nov	0.16
Dec	0.16

Site topography at reach 2 included local high points that would require excavation to achieve the assumed reservoir geometry. The DEM was therefore used to establish the reservoir's boundary/footprint and approximate base elevation (~1,100 ft) rather than to generate a stage-storage (elevation–area–capacity) relationship; storage volume was estimated from the assumed uniform-basin geometry (58.2 ha surface area, 9.1 m average depth, 3:1 side slope) applied across that footprint, rather than from a DEM-based cut/fill calculation.

Appendix B - Filter Strips

Filter strips (also called vegetated or grassed filter strips) are permanent bands of dense vegetation at the downslope edge of a field. As runoff crosses the area carrying soil particles, the vegetation slows the flow and lets suspended sediment settle out before it reaches a waterway, while also increasing infiltration and reducing runoff volume. They're conceptually similar to buffer strips, but sit specifically at the downstream edge of a field or drainage path rather than along contours. The EPA/NPDES fact sheet adds that flow length into the strip should generally stay under 75 ft to 150 ft, topsoil should be 8–18 in deep with good infiltration (0.5–12 in/hr), and the strip should sit 2 to 4 ft above the water table.

Reported performance: a 15-ft agricultural buffer can remove ~50% of nitrogen, phosphorus, and sediment, and a 100-ft buffer up to 70% (Barr/Metro Council). A Chesapeake Bay Program review found average reductions of 51% for stormwater volume and 56–86% for nitrogen, phosphorus, and total solids (EPA/NPDES), though effectiveness drops for large storms or flows over ~1.3 ft/s. Filter strips do not reduce peak flow rate much, so they work best as pretreatment ahead of another BMP.

Appendix Figure B.1: Filter strip in a field (Source: Xiaoqiang Liu, Food, Agricultural and Biological Engineering, The Ohio State University, via Ohio State University AgBMPs guide, "Filter Strips/Grassed Riparian Buffers (NRCS 393 & 390))

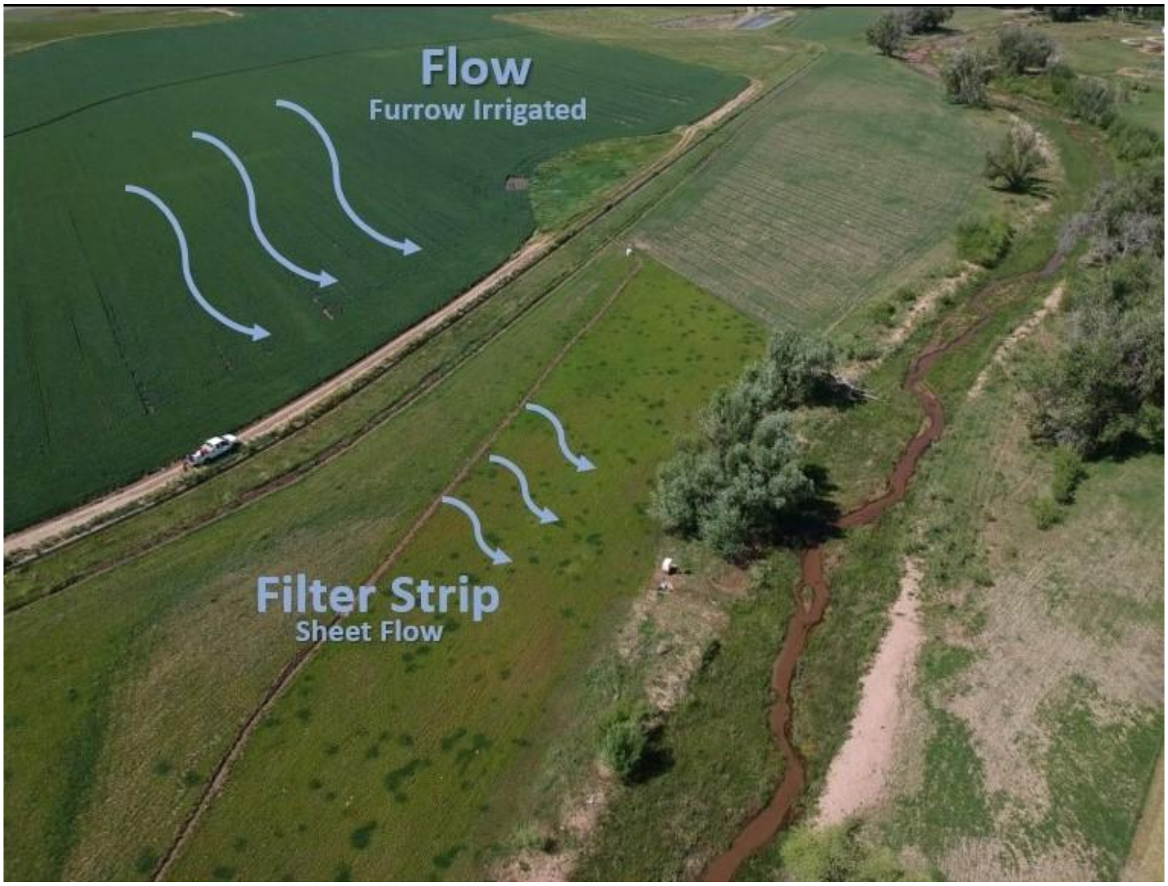

Appendix Figure B.2: Example of filter strips slowing field runoff and dropping sediment before it enters a waterway (Source: https://vernonbmpguide.ericbarefoot.com/bmp_pages/filter-strips.html)

Appendix Figure B.3: Photo of a functioning vegetated filter strip with a stone-lined channel and dense native vegetation (Source: Steven Chase for USEPA, 2019, via EPA NPDES fact sheet